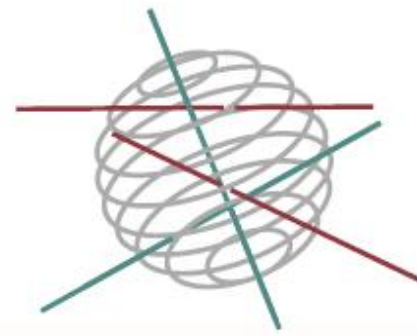


# SSD

SCIENCE FOR A SUSTAINABLE DEVELOPMENT



## MICROBIAL DIVERSITY AND METAL FLUXES IN CONTAMINATED NORTH SEA SEDIMENTS

"MICROMET"

D. C. GILLAN, K. SABBE, A. PEDE, G. BILLON,  
L. LESVEN, Y. GAO, M. LEERMAKERS,  
W. BAEYENS, B. LOURIÑO CABANA



ENERGY 

TRANSPORT AND MOBILITY 

AGRO-FOOD 

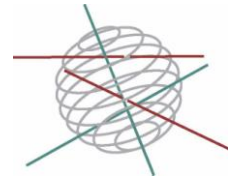
HEALTH AND ENVIRONMENT 

CLIMATE 

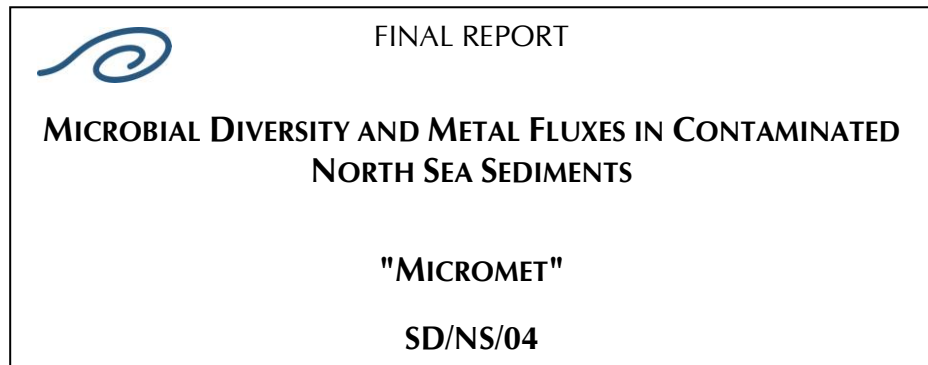
BIODIVERSITY   

ATMOSPHERE AND TERRESTRIAL AND MARINE ECOSYSTEMS   

TRANSVERSAL ACTIONS 



***Biodiversity, Terrestrial and Marine Ecosystems***



**Promotors**

**David C. Gillan & Philippe Dubois**  
Université Libre de Bruxelles (ULB)

**Koen Sabbe**

Universiteit Gent (Ugent)

**Willy Baeyens & Martine Leermakers**

Vrije Universiteit Brussel (VUB)

**Jean-Claude Fisher**

University of Science and Technology - Lille (USTL)

**Authors**

David C. Gillan (Université Libre de Bruxelles)

Koen Sabbe (Ghent University)

Annelies Pede (Ghent University)

Gabriel Billon (Université Lille-1)

Ludovic Lesven (Université Lille-1)

Yue Gao (Vrije Universiteit Brussel)

Martine Leermakers (Vrije Universiteit Brussel)

Willy Baeyens (Vrije Universiteit Brussel)

Beatriz Lourião Cabana (Université Libre de Bruxelles)





D/2012/1191/9

Published in 2012 by the Belgian Science Policy Office

Avenue Louise 231

Louizalaan 231

B-1050 Brussels

Belgium

Tel: + 32 (0)2 238 34 11 – Fax: + 32 (0)2 230 59 12

<http://www.belspo.be>

Contact person: David Cox

+ 32 (0)2 238 34 03

Neither the Belgian Science Policy Office nor any person acting on behalf of the Belgian Science Policy Office is responsible for the use which might be made of the following information. The authors are responsible for the content.

No part of this publication may be reproduced, stored in a retrieval system, or transmitted in any form or by any means, electronic, mechanical, photocopying, recording, or otherwise, without indicating the reference :

Gillan DC, Sabbe K, Pede A, Billon G, Lesven L, Gao Y, Leermakers M, Baeyens W, Lourião Cabana B. ***Microbial Diversity and Metal Fluxes in Contaminated North Sea Sediments – Micromet***. Final Report. Brussels : Belgian Science Policy Office 2012 – 107 p. (Research Programme Science for a Sustainable Development).

## **TABLE OF CONTENT**

|  |            |
|--|------------|
| <b>SUMMARY .....</b>   | <b>5</b>   |
| <b>1. INTRODUCTION .....</b>   | <b>9</b>   |
| <b>1.1. Subject and objectives .....</b>                                   | <b>9</b>   |
| 1.1.1. Trace metals in marine sediments and benthic fluxes.....            | 9          |
| 1.1.2. Sediment-associated microbial communities.....                      | 9          |
| 1.1.3. Benthic microbes and trace metals.....                              | 10         |
| <b>1.2. Aim of the MICROMET research program .....</b>                     | <b>11</b>  |
| <b>1.3. The MICROMET research program and sustainable development.....</b> | <b>12</b>  |
| <b>2. METHODOLOGY AND RESULTS .....</b>                                    | <b>13</b>  |
| <b>2.1. Methodology .....</b>  | <b>13</b>  |
| 2.1.1. Sampling and microelectrode analysis.....                           | 13         |
| 2.1.2. Determination of the microbial diversity.....                       | 14         |
| 2.1.3. Determination of microbial biomass.....                             | 16         |
| 2.1.4. Bacterial production .....  | 17         |
| 2.1.5. Geochemical properties of the sediment.....                         | 18         |
| 2.1.6. Laboratory simulation approaches.....                               | 20         |
| 2.1.7. Data analysis.....  | 23         |
| 2.1.8. Numerical modelling.....  | 24         |
| <b>2.2. Results.....</b>   | <b>26</b>  |
| 2.2.1. Field campaigns .....   | 26         |
| 2.2.2. Field campaigns conclusions .....                                   | 55         |
| 2.2.3. Laboratory simulation approaches.....                               | 57         |
| 2.2.4. Laboratory simulation approaches conclusions.....                   | 76         |
| 2.2.5. Numerical modeling.....   | 81         |
| <b>3. POLICY SUPPORT .....</b>   | <b>95</b>  |
| <b>4. DISSEMINATION AND VALORISATION .....</b>                             | <b>97</b>  |
| <b>4.1. PhD thesis including MICROMET data.....</b>                        | <b>97</b>  |
| <b>4.2. Poster presentations and oral communications .....</b>             | <b>97</b>  |
| <b>4.3. Other activities.....</b>  | <b>98</b>  |
| <b>5. PUBLICATIONS OF THE TEAM.....</b>                                    | <b>99</b>  |
| <b>5.1. Published manuscripts .....</b>                                    | <b>99</b>  |
| <b>5.2. Submitted manuscripts.....</b>                                     | <b>99</b>  |
| <b>5.3. Manuscripts in preparation .....</b>                               | <b>99</b>  |
| <b>6. ACKNOWLEDGMENTS.....</b>   | <b>101</b> |
| <b>7. REFERENCES .....</b>   | <b>103</b> |



## SUMMARY

### A. CONTEXT

Many coastal areas worldwide are contaminated by metallic toxicants such as Cd, Ag, Pb, Hg and Ni, and these contaminants usually accumulate in sediments. On the Belgian Continental Plate (BCP) the concentration of metallic pollutants in sediments is above, or just at the level of, the Ecotoxicological Assessment Criteria (EAC), which are defined by the OSPAR Commission as concentration levels above which concern is needed.

As the most abundant organisms in the sediments, microorganisms are key players in the biogeochemistry of benthic ecosystems, acting on a variety of processes which may affect metal mobility and bioavailability. For example, benthic microbial communities are responsible for a substantial part of organic matter mineralization, essentially produced by local phytoplankton blooms and/or imported from adjacent estuaries. As most metals may be complexed by organic matter, metals are mobilized when organic matter is degraded. This may lead to both the alteration of microbial biodiversity and to metal bioaccumulation in higher trophic levels through increased leaching of metals from the sediments. To date, the composition, structure and physiology of microbial communities in marine sediments remain poorly studied, and there is virtually no information on microbial assemblages and their functioning in metal contaminated zones. Nothing is known about the impact of metallic toxicants on microbial diversity in sediments of the BCP or about the importance of microbial communities in the leaching of metallic pollutants from the sediments in this area. This is problematic as the BCP is characterized by massive algal blooms in spring (mainly *Phaeocystis globosa*) and receives large amounts of nutrients and organic matter from the Scheldt estuary.

### B. OBJECTIVES AND MAIN RESULTS

The aim of the MICROMET project was to study the interactions between metallic contaminants and microbial communities (Archae, Bacteria, and micro-Eukarya) living in marine sediments of the BCP. The research was composed of three main parts in which microbiological and geochemical approaches were closely integrated. The first part (Work Package 1 - WP 1) was devoted to an in depth analysis of the impact of metallic contaminants on the microbial diversity of sediments using a combination of state-of-the-art molecular and geochemical tools. For that, 9 stations were selected on the BCP. The aim of the second part (WP 2) was to assess the importance of microorganisms in the leaching of metallic contaminants from the sediments into the water column. In the third part (WP 3) geochemical modelisation was performed with the results obtained previously in order to better characterize metal fluxes in the sediments. During the whole MICROMET project, special attention was paid to the influence of organic matter, particularly phytodetritus, on the relationship between benthic microbes and metals. Organic matter has been identified in previous researches as one of the main force affecting the diversity and activity of microbial communities.

Field campaigns indicated that the most abundant Bacteria in the sediments belong to the  $\gamma$ -Proteobacteria,  $\delta$ -Proteobacteria and CFB bacteria. Acidobacteria represent 2.6–14.6% of the 16S rRNA clones in most of the stations. For micro-

Eukarya, 18S rRNA based DGGE and clone libraries revealed a surprisingly high diversity mainly comprising Stramenopiles (diatoms and oomycetes), Protozoa (Alveolata, Cercozoans and Amoebozoa) and Fungi, many of which are as yet unidentified (or ambiguously identified) in the existing genetic databases (Pede et al., in prep a). Microbial diversity (Bacteria and micro-Eukarya), as measured with the DGGE approach, was not correlated to environmental variables. This might be explained by methodological biases but also by the present-day adaptation of the microbial communities to elevated metal concentrations. Future studies should concentrate on metal resistance and metal bioavailability. Other methods of biodiversity measurement should also be tested. Contrary to biodiversity, bacterial biomass (DAPI counts) displayed elevated and significant correlations to some environmental variables, particularly to dissolved Mn, Fe and As (Gillan et al., in press). Field campaigns have also indicated that trace elements measured by the DET/DGT approaches are mobilized at specific depths. Seasonal variations of these elements have been observed and flux calculations based on DGT profiles indicate that metals may diffuse out of the sediment into the overlying water at least in one of the stations investigated (station 130) (Gao et al. 2009). Flux calculations based on DGT piston experiments confirmed that metals may reach the sediment-water interface (SWI) and be released in the seawater. Microbial eukaryotic communities showed pronounced changes across a phytoplankton bloom deposition event, both in time and with depth in the sediment; community dynamics were strongly related to changes in redox and pH, but an independent impact of trace metals was also observed (Pede et al., in prep b).

Laboratory microcosm experiments performed during the MICROMET project have clearly demonstrated that microbial mineralization of phytoplankton-derived phytodetritus accumulated at the surface of contaminated muddy sediments leads to increased effluxes of trace elements from these sediments (Gao et al. 2011, Gillan et al., subm.; Pede et al., in prep c & d). During one of these experiments, muddy sediments were overlaid by phytodetritus, i.e. a mix of *Phaeocystis globosa* and *Skeletonema costatum* (final chlorophyll a content :  $750 \pm 35 \mu\text{g L}^{-1}$ ). This exposure produced large benthic effluxes of metals reaching  $1084 \text{ nmol m}^{-2} \text{ d}^{-1}$  for arsenic,  $512 \text{ nmol m}^{-2} \text{ d}^{-1}$  for cobalt, and  $755 \mu\text{mol m}^{-2} \text{ d}^{-1}$  for manganese. A clear link was established between heterotrophic microbial activity at the SWI and metal effluxes. Calculations have suggested that during phytoplankton blooms microbial activity alone may release substantial amounts of dissolved arsenic in areas of the BCP covered by muddy sediments. Active (RNA) bacterial and protozoan communities respond with significant changes in community composition to phytodetritus deposition, with most pronounced changes in Protozoa lagging 5 days behind those of bacteria (Pede et al., in prep c). In another experiment we also demonstrated that micro-eukaryotic communities are significantly influenced by the contamination with arsenic, with diversity decreasing at high As concentrations ( $> 240 \mu\text{g L}^{-1}$ ); ciliates were the most tolerant organisms (Pede et al., in prep d).

Geochemical modelisations have shown that sulfides play an important role for all metals on muddy sediments of the BCP, whereas none of the studied metals seemed to be highly dependent on temperature or pH. Organic matter level was observed to be an important parameter to take into account for Fe, Co, Cu, As(III), Pb and Cd. It was also found that carbonates do not play a significant role in the speciation of trace metals. On the other hand, most of the metallic sulfides were found to precipitate, such as FeS, PbS, ZnS, CdS, CoS, CuS, NiS and  $\text{CuFeS}_2$ , which clearly indicates that metal speciation in these sediments is controlled by

sulfides, but also by organic matter. Bacterial reductive dissolution of Mn(III and IV) and Fe(III) oxides/hydroxides is clearly associated to microbial degradation of organic matter and leads increased metal levels in porewaters. Overall, results obtained from thermodynamic calculations showed good agreement with experimental data (microcosm experiments) and field surveys.

### **C. CONCLUSION**

As a conclusion, relationships between microbial diversity and metal levels are highly complex and bacterial biomass is a variable which is a better indicator for marine sediment quality, especially for arsenic in porewaters. Metal levels on the BCP are striking (particularly the metalloid arsenic) and efforts should be made to reduce the human impact, especially in the area extending up to 3–4 km in the open sea between Oostende and Zeebrugge. Sediments are able to accumulate and release large quantities of contaminants like arsenic and benthic ecology may be affected.

The MICROMET project has resulted in three completed PhD's (Ludovic Lesven, USTL, 2008; Yue Gao, VUB, 2009; Annelies Pede, UGent, Dec. 2011). Another PhD based on MICROMET results & methodologies will be presented in 2013 (Stephanie Roosa, UMons). Two papers have been published during the project (Gao et al. 2009, 2011), others have been submitted or just accepted (Gillan et al., in press); others are very close to submission to peer-reviewed journals (Pede et al., a, b, c & d – these are finished, manuscript-format chapters in the PhD of A. Pede). Results of the MICROMET projects have been presented at various national and international meetings (e.g., ASLO, EMBS, SedNet, VLIZ-meetings, International Estuarine Biogeochemistry Symposium, Symposium on Environmental Analytical Chemistry).

### **D. CONTRIBUTION OF THE PROJECT IN A CONTEXT OF SCIENTIFIC SUPPORT TO A SUSTAINABLE DEVELOPMENT POLICY**

Products from fisheries (especially benthic and demersal fishes) and mussel-farming from the BCP zone should be carefully monitored for metals and metalloids, especially arsenic. The large phytoplankton blooms which inevitably occur each year on the Belgian continental plate are expected to increase effluxes of toxic metals from the sediments, especially from coastal muddy sediments on the eastern part of the Belgian coast. Efforts should also be maintained to reduce nutrient inputs from the Scheldt estuary. The implementation of the EU Water Framework Directive (WFD) is currently raising a number of technical challenges for the Member States, particularly for Belgium, which should meet the WFD environmental objectives in 2015. Clearly, measurements performed during the MICROMET project between 2007 and 2010 suggested that a "good ecological and chemical status" will not be met in 2015 for the Belgian coastal ecosystem extending up to 3-4 km in the open sea between Oostende and Zeebrugge.

### **E. KEYWORDS**

Sediment, metals, porewater, bacteria, microorganisms, micro-eukaryotes, arsenic, cobalt, manganese, marine environment, biodiversity, metal fluxes, contamination, phytoplankton bloom, *Phaeocystis*, modelling.



## 1. INTRODUCTION

### 1.1. Subject and objectives

#### 1.1.1. Trace metals in marine sediments and benthic fluxes

As a consequence of human activities, many coastal areas all around the world are contaminated by metals such as Cd, Cu, Pb, Zn, Hg and Ni (Clark 2001, Green et al. 2003). These elements are usually accumulated in sediments where concentrations in pore-waters can exceed those in overlying waters by several orders of magnitude (Calmano & Förstner 1996). According to the Quality Status Report 2000 of the OSPAR commission (QSR 2000) concentrations of Cd, Cu, Pb, and Zn in most coastal sediments of the North Sea are above, or just at the level, of the Ecotoxicological Assessment Criteria (EAC), which are defined as concentration levels above which concern is needed. Recent studies, conducted on the Belgian Continental Plate (BCP), confirmed the observations of the Quality Status Report (Danis et al. 2004, Gillan & Pernet 2007).

Once in the sediments, metals are highly persistent and are accumulated over time. Even when the primary source of pollution has disappeared sediments may act as a long-term metal source for bottom waters. This was demonstrated in many coastal areas where benthic fluxes of metals were quantified (Holmes 1986, Heggie et al. 1987, Rivera-Duarte & Flegal 1994, Berelson et al. 2003, Alongi et al. 1996, Skrabal et al. 2000, Fones et al. 2004). For instance, in coastal California, the net diffusive benthic flux of Pb from sediments ( $3\text{-}31 \text{ moles d}^{-1}$ ) was at least an order of magnitude greater than the fluvial input of dissolved Pb to the estuary ( $0.2 \text{ moles d}^{-1}$ ) during low flow periods (Rivera-Duarte & Flegal 1994). Despite the high concentration levels of metals in sediments from the BCP (Danis et al. 2004), the importance of benthic fluxes in the area is unknown. This is a problem because toxic metals such as Cd, Hg and Pb are bioaccumulated in many organisms (Kennish 1998, De Gieter et al. 2002, Baeyens et al. 2003, Coteur et al. 2003, Danis et al. 2004). In addition, metals are on the European Union's list of priority substances for the Water Framework Directive (2000/60/EC), which goal is to evaluate all inputs of hazardous substances and try to achieve concentrations in the marine environment near background values by 2020.

#### 1.1.2. Sediment-associated microbial communities

Despite the advent of the recent "omics" era (e.g., Venter et al. 2004, Konstantinidis et al. 2009, Morris et al. 2010), the diversity of marine microbial communities is still largely unknown in the coastal subtidal zone, and so is the true extent of its ecological and evolutionary importance (e.g. Richards & Bass 2005 and references therein). Many studies based on environmental gene libraries have shown that the true diversity of these communities far exceeds our current knowledge. There are strong indications that especially anoxic environments harbour many more species than hitherto expected (e.g. Madrid et al. 2001, Countway et al. 2005, Köpke et al. 2005, Stoeck et al. 2006, Wilms et al. 2006). However, most studies to date pertain to pelagic samples, with marine sediments being severely understudied.

The fact that many of the novel sequences belong to as yet uncultivable organisms underscores the importance of the integration of molecular tools in ecological studies.

Benthic protozoa inhabiting marine sediments are particularly understudied, especially in the North Sea (Kröncke et al. 2004). It can be expected, however, that by analogy with pelagic systems, where they play a key role in the microbial loop, protozoa are instrumental in the functioning of benthic ecosystems. Their high functional diversity combined with potentially high growth and grazing rates suggest a crucial role in remineralization rates and the transfer of matter and energy to higher trophic levels (Epstein 1997, Hamels et al. 2004). As for prokaryotes, quantification and identification are problematic. Traditional identification methods require the study of living materials and/or dedicated staining techniques, and in both cases a thorough taxonomic expertise (Dietrich & Arndt 2000, Hamels et al. 2005).

For quantification, protozoa are usually stained (e.g. with DAPI) and enumerated using epifluorescence microscopy, which precludes proper identification, and only allows to distinguish broad categories (morphotypes and/or size classes, e.g. Hamels et al. 2004, Polymenakou et al. 2005). Other quantification methods such as the most probable number method (e.g. Ekelund et al. 2001) are time-consuming and therefore less suitable for the quantitative processing of large numbers of samples.

Studies using molecular methods for identification and/or quantification of benthic marine protozoa are virtually lacking. While subtidal benthic communities commonly consist of flagellated, ciliated or amoeboid species (Dietrich & Arndt 2000, Hausmann et al. 2002), studies on protozoa of North Sea sediments have so far been largely focused on heterotrophic nanoflagellates (Hondeveld et al. 1994, 1999). Spatial and temporal dynamics of this group have been related to a.o. bacterial biomass and production, granulometry (Hondeveld et al. 1994), organic sedimentation (Van Duyl et al. 1992, Bak et al. 1995), oxygen conditions (Hondeveld et al. 1994) and various activities of meio- and macrofauna, such as bioturbation and grazing (e.g. Bak et al. 1995, Hamels et al. 2005). If light penetration is sufficient, subtidal areas can also support benthic microalgal growth (e.g. on the Dogger Bank, Kröncke et al. 2004).

### **1.1.3. Benthic microbes and trace metals**

The impact of metal contamination on the biology and diversity of sedimentary macrobiota is well chronicled (Kennish 1998). For instance, macrofaunal species diversity in Norwegian fjords showed a strong negative correlation with copper concentrations (Rygg 1985, Kennish 1998). In contrast, virtually nothing is known about the biodiversity, the structure, and the physiology of prokaryotic microbial communities in metal contaminated coastal sediments (Gillan et al. 2005, Powell et al. 2003). At the start of the MICROMET project in 2006 only three quantitative studies were conducted within metal contaminated environments : two of them were carried out in the same intertidal mudflat of the German Wadden Sea, mostly contaminated with Pb and Zn (Böttcher et al. 2000, Mußmann et al. 2005), and the third in the Sørøfjord (Norway), which has been contaminated for more than 80 years with Cd, Cu, Pb and Zn (Gillan et al. 2005). The latter study concluded that biomass was not correlated to metal levels and that HCl-extractable Cu, Pb, and Zn were negatively correlated with the abundance of  $\gamma$ -Proteobacteria and CFB bacteria. However, a recent study conducted on the BCP area (Gillan & Pernet 2007) showed

that total bacterial biomass was negatively correlated to HCl-extractable metals, and that the abundance of  $\gamma$ - and  $\delta$ -Proteobacteria, and CFB bacteria, was not correlated to HCl-extractable metal levels.

The impact of metals on marine benthic protozoa has, to our knowledge, never been studied. The only available studies deal with terrestrial soils and have shown that protozoa and protozoan grazing can be negatively affected by metal contamination (e.g. Holtze et al. 2003, Ekelund et al. 2003, Du Plessis et al. 2005). The general lack of studies about the relation between benthic marine microbes and heavy metals is surprising given the fact that these organisms are abundant and fulfill a pivotal role in the biogeochemistry of marine sediments, including a variety of processes which can influence metal mobility and bioavailability (Ford & Ryan 1995, Ehrlich 1997, Gadd 2004). It is clear that in order to elucidate the impact of microbial communities on pore-water metal concentrations and the subsequent release of metals in the water column there is an urgent need for integrated studies including biogeochemical approaches and molecular microbiological methods (Böttcher et al. 2000).

## 1.2. Aim of the MICROMET research project

The aim of the project was to study the interactions between metallic contaminants and the microbial communities (archaeobacteria, eubacteria, and eukaryotes) living in marine sediments of the BCP area. The research was composed of three main parts in which microbiological and geochemical approaches were closely integrated. The first part (WP 1) was devoted to an in depth analysis of the impact of metallic contaminants on the microbial diversity of sediments using a combination of state-of-the-art molecular and geochemical tools. This aim is directly related to one of the seven priority research domains of the SSD program (i.e., the "Biodiversity" domain). The aim of the second part (WP 2) was to assess the importance of microorganisms in the leaching of metallic contaminants from the sediments into the water column. The aim of WP 2 is directly connected with another priority research domain of the SSD program (i.e., the "Marine Ecosystems of the North Sea"), as the study of benthic metal fluxes is necessary to fully understand their importance and role in the functioning of benthic ecosystems of the North Sea. In the third part (WP 3), results obtained during the research project are used to run geochemical models. These models may be used for the prediction and, ultimately, for the remediation of metal remobilization events.

Special attention was paid to the influence of oxygen and organic matter on the relationship between microbes and metals. These factors have been identified as the main forces affecting the diversity and activity of microbial communities (Giller et al. 1998, Bak et al. 1995). Organic matter and nutrient levels can be expected to change in the near future as inputs from the Scheldt estuary are progressively reduced since the activation of the Brussels North wastewater treatment plant in March 2007 ([www.aquiris.be](http://www.aquiris.be)). In addition, the continuing implementation of various EU directives on surface water quality (such as the Water Framework Directive) is also expected to have an effect on nutrient and organic matter inputs from the Scheldt estuary.

### 1.3. The MICROMET research project and sustainable development

Sediment-associated microbial communities have long been recognized as a key component of marine ecosystems as they are implicated in all major biogeochemical cycles (Canfield et al. 2005), are directly consumed by many deposit feeders (Newell 1965, Phillips 1984, Lopez & Levinton 1987) and play an important role in the recruitment, settlement and metamorphosis of many benthic invertebrates (Pearce & Scheibling 1991, Lam et al. 2003). Understanding how metal contaminants impact these communities, and vice versa, how and under which circumstances the microorganisms mediate fluxes of these contaminants to and from the water column is fundamental to ensure the long-term integrity of these benthic ecosystems and their sustainable exploitation.

The relationship between organic matter deposition, metals in sediments and benthic microbial communities is specially important. Most metals are complexed by organic matter, and organic matter provides the primary food source for microorganisms. Benthic remineralization has been shown to be an important process in BCP sediments (Riebesell 1993, Cadée 1996, Peperzak et al. 1998, Schoemann et al. 1998, Lancelot et al. 2005), but little is known about the influence of this process on metal mobilization. During the last decades, excess input of nitrogen and phosphorus (with respect to Si) have led to recurrent, massive spring blooms of opportunistic non-siliceous phytoplankton such as the haptophyte *Phaeocystis globosa* (Rousseau et al. 2000, Lancelot et al. 2005, Muylaert et al. 2006). New and existing measures are expected to lead to a further reduction in the input of N and P into the Belgian coastal zone, which may alter bloom development and composition, and hence also the amount and nature of organic matter input into the sediments, and oxygen profiles within these sediments. Using dedicated microcosm experiments, in which organic matter levels have been manipulated, the MICROMET project will lead to a better understanding of the interaction between organic matter input and decomposition, oxygen, microorganisms and metal fluxes in coastal sediments. As such, the results of MICROMET will further contribute to the sustainable development of the Belgian coastal zone.

## 2. METHODOLOGY AND RESULTS

The MICROMET project is interdisciplinary and strives for a close-knit integration of microbiological and geochemical approaches in the context of field surveys to study the relationship between microbial diversity and metal contaminants as well as laboratory experiments to study the impact of various biological and chemical factors on benthic metal fluxes. The project was started in January 2007. The data generated in this study is used to feed existing geochemical models and predict benthic fluxes of metals on the BCP in relation to key environmental factors such as organic matter and oxygen levels.

### 2.1. Methodology

#### 2.1.1. Sampling and microelectrode analysis

Nine sampling stations were selected on the BCP on the basis of previous research (Danis et al. 2004, Gillan & Pernet 2007) and SPSD 2 programs (Figure 1): stations 120, 130, 140, 230, 330, 435, 700, DCG, ZG03. The coordinates of the stations were 51°11.10 N - 02°42.07 E (120), 51°16.25 N - 02°54.30 E (130), 51°19.57 N - 03°02.93 E (140), 51°18.50 N - 02°51.00 E (230), 51°26.00 N - 02°48.50 E (330), 51°34.84 N - 02°47.42 E (435), 51°22.60 N - 03°13.20 E (700), 51°45.00 N - 02°42.00 E (DCG), and 51°15.70 N - 02°40.00 E (ZG03). Sediments encompassed a wide range of metal loads and granulometries.

In 2007, all sampling stations were sampled in two periods to take different organic matter sedimentation patterns into account [before (7-9<sup>th</sup> February) and after (4-6<sup>th</sup> July) the spring bloom]. In 2008, the two stations with the highest metal loads were sampled monthly between February and July (St. 130 & 700). Sandy stations were not selected as porewater metal concentrations (see DET/DGT analyses) were very low (see results of the 2007 campaign). Each month, 10 cm cores were subdivided into 1cm slices which were further analysed using the same methods as 2007. In 2009 and 2010 sediments of station 130 were collected and studied in microcosms experiments (see below).

Sediments were sampled using a Reineck corer ( $\varnothing$  15 cm) onboard the RV Zeeleeuw. Subcores were obtained using 11 cm plastic corers ( $\varnothing$  3 cm and  $\varnothing$  7-10 cm). From each Reineck core, one or two narrow subcores were used for molecular analyses (DGGE, cloning) and another one was used for determination of microbial biomass. The largest plastic subcores ( $\varnothing$  7-10 cm) were used for DET/DGT and microelectrode analyses. For microbiology, only two sediment horizons (0-1 and 9-10 cm) were considered in 2007. In 2008, ten depths (every 1 cm up to 10 cm) were sampled. In 2007, subsamples for molecular analyses were taken on board, stored in cryovials and transported in liquid nitrogen to the lab, where they were stored at -80°C. In 2008, whole cores were frozen on board in liquid nitrogen and subdivided in the lab. The subsamples for biomass determination (DAPI counts) were fixed with an equal volume 2.5 % glutaraldehyde (micro-eukaryotes) or 4% paraformaldehyde (bacteria), and stored in darkness at 4°C until processing. At each station, replicate pigment samples were also collected for all depths considered.

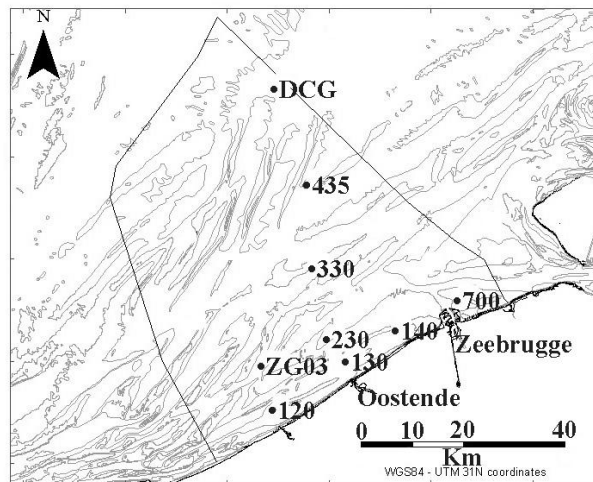


Figure 1. Sampling stations of the MICROMET project in 2007 and 2008.

Oxygen, pH and Eh were determined in sediments using microelectrodes. These parameters are important because they directly influence microbiology as well as the type of metals released in the pore-waters and consequently in the water column (Petersen et al. 1996). Oxygen profiles were obtained with a microelectrode of 500  $\mu\text{m}$  in diameter fixed on a micromanipulator (Unisense company). pH was estimated directly in the field by means of a glass micro-electrode (Ingold). It was combined with an Ag/AgCl reference electrode with a potential equal to +0.22 V vs a hydrogen normal electrode (HNE). Redox potential (Eh) profiles were measured with a home-made platinum micro-electrode associated with a reference electrode Ag/AgCl, [KCl] = 3 M. For the microcosm experiments Eh was measured using a platinum electrode (Mettler-Toledo/Pt 4800) as indicator electrode. This electrode was also combined with an Ag/AgCl, [KCl] = 3 M reference electrode with a potential equal to +0.22 V vs a hydrogen normal electrode.

## 2.1.2. Determination of the microbial diversity

### 2.1.2.1. DGGE analysis (Denaturing Gradient Gel Electrophoresis)

In 2007 and 2008, the *in situ* genetic diversity of microbial communities was determined using DGGE analysis of the 16S (for eubacteria and archaeobacteria) and 18S (for eukaryotes) rRNA gene.

For bacteria, DNA extraction was performed as described in Gillan & Pernet (2007). The general eubacterial primers GM5F and 518r were used (Muyzer et al. 1993). They amplify a fragment of the 16S rDNA, approximately 195 bp long. For Archaeobacteria, we designed two new primers: ARC-349-F and ARC-853-R (see below). A 40 bp GC clamp was attached to the 5' end of all the forward primers. DGGE was performed in 10% polyacrylamide gels submerged in 1X TAE buffer at 60°C. Electrophoresis conditions were: 16h at 75V in a linear 25 to 75% denaturant gradient. The gels were stained for 60 min in 1X TAE buffer with ethidium bromide and visualized with UV radiation.

For micro-eukaryotes, DNA extraction was performed using zirconium beads (Zwart et al. 1998). Elimination of extracellular DNA was performed as described by Corinaldesi et al. (2005). Extracted DNA was amplified for DGGE analysis using the PCR procedure described by Muyzer et al (1993). We used the general eukaryotic primers 1427f-GC and 1637r, designed by Van Hannen et al. (1998), which amplifies a  $\pm$  180 bp fragment of the 18S rDNA. DNA-based DGGE analyses are generally used to study the whole microbial community composition. In addition, to elucidate the effect of experimental conditions to the microeukaryotic community, SSU rRNA extractions were performed for the LABOSI-4 and LABOSI-5 experiments. Ribosomal RNA is an essential structural component of the ribosome, which is the organelle responsible for protein synthesis in all prokaryotes and eukaryotes. The number of cellular ribosomes, and thus also the rRNA content, increases with growth rate and decreases with starvation. Therefore, rRNA extracted from environmental samples serves as a phylogenetic marker for the identification and relative abundance of metabolically active microorganisms. Ribosomal RNA was isolated using bead-beating, phenol-chloroform extraction, and ethanol precipitation, as described by Chang et al (1993). RNA extracts were treated with RNase-free DNase, to eliminate the DNA. Total RNA was transcribed into cDNA using Qiagen OneStep RT-PCR Kit, according to the manufacturer's instructions. For LABOSI-4, the cDNA was used for analyses of both microeukaryotic and bacterial communities. Subsequent PCR and DGGE were proceeded as described above.

In addition, we tested the general eukaryotic primers Euk1A and Euk516r-GC designed by Diez et al. (2001), as these yield a larger DNA fragment ( $\pm$  560 bp). We also adapted 3 specific primer sets for important benthic protozoan groups (Alveolata:ciliates, Excavata:kinetoplastids and Rhizaria:cercozoans) for use in DGGE (nested PCR approach) to check whether the diversity of these groups may be underestimated due to the presence of high amounts of diatom DNA (see task 1.2.1) [ciliate-specific primers (Cil-315f; Cil-959r(I-II-III): 600-670bp, Lara *et al.* (2007), Kinetoplastida-specific primers (Kineto14F; Kineto2026R: 1900-2200bp, Von der Heyden & Cavalier-Smith 2005) and Cercozoa-specific primers (25F; 1256R:  $\pm$ 1260bp, Bass and Cavalier-Smith 2004), all in combination (second step in nested PCR) with the general eukaryotic primers (1427f-GC and/or Euk516r-GC)]. DGGE was performed with 7% polyacrylamide gels submerged in 1X TAE buffer at 60°C. Electrophoresis conditions were: 16h at 100V in a linear 30 to 55% denaturant gradient. The gels were stained for 30 min in 1X TAE buffer with SybrGold and visualized with UV radiation. DGGE bands were excised from the gel, resuspended in 30 $\mu$ l 1X TE buffer, reamplified, and sequenced.

#### **2.1.2.2. SSU rRNA clone libraries (CL) and sequencing**

Complete 16S and partial 18S rRNA genes were amplified from environmental DNA using universal archaeal, bacterial or eukaryotic primers (Gillan et al. 2005, Van Hannen et al. 1998, Wilms et al. 2006) and sequenced.

For micro-eukaryotes, three 18S clone libraries were constructed for stations 130 and 700 for 2008, using group-specific eukaryotic primers (first tested using PCR-DGGE-see 2.2.1.2) for three major protozoan groups, viz. ciliates, Cercozoa and Kinetoplastida (cf. above). The 18S rRNA genes were PCR amplified; PCR products from several reactions (2008 samples) were pooled to provide adequate amounts of product for the preparation of the clone library, positive (white and light

blue) colonies were picked out; 250 colonies for ciliates, 100 c for Cercozoa, 250 c for Kinetoplastida. Presence of the 18S rRNA gene insert was checked by PCR using T7 and SP6 primers and agarose gel electrophoresis. No insert was found for clones of Kinetoplastida. Clones with the correct insert size were PCR amplified for fast screening by DGGE using the nested PCR approach described above. Clones which showed different DGGE banding patterns, were selected to be sequenced. Sequencing was performed with forward primer cil-315f and reverse primers cil-959r(I-II-III) for ciliates, and with forward primer 25F, reverse primer 1256R, and internal primers 528 and Euk516r for Cercozoa (Bass & Cavalier-Smith 2004, Lara *et al.* 2007, Diez *et al.* 2001). Forward, reverse and internal sequences were aligned in Bionumerics 5.10.

### **2.1.2.3. Isolation of microorganisms**

For bacteria, five types of medium were used in February 2007. The purpose of these isolations was to evaluate biodiversity and to determine the bacterial biomass using the MPN approach (Most Probable Number). The media are described in Köpke *et al.* (2005). Briefly, medium I was used for oxic incubations and media II to V were used for anoxic incubations. Medium II is the standard anoxic medium for sulfate reducers (with sulfate); medium III is the standard anoxic medium without sulfate (for fermenters); and medium IV & V are the standard anoxic medium with manganese or iron oxides (5 mM). The MPN plates were incubated 3 months at 15°C in the dark. After that, MPN counts were obtained and subcultures were then incubated for 3 months. Isolations of pure cultures were then performed on agar plates.

### **2.1.3. Determination of microbial biomass**

For bacteria, total direct counts were determined in the two selected sediment sections for the February and July 2007 samples (0-1 and 9-10 cm), and in all sediment sections (from 0-10 cm) for the 2008 samples. Due to initial problems in methodology in February 2007 eukaryotic DAPI counts could not be obtained. For July 2007, eukaryotic DAPI counts were obtained for all samples except those of stations 330, 435 and DCG.

Total bacterial biomass was obtained using DAPI counts as described in Gillan *et al.* (2005) and MPN counts as described in Köpke *et al.* (2005). Bacteria were counted manually and by using the Image J software (14 pictures were counted for each filter, as explained in Gillan *et al.* (2005).

For isolation of micro-eukaryotes from the fixed sediment samples we used the density gradient centrifugation technique described by Starink *et al.* (1994, see also Hamels *et al.* 2004). This involves creating a 50 % Percoll density gradient (ultracentrifugation during 30 min at 38 800 g) and loading of the fixed sediment samples onto Percoll density gradients and centrifugation during 15min at 4.300 g. After centrifugation, the supernatants containing the extracted micro-eukaryotes is filtered onto 0.8 µm polycarbonate filters and stained with DAPI (10 µg mL<sup>-1</sup> final concentration). The filters are then immersed in immersion oil, covered with a cover slip and kept frozen and dark until epifluorescence microscopic analysis.

#### **2.1.4. Bacterial production**

Bacterial production measurements were performed during the LABOSI-4 microcosm experiment (see below). It included (i) incorporation of tritiated thymidine, (ii) community level physiological profiling (CLPP), and (iii) fluorescein diacetate analysis (FDA).

##### **2.1.4.1. Incorporation of tritiated thymidine**

For bacterial production, the tritiated thymidine incorporation approach was used with 1.0 g (ww) of living surface sediments that was suspended in 6 mL of autoclaved sterile seawater (LABOSI-4 experiment). These sediments were collected over a surface of ca 1 cm<sup>2</sup>. The sediment suspension was then sonicated for 30 sec to detach bacteria from particles (Gillan & Pernet, 2007). The suspension was then centrifuged 5 min at 180 g (4°C) to precipitate mineral particles. A volume of 5 mL of supernatant (containing bacteria) was placed in a clean tube with 6.4 µL of a <sup>3</sup>H-thymidine stock solution (specific activity, SA : 64 Ci mmol<sup>-1</sup>; 1.0 mCi mL<sup>-1</sup>) (MP Biomedicals). The final concentration of tritiated thymidine was 0.1 nmol in 5 mL. Tubes were then incubated for 90 min in the dark at 15°C under orbital agitation. The incorporation was stopped using 1.5 mL of 25% cold trichloroacetic acid. For the incorporation blanks (controls) the trichloroacetic acid was added before the 90 min incubation. All samples were then filtered using Sartorius cellulose acetate filters (0.2 µm). Filters were placed in scintillation vials with 5 mL of scintillation fluid (Filter Count). Radioactivity of the samples was determined using a Packard Tri-Carb scintillation counter. Counts per minute (CPM) were automatically converted to disintegrations per minute (DPM) using a quench curve stored in the counter. Incorporation blanks were then subtracted from the experimental tubes and the rate of incorporation of thymidine was expressed in mg C m<sup>-2</sup> d<sup>-1</sup>. We considered that 2x10<sup>18</sup> cells were produced per mol of thymidine incorporated (Moriarty et al. 1985) and that one cell of 0.1 µm<sup>3</sup> contained 2.44x10<sup>-11</sup> mg C (Servais 1990).

##### **2.1.4.2. Community level physiological profiling (CLPP)**

Community level physiological profiling (CLPP) was determined using living sediments from the LABOSI-4 experiment and the Biolog EcoPlate system (Garland & Mills, 1991). Bacteria were first extracted from the sediments. Fresh sediments (2.0 g, wet weight) were placed in 5 mL of autoclaved artificial seawater (Sigma, 40 g L<sup>-1</sup>). The sediment suspension was sonicated (same protocol as above). The suspension was then centrifuged 5 min. at 180 g (4°C) to precipitate mineral particles. A volume of 150 µL of supernatant (containing bacteria) was placed in each well of an EcoPlate and the microplates were incubated 48 h at 15°C in the dark. The optical density of each well was recorded at 590 nm using a FLUOstar Optima microplate reader (BMG Labtech). The absorbance value of the least utilized substrate (among the 31 substrates) was subtracted from the absorbance value of the remaining wells (Hitzl et al., 1997; Stefanowicz, 2006). Absorbance values obtained with control and experimental microcosms were then compared to each other using the Mann-Whitney U test.

### 2.1.4.3. Fluorescein diacetate analysis (FDA)

FDA estimates the total esterase activity of microbial communities (Battin 1997). When fluorescein diacetate is cleaved by microorganisms fluorescein is released and measured by spectrophotometry. Sediments (500 mg ww) were placed in sterile 15 ml polypropylene tubes and diluted with 2750  $\mu\text{l}$  of sterile artificial seawater (Sigma salts 40 g  $\text{L}^{-1}$ ; autoclaved). Samples were then sonicated 30 seconds as explained above. A volume of 250  $\mu\text{l}$  of a FDA working solution (Sigma) in 100% acetone (analytical grade) was then added to the samples to a final concentration of 200  $\mu\text{M}$ . Control tubes were immediately inactivated with acetone 100% to a final concentration of 50% (v/v). Samples were incubated for 60 min in the dark at 15°C. Incubation was stopped with 3 ml of acetone 100%. Absorbance of the supernatant at 490 nm was then measured spectrophotometrically against a water/acetone (50% v/v) blank. A standard curve was prepared with a fluorescein disodium salt (Sigma). FDA hydrolysis was expressed per g of wet weight.

### 2.1.5. Geochemical properties of the sediment

#### 2.1.5.1. General properties of the sediment

Granulometry was determined by laser analysis and the specific area of the sediments was determined by nitrogen adsorption and the BET theory. Acid Volatile Sulfides (AVS) and Chromium Reducible Sulfur (CRS) have been determined in the sediments because they are closely linked to the behaviour of heavy metals. AVS are mainly amorphous FeS, but also crystallized iron sulfides precipitates, mostly  $\text{Fe}_3\text{S}_4$  (greigite) and  $\text{FeS}_{1-x}$  (mackinawite). Other metal sulfides such as PbS, CdS and ZnS are also included in the AVS but generally at significant lower amount. CRS are mainly composed of elemental S and  $\text{FeS}_2$  (pyrite). The sequential extraction of AVS and CRS has been previously described in detail and reviewed elsewhere (Canfield et al. 1986, Billon et al. 2001). Dilute HCl-extractable metals (SEM - Simultaneously Extracted Metals) have also been obtained as they reveal the easily exchangeable metals (Gillan et al. 2005). A solution of HCl (1M) was used. To determine the concentration of dissolved sulfides in the sediments with high resolution AgI DGT probes were used (see Task 1.4.2. for a description of the DGT approach). Briefly, in presence of sulfides, the white AgI compound present in the probe is replaced by a dark  $\text{Ag}_2\text{S}$  precipitate. The colour intensity is then digitised and calibrated to achieve the concentrations initially present in the porewaters (Teasdale et al. 1999). For pigment analyses, sediment samples were extracted in acetone using sonication. Pigments were analyzed using HPLC with standard protocols (cf. Wright et al. 1991). Chlorophyll a concentrations ( $\mu\text{g g}^{-1}$  DW) were determined.

### 2.1.5.2. DET/DGT analysis

In this study, high-resolution vertical profiles of metals in sediment porewaters were obtained by the DET (Diffusive Equilibrium in Thin films) and the DGT (Diffusive Gradients in Thin films) approaches (Davison et al. 1991; Davison & Zhang 1994; Fones et al. 2004; Gao et al. 2006; Zhang et al. 2002; Leermakers et al. 2005). Porewaters were also analysed by conventional sampling (centrifugation technique).

For the DET approach the preparation procedure was similar to that of Docekalova et al. (2002). A gel containing 1.5% agarose was prepared by dissolving it in an appropriate volume of 80°C warm Milli-Q water. The mixture was placed in a boiling water bath, covered and gently stirred until all the agarose was dissolved and the solution was immediately pipetted into a preheated gel-casting probe and left to cool down to its gelling temperature (36°C or below). The constrained DET probe's material was obtained from DGT Research Ltd. The size of the DET probes was 180 mm \* 40 mm, with a window of 150 mm \* 18 mm open to the aquatic system. After the gels were set, they were covered with a 0.45 µm cellulose acetate filter (Millipore). Finally the window plate was put on top of the probe and all the elements gently pressed together.

For the DGT technique, diffusive and resin gels were prepared as described by DGT Research Ltd ([www.dgtresearch.com](http://www.dgtresearch.com)). The probes were 180 mm\*40 mm in size, with a window of 150 mm\*18 mm open to the aquatic system. The resin gel was covered by diffusive gel (polyacrylamide) and a 0.45 µm pore size cellulose acetate filter. The front window plate gently pressed the various layers together.

Before deployment, the entire gel assemblies (DET and DGT) were de-oxygenated by immersing them for 24 hours in a container filled with 0.40 M NaCl trace metal free solution and by bubbling with nitrogen. A pair of DET and DGT probes, arranged back to back, was inserted vertically into one core. The water-sediment interface was marked when the probes were retrieved from the sediment core. In the laboratory, all manipulations of the gels were carried out in a laminar flow hood located in a clean room. The DET gels (typically 20 µl) were transferred into pre-weighed 2 ml tubes, weighed and eluted in 1 ml 1 N HNO<sub>3</sub>. They were generally not further diluted for analysis. The DGT probes were opened, the filter and diffusive gel were removed and the resin gel was cut into 5 mm intervals using a Plexiglas gel cutter. Each gel slice was eluted in 1 ml 1 N HNO<sub>3</sub> for 24 hours (elution factors of 0.8) and further diluted to 10 ml for analysis by Inductively Coupled Mass Spectrometry (ICPMS).

Blank DET and DGT probes went together with the sample probes through all previous described steps including casting, probe construction, and deoxygenation except for the last step, the deployment. After the deployment, blank and sample probes were again treated in the same way. The resin gel of DGT was sliced into 32 intervals of 5 mm; 10 slices were randomly chosen for analysis. For the DET probe 10 out of 75 blank slices were randomly chosen for analysis.

Conventional sampling and centrifugation. In addition to the DET/DGT approaches, porewaters were also analysed using a conventional approach. All handling, including sample sectioning and filtration, was carried out inside a nitrogen flushed glove-bag. The sediment samples collected with conventional presectioned core samplers were cut after removing each time the plastic cover, and split into two parts: one part was put in the centrifuge vessels and another small part about

2 grams was kept inside a small container used for AVS analysis (USTL, Lille). The samples were then all sealed in order to prevent oxidation. The samples in the centrifuge vessels were centrifuged for 30 minutes at 2500 rpm. To eliminate residual small size particles, the obtained pore waters were further filtered through a 0.45  $\mu\text{m}$  cellulose acetate disposable filter, collected in a clean polyethylene tube and acidified with 1%  $\text{HNO}_3$ . HR-ICPMS (Thermo Finnigan Element II) was then used to determine the concentrations of metals and major elements.

### 2.1.5.3. Dissolved organic carbon (DOC) in porewaters

Sediments were centrifuged and the porewater was collected using a baked ( $450^\circ\text{C}$ ) glass syringe. The porewater was then filtered using baked Whatman GF/F glass fiber filters. Porewaters were preserved with phosphoric acid (5  $\mu\text{L}$  of  $\text{H}_3\text{PO}_4$  per mL of sample) and stored at  $4^\circ\text{C}$ . All glassware receiving the samples was treated at  $500^\circ\text{C}$  for 4 hours. Before analysis samples were diluted 9 times with MilliQ water. DOC concentrations were measured by a total organic carbon analyzer Dohrman Apollo 9000 in which inorganic carbon is eliminated by bubbling in the presence of phosphoric acid and organic carbon is oxidized at high temperature ( $680^\circ\text{C}$ ); the produced  $\text{CO}_2$  is then detected by non-dispersive infra-red (NDIR) analysis. The instrument response was calibrated by the method of standard additions.

### 2.1.6. Laboratory simulation approaches

Five laboratory simulation experiments (LABOSI 1–5) have been conducted using sediments of station 130. These experiments used a static setup, i.e. sediments incubated in the laboratory with stagnating seawater at the surface. The stagnating seawater is then enriched (or not) with phytodetritus and sediments are followed over time. The phytodetritus are composed of algae which are naturally present on the BCZ and are dominant members of the phytoplankton at certain periods such as *Phaeocystis globosa* and diatoms (Rousseau et al. 2002). These algae were cultivated in medium F20 which contains natural seawater as *Phaeocystis* cultured in artificial seawater does not form colonies. Medium F20 (1 liter) is composed of 990 mL of natural seawater and 10 mL of medium F2. Medium F2 (100 mL) is composed of 70 mL of distilled water, 10 mL of  $\text{KNO}_3$  (50 mM), 10 mL  $\text{NH}_4\text{Cl}$  (25 mM), 5 mL  $\text{NaH}_2\text{PO}_4 \cdot 2\text{H}_2\text{O}$  (10 mM), 5 mL  $\text{Na}_2\text{SiO}_3 \cdot 9\text{H}_2\text{O}$  (10 mM), 0.25 mL of trace elements 1, 0.25 mL of trace elements 2 and 0.25 mL of vitamins. Trace elements 1 & 2 as well as the vitamin solution are given in Veldhuis & Admiraal (1987). All solutions were autoclaved except the vitamin solution which was filtered. The natural seawater used was sampled on the BCZ and was filtered through 0.2  $\mu\text{m}$  Sartorius membrane and autoclaved for 20 min at  $121^\circ\text{C}$  before use. Cultures were performed at  $9\text{--}10^\circ\text{C}$  with an irradiance of  $100 \mu\text{E m}^{-2} \text{s}^{-1}$  and a gentle agitation of the culture flasks.

LABOSI-1. This experiment was designed to test the laboratory experimental setup and particularly to test the reestablishment of the biological and geochemical gradients after homogenization of the sediments. The experiment was conducted from the 12th to the 21st November 2008 at the ULB. Sediments (height: 10 cm)

were gently hand-mixed and placed in 3 large containers. Sediments were incubated in darkness at 11°C for 7 days. Various parameters were followed (Eh, pH, O<sub>2</sub>, salinity, sulfides, trace metals, DAPI counts, DGGE).

LABOSI-2. This experiment was designed to test the effect of an early spring diatom bloom on the sediments. A mix of 3 diatom species was used (*Skeletonema sp.*, 80%; *Thalassiosira sp.*, 10%; *Chaetoceros sp.*, 10%). The culture was prepared at the ESA lab of the ULB. Diatoms were rinsed with seawater and placed on top of the sediments. This corresponded to 336.8 µg L<sup>-1</sup> of chlorophyll *a* or 0.39 µg cm<sup>-2</sup>. The height of overlying water was 4 cm. The experiment was conducted from the 19th February 2009 to the 5th March 2009 at the ULB. Sediments (height : 7 cm) were not mixed (the stratification was maintained). Sediments were incubated in darkness at 4°C for 14 days. The same parameters were followed (Eh, pH, O<sub>2</sub>, salinity, sulfides, trace metals, DAPI counts, DGGE) in addition to chlorophyll *a* and DOC.

LABOSI-3. This experiment was designed to test the effect of a late spring *Phaeocystis* bloom on the sediments. A pure culture of *Phaeocystis globosa* was prepared at the ESA lab of the ULB. The culture (15 000 colonies L<sup>-1</sup>) was not rinsed with seawater in order to maintain the structure of the *Phaeocystis* colonies. A volume of 563 ml of culture (i.e., ± 3 cm for each microcosm) was placed on top of the sediments. Controls included microcosms with only seawater and microcosms only with culture medium (without *Phaeocystis*). The microcosms exposed to *Phaeocystis* received a biomass evaluated at 0.225 mg of carbon per liter (i.e., 0.127 mg per microcosm). The experiment was conducted from the 15th June 2009 to the 22th June 2009 at the ULB. Sediments (height: 7 cm) were not mixed (the stratification was maintained). Sediments were incubated in darkness at 15°C for 7 days. The same parameters were followed (Eh, pH, O<sub>2</sub>, salinity, sulfides, trace metals, DAPI counts, DGGE) in addition to chlorophyll *a* and DOC.

LABOSI-4. This experiment was designed to test the effect of two types of phytodetritus at the same time on sediments from station 130. The experiment was conducted from the 29th March 2010 to the 5th May 2010 at the ULB. Sediments (height ± 7 cm) were not mixed (the stratification was maintained). Two 20 liters cultures of unicellular algae were prepared : *Phaeocystis globosa* and *Skeletonema costatum* (an early spring diatom). Inocula were obtained from the ESA Lab, ULB, Brussels. After a few days of development, cultures were decanted and centrifuged. Cell pellets were kept at -20°C until the start of the experiment. At the start of the experiment (Day-0) cell pellets were thawed and combined in 8 liters of natural seawater. This algal suspension was then immediately used for the microcosm experiment. The proportion of the two algae in the algal suspension was 50:50 (w/w), the total chlorophyll *a* content was 750 ± 35 µg L<sup>-1</sup> (mean ± SD), and the salinity was 30‰. The biomass of the algal suspension was 130.6 mg L<sup>-1</sup> (dry weight, measured after centrifugation and lyophilisation of three 50 ml samples). Metal concentrations of the algal biomass were as follows (in µg g<sup>-1</sup> dry weight): Cd, 0.53; Pb 38.6; Cr, 5.1; Mn, 64.5; Fe, 7533; Co, 0.54; Ni, 5.1; Cu, 246; Zn, 381; As, 4.4. Dissolved metal concentrations of the algal suspension (after filtration on 0.45 µm) were as follows (values in µg L<sup>-1</sup>): Cd, 0.71; Pb, 0.26; Cr, 0.94; Mn, 12.4; Fe, 6.9; Co, 0.28; Ni, 2.1; Cu, 9.9; Zn, 12.0; As, 2.8).

The experimental design used for LABOSI-4 featured a total of 18 large microcosms (15 cm  $\varnothing$ ). These microcosms were used to test two conditions (algal exposition & unexposed controls) at three different sampling points (Day-0, Day-2, Day-7) with three replicates. For the DET-DGT measurements (see below) 6 small cores were used (6.5 cm  $\varnothing$ ). At the start of the experiment the overlying seawater was slowly removed from all the microcosms and cores without disturbing the sediment-seawater interface. A volume of 710 mL of algal suspension was then slowly deposited on half of the microcosms, the other half receiving 710 mL of natural seawater (controls). The small cores received 132 mL of algal suspension (3 experimental cores) or 132 mL of seawater (3 control cores). The height of the overlying seawater in all microcosms and cores was 4 cm. After two hours of sedimentation 6 microcosms (3 experimental and 3 controls) and two small cores (1 experimental & 1 control) were used for the Day-0 analyses (Day-0-2h). These analyses include microbial and geochemical parameters (see below). After two days (Day-2) and 7 days (Day-7) the same analyses were repeated. Salinity variations due to evaporation were avoided by regular MilliQ additions and monitoring by a salinometer. The temperature of the water was maintained at  $15.0 \pm 1^\circ\text{C}$  during all the experiment. This temperature was chosen because (i) previous experiments suggested a very low bacterial activity at lower temperatures (data not shown), and (ii) such a temperature is reached at the end of spring and even exceeded during the summer period, which are periods of intense biological activity (Hondeveld et al. 1994).

In parallel to the LABOSI-2-4 experiments sediments were also incubated in large plexiglass cores (9 cm inner  $\varnothing$ , 10 cm of height) at the Geosystems Laboratory of the USTL and the ANCH laboratory of the VUB. These sediments were sampled at the same moment and were exposed to the same phytoplankton cultures (i.e., diatoms and *Phaeocystis*) for exactly the same time and at the same temperature. These 9 cm  $\varnothing$  cores were used to monitor metal fluxes, alkalinity and  $\text{O}_2$  levels during the incubations.

**LABOSI-5.** The LABOSI-5 experiment was designed to test the effect of arsenic on benthic microbial communities from 2 different sediment types. Sediment samples were collected on 12<sup>th</sup> May 2010, from the subtidal stations 130 and 230. Only the top sediments (first cm) were sampled, and three replicate samples were collected at both sites. Microcosms consisted of 50 ml falcon tubes, containing 5 g of sediment and 25 ml of filtered seawater. A total of 36 microcosms were prepared, and used to test for the effect of treatment (6 different levels of arsenic contamination) and station (with different sediment composition and contamination history) on microbial communities; all doses for both stations were tested in triplicate (n=3).

A  $1\text{g L}^{-1}$  (filtered seawater) stock solution of an arsenic-salt ( $\text{KH}_2\text{AsO}_4$ ) was prepared, and used to make a dilution series of 0 (control), 60, 120, 240, 480 and  $960\ \mu\text{g L}^{-1}$  of As (final concentration in microcosms). The arsenic stock-solution was added to the falcon tubes by pipetting into the water column in the correct concentration, and falcon tubes were stirred gently to evenly distribute the toxicant. Falcon tubes were incubated at  $15^\circ\text{C}$  and in the dark, for 46-48h. After this incubation period, water was removed by decantation and pipetting, and 0.5 g of sediment was brought into a 2 ml sterile eppendorf, immediately frozen on dry ice and stored at  $-80^\circ\text{C}$  until RNA extraction (see 2.1.2.1).

The stations used for this experiment were chosen on the basis of previous research and the results of phase I of the MICROMET project. Station 130 is located near the Zeebrugge harbor outlet, and high metal contamination levels have been measured, including arsenic (Gillan & Pernet 2007; results phase I). Station 230 is situated more offshore and contains low(er) amounts of heavy metals (results phase I). Due to the different contamination history, we expect differences in arsenic tolerance between the microbial communities of these sediments.

### 2.1.7. Data analysis

Microbial diversity, composition and biomass data were analyzed and related to the measured geochemical variables using standard correlation and (multiple) regression statistical analyses. DGGE gels were digitized and analyzed using Bionumerics 1.5 (Applied Maths BVBA, Kortrijk, Belgium) and Quantity One v. 4.2 (Bio Rad). The DGGE data on microbial community structure were analysed using multivariate statistical tools using Statistica 7.0, PRIMER 6 (Clarke & Gorley 2006) with the PERMANOVA+ add-on (Anderson et al 2008) and the Canoco 4.5 software package. A toxicity index (TI) was calculated for the simultaneously Extracted Metals (Di Toro et al. 1992):  $TI = [Cd + Co + Cu + Ni + Pb + Zn]_{SEM} / [S]_{AVS}$ . In this formula, all concentrations are expressed in  $\mu\text{mol kg}^{-1}$ . Biodiversity (i.e., the Shannon index) was calculated as described in Gillan (2004).

Two different approaches were used to estimate dissolved metal fluxes at the SWI during the LABOSI experiments. The first one was based on the estimation of the concentration gradient at the interface. It is an indirect method, which uses the first Fick's law, as follows :

$$J = \varphi \cdot D_s \cdot (dC/dz)_{z=0}$$

where  $\varphi$  is the porosity of the interface and  $D_s$  the diffusive coefficient of the metal species. As  $D_s = D_m / \theta^2$  (with  $D_m$  being the molecular diffusive coefficient, and  $\theta$  the tortuosity of the interface), a flux, called diffusive flux, can be calculated. The knowledge of the interface properties is not so straightforward, particularly because of the presence of a biofilm with unknown diffusive characteristics. As a result, diffusive fluxes have not been calculated but the concentration profiles of the metals observed in the sediments have given some information on the direction of the diffusive fluxes.

The second approach of flux measurement was a direct method. It was used in the LABOSI-4 experiment. It consisted in the evaluation of the concentration change in the overlying seawater, assuming that the observed change was the result of a metal release from the sediments (or a metal consumption in the sediments). This flux, called benthic flux, takes into account all types of exchanges of dissolved species at the interface including bioturbation. Dissolved metal concentrations in the overlying waters after 2 and 7 days of exposure were first measured by HR-ICP-MS (concentrations at Day-0 were subtracted from those at Day-2, and concentrations at Day-2 were subtracted from those at Day-7, respectively). The volume of the overlying water was 710 mL (V) and the surface area (A) of the microcosms was 0.0176 m<sup>2</sup>. The efflux was calculated as  $F = C \times V / (A \times T)$ . Effluxes were expressed in mol m<sup>-2</sup> d<sup>-1</sup>.

### 2.1.8. Numerical modelling

Chemical equilibrium calculations have been carried out with data from LABOSI-4 experiments, mostly by using the software Visual MINTEQ version 3.0 beta. This software has been developed by Jon Petter Gustafsson, and can be downloaded as a freeware from the following website: <http://www2.lwr.kth.se/English/OurSoftware/vminteq/download.html>. It is a Windows version of the MINTEQA2 version 4.0 which was previously developed by USEPA (United States Environmental Protection Agency) in 1998 (USEPA 1998). The software was mainly used to predict the speciation of the principal elements in the liquid phase, including some trace metals, and to check the saturation index (SI) of several precipitates. SI is defined as follows:

$$SI = \log \left( \frac{IAP}{K_{sp}} \right)$$

*IAP* is the ionic activity product and  $K_{sp}$  is the solubility product constant of the studied precipitate. If  $SI < 0$ , the precipitate should not exist in the medium and an undersaturated state occurs, whereas if  $SI \geq 0$ , the precipitate should be generated with the possibility of an (over)saturation state.

For computational calculations, the MinteqA2 database updated from the NIST Data was used in the present work. The existence of metal/organic-matter complexation models, such as NICA-Donnan and Stockholm Humic model (SHM) (Tipping & Hurley 1992; Benedetti et al. 1996) has allowed us to examine interactions between dissolved organic matter and metals in the liquid phase, particularly by treating data using the NICA-Donnan sub-model, which supposes a bimodal and continuous distribution of site affinities (Benedetti et al. 1995). To include organic matter, the NICA-Donnan model was used and organic matter was added in the form of DOC concentrations, using the parameters by default, assuming that 70% of the DOC is composed of fulvic acid, having a C content of 50% (this mean a ratio of DOM to DOC ratio of 1.4) (help file in Visual Minteq software version 3.0 beta). We are aware that the values (present in the database we used) relative to the metal complexation by humic substances only permit to get a first approach of the role played by the natural organic matter on the metal speciation, but to our best knowledge, no more adapted organic model exist in the literature.

The computational procedure was performed by taking into account the following physicochemical parameters: pH, temperature, alkalinity, DOC,  $\text{Na}^+$ ,  $\text{Ca}^{2+}$ ,  $\text{Mg}^{2+}$ ,  $\text{K}^+$ ,  $\text{Al}^{3+}$ ,  $\text{Fe}^{2+}$ ,  $\text{Cu}^{2+}$ ,  $\text{Cd}^{2+}$ ,  $\text{Mn}^{2+}$ ,  $\text{Co}^{2+}$ ,  $\text{Ni}^{2+}$ ,  $\text{Zn}^{2+}$ ,  $\text{PO}_4^{3-}$ ,  $\text{NO}_3^-$ ,  $\text{Cl}^-$ ,  $\text{SO}_4^{2-}$ ,  $\text{S}^{2-}$ ,  $\text{CO}_3^{2-}$ , As(III) and As(V) oxoanions, and  $\text{Si}(\text{OH})_4$ .

From computational calculations, the output file gives the following data: (i) the concentrations and activities of all the species; (ii) the saturation index of possible authigenic minerals generated in the medium; (iii) the ionic strength; and (iv) the ionic balance or the charge difference between cations and anions. This latter was found to be better than 15% in most of the studied cases, showing that the majority of ionic species was effectively taken into account in our systems. If necessary, the ionic balance was adjusted by increasing the concentration of either  $\text{Na}^+$  or  $\text{NO}_3^-$ . These

two ions were chosen because of their weak complexation/precipitation characteristics towards metallic cations.

The principle of the computational calculation used by this thermodynamic-equilibrium software is based on an iterative process that ends only when the calculated concentrations of the different components implicated are close enough to the measured ones. Mathematically, these components are assumed to be the independent variables of the mass balance equations, whereas the generated species are considered as reaction products derived from components. The system is found to be essentially nonlinear.

Briefly, the equation of mass conservation relates the activity of each component  $j$  ( $X_j$ ) to the activity of its different species  $i$  ( $S_i$ ):

$$X_j = \sum a_{ij} S_i \quad (1)$$

where  $a_{ij}$  is the stoichiometric coefficient of the component  $j$  in the species  $i$ .

For instance, for the component  $\text{Ca}^{2+}$ , the mass conservation equation relates the total activity of this component to the activity of the different species in the following way:

$$(\text{Ca}^{2+})_t = (\text{Ca}^{2+}) + (\text{CaCl}^+) + (\text{CaSO}_4)_{\text{aq}} + (\text{CaNO}_3^+) + (\text{CaHCO}_3^+) + (\text{CaCO}_3)_{\text{aq}}$$

A second equation (mass action law) relates the equilibrium between the different components:

$$K_i = S_i \prod X_j^{-a_{ij}} \quad (2)$$

where  $K_i$  is the formation equilibrium constant of the species  $i$  and  $\prod$  is the product of all the components  $X_j$  of the species  $S_i$  affected by their stoichiometric coefficient.

As an example, regarding the formation reaction of  $(\text{CaHCO}_3^+)$ :



its equilibrium constant can be written as follows:

$$K = \frac{(\text{CaHCO}_3^+)}{(\text{Ca}^{2+})(\text{H}^+)(\text{CO}_3^{2-})} \quad (3)$$

Activities ( $S_i$ ) can be replaced by concentrations  $[S_i]$  by using equation 4:

$$S_i = \gamma_i [S_i] \quad (4)$$

where  $\gamma$  represents the activity coefficient of the species  $i$ . Equation (2) can then be transformed as follows:

$$S_i = \left( \frac{K_j}{\gamma_i} \right) \cdot \Pi \cdot X_j^{a_i} \quad (5)$$

In addition to these mass action law expressions, the independent components follow the mass balance equations according to:

$$Y_j = \sum a_{ij} [X_i] - [X_j] \quad (6)$$

Where  $[X_j]_t$  is the measured total concentration of the component j (input parameter), and  $Y_j$  represents the difference between the calculated and the experimental total concentration of the component j.

To solve this problem, the concentration of each species must be calculated from the activity of each component using equation 5. Total concentration of every component is calculated from equation 1 and compared to the input data corresponding to experimental values. If the difference between calculated and measured concentrations is not sufficiently small,  $X_j$  is re-adjusted and a new iteration is accomplished. The solution is finally obtained when the ratio corresponding to the difference between the calculated and measured concentrations on the measured one as:  $\{[X]_{\text{calculated}} - [X]_{\text{measured}}\} / [X]_{\text{measured}}$  is found to be lower than 1‰ (USEPA 1998).

## 2.2. Results

### 2.2.1. Field campaigns

#### 2.2.1.1. Micro-electrode analyses

Oxygen and redox profiles for the 2007 sampling campaigns are shown in Figs 2-3. For sandy sediments (stations 330, 435 and DCG), no significant decreases in dissolved oxygen were measured within the upper cm, indicating either a poor bacterial activity or a quick resupply of oxygen because of the high porosity of the sediment (Fig. 2, 330 and DCG not shown). For the other, muddier stations, the drop of the oxygen concentrations is sharp, immediately below the water-sediment interface. In these sediments, oxygen is completely consumed in the upper 2-4 mm (Figure 2).

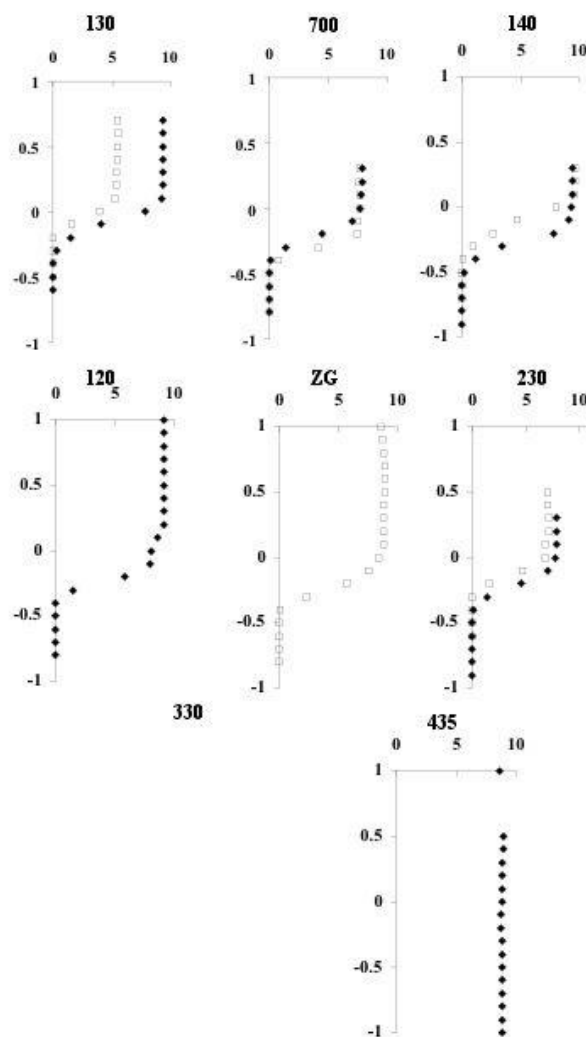


Figure 2. Oxygen profiles ( $\text{mg L}^{-1}$ ) in 7 stations in function of depth (cm).  $\blacklozenge$ : February 2007;  $\square$ : July 2007.

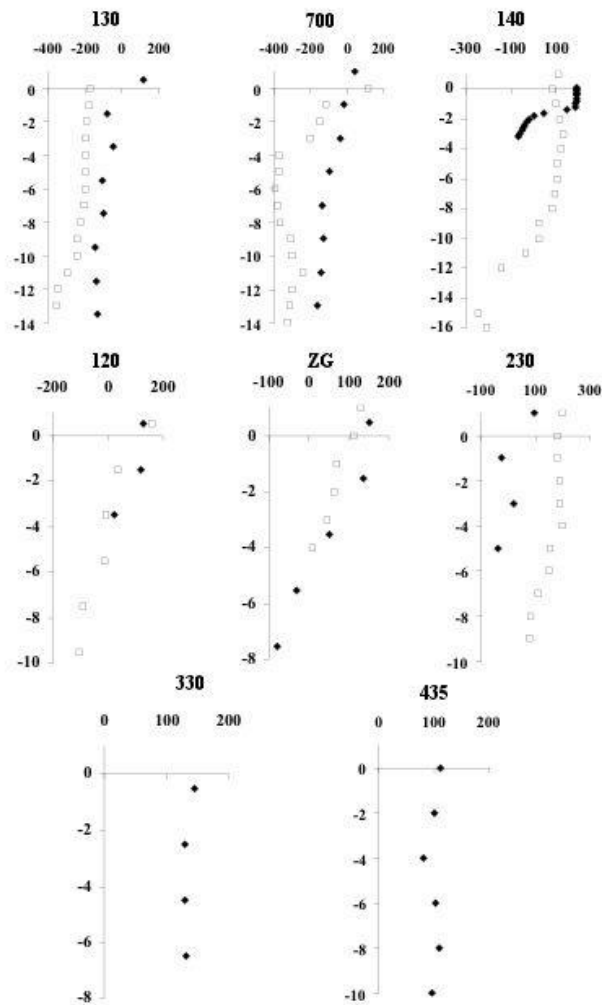


Figure 3. Eh profiles (mV) in 8 stations function of depth (cm). ◆ : February 2007; □ : July 2007.

For the two muddy stations sampled in 2008 (130 and 700, not shown), we also noticed that oxygen decreased sharply at the WSI down to 0 at around 2-3 mm. Oxygen concentrations just above the interface are usually lower in summer than in winter, which could be explained by higher bacterial activity during the warmest periods.

Redox potential profiles are displayed in Figure 3 and corroborate the differences between sandy (330, 435, DCG) and muddy sediments (130, 140, 700). Oxic conditions remained stable in function of depth in the sandy stations with redox potential values higher than 100 mV (vs reference electrode). In contrast, a drop of 200 mV occurs in the 2-4 cm of the muddy sediments (stations 130 and 700), indicating that other oxidants (than O<sub>2</sub>) are thereby consumed by microorganisms. For the other stations (especially stations 120, 140 and ZG03), the evolution of the redox potential is more slow, suggesting lower microbial activities. Measurements of pH profiles give information on early diagenetic processes since degradation of organic matter produces alkalinity but also hydronium ions. Our data (not shown here) show a distinct drop of  $\pm 0.5$  pH units in the muddy stations between the interface and -10 cm (stations 130 and 700), down to pH 6.9. In sandy sediments

(DCG, 435 & 330), most of the pH values remain higher than 8, while in station 120, 140 and ZG03, values are between 7.1 and 8.5.

In 2008, Eh and pH values were recorded every month in stations 130 & 700. Values of pH did not indicate any clear seasonal trend. A decrease of  $\pm 0.5$ -1.0 pH unit generally occurred at the interface and pH stabilized between 7.0 and 7.5 below 2 cm of depth. Strongly reduced sediments have been observed each time through Eh measurements. Eh values (given vs the Ag/AgCl reference electrode) were always negative below 1-2 cm depth and could reach -400 mV at -10 cm depth. We may conclude that sulphide compounds (and especially AVS, which are very sensitive to oxygen and that are known to trap several metallic pollutants), will never easily oxidize whatever the season (unless sediments are physically remobilized).

### 2.2.1.2. Determination of the microbial diversity

#### DGGE of Bacteria.

In 2007, the total number of DGGE bands (i.e., diversity or band richness) observed for 500 mg (ww) of sediments varied between 6 and 27 (TABLE 1). For the surface sediments (0-1 cm) in February, bacterial biodiversity values were significantly higher in sandy stations 120/DCG than in coastal station 700; in July, it was significantly higher in stations 130/DCG than in station 120. For the 9-10 cm layer of the sediments in February, biodiversity was significantly higher in station DCG than in stations 330/140; in July, it was at the same level in all the stations (TABLE 1). Significant seasonal differences were observed between February and July : for the 0-1 cm sediments, diversity increased in stations 130/700 and decreased in stations 120/230; for the 9-10 cm sediments diversity increased in station 330 (Table 1).

TABLE 1. Number of DGGE bands (range; n=4) observed in marine sediments of 9 stations on the BCP in February 2007 (FEB) and July (JUL) 2007. Two sediment sections were considered (0-1 cm and 9-10 cm). Values in boldface refer to significant seasonal differences, within the same station and sediment layer (Mann Whitney U-test,  $P < 0.05$ ). Letters (a, b) refer to comparisons between stations (within one sediment layer); stations are not significantly different if at least one letter is shared (Dunn's test,  $P < 0.05$ ).

|             | 120              | 130              | 140        | 230               | 330              | 435        | 700               | DCG       | ZG03       |
|-------------|------------------|------------------|------------|-------------------|------------------|------------|-------------------|-----------|------------|
| FEB 0-1 cm  | <b>20 - 27</b> a | <b>9 - 19</b> ab | 13 - 17 ab | <b>17 - 19</b> ab | 15 - 15 ab       | 18 - 21 ab | <b>7 - 13</b> b   | 22 - 23 a | 16 - 19 ab |
| FEB 9-10 cm | 14 - 20 ab       | 16 - 18 ab       | 10 - 12 b  | 12 - 14 ab        | <b>10 - 13</b> b | 16 - 19 ab | 11 - 15 ab        | 20 - 22 a | 15 - 18 ab |
| JUL 0-1 cm  | <b>10 - 13</b> b | <b>20 - 21</b> a | 14 - 14 ab | <b>11 - 16</b> ab | 15 - 19 ab       | 17 - 21 ab | <b>14 - 14</b> ab | 19 - 22 a | 11 - 17 ab |
| JUL 9-10 cm | 10 - 16 a        | 17 - 22 a        | 15 - 18 a  | 6 - 15 a          | <b>13 - 18</b> a | 17 - 21 a  | 12 - 14 a         | 16 - 21 a | 15 - 21 a  |

In 2008, vertical profiles of DGGE taxon richness were obtained for stations 130 and 700. About 15 band positions were followed each month in both stations between 0 and 10 cm. An example of a profile, (DGGE band 2/2) is shown in Figure 4. In that figure, it can be seen that reproducibility is good and that the relative intensity of the band varies with sediment depth, with a peak in the 8-9 cm section of the sediments. Some of these DGGE profiles were positively or negatively correlated to environmental parameters (see below).

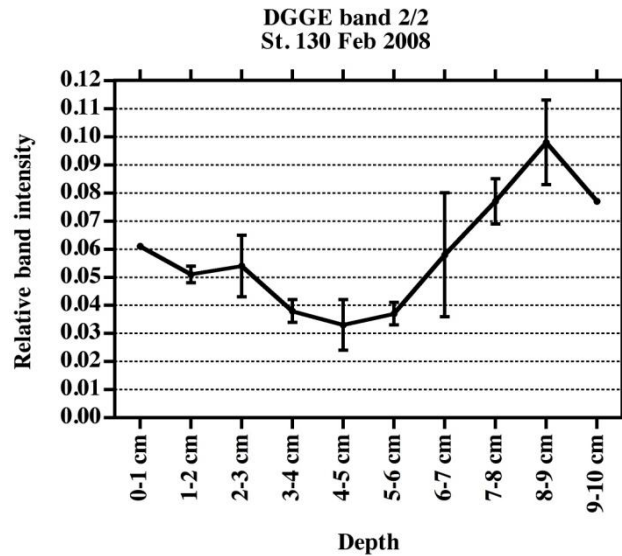


Figure 4. Relative DGGE band intensity according to depth for band 2/2 in February 2008 (station 130); n=2.

### DGGE of Archaea.

On the basis of the 16S rRNA sequences obtained in the cloning approach the existing PCR primers for studying archaeal communities by DGGE were first adapted to the BCP communities. The adapted primers (ARC-349-F and ARC-853-R) are homologous to primers S-D-Arch-0344-a-S-20 and 907r (Wilms et al. 2006), but contrary to them they amplify the rDNA genes from both Euryarchaeota and Crenarchaeota of the BCP (the two major groups of Archaea). A 40 bp GC-clamp was attached to the 5' end of primer ARC-349-F. These new primers amplify a 544 bp region of the archaeal 16S rRNA gene over the V3 and V5 regions (bp 330-874, *Methanococcus jannaschii* M59126 numbering).

As the quantity of archaeal DNA in the BCP sediments was very low, a nested PCR approach was used with a first amplification of the complete 16S rDNA with primers ARC21F and U1492R (Gillan & Danis 2007) followed by a nested PCR with primers ARC-349-F-GC-clamp and ARC-853-R. This approach was tested in stations 700 and DCG (sediments of February 2007). No PCR amplifications were observed in station 700, which can be explained by the very low levels of Archaea in that station (various PCR conditions were tested). On the contrary, PCR amplifications were successful in station DCG and the DGGE profiles featured only one band. The diversity of Archaea is probably very low in that station. No PCR amplifications have been obtained in the other stations. This might be due to the absence, or very low numbers, of Archaea on the BCP.

## DGGE of microeukaryotes

DGGE profiling of the samples has been completed using the Van Hannen (1998) primer set. For 2007, the DGGE analyses revealed a surprisingly high number of eukaryotic phylotypes (DGGE bands), with values ranging between  $\pm 20 - 50$  bands per sample (data not shown). There were no clear trends in total diversity between stations, depths or seasons.

In order to get an idea of the identity of these bands, a total of 404 bands was excised, of which 114 have been sequenced. BLAST analyses and alignments revealed 54 unique sequences for 2007 (submitted in GenBank under accession numbers HQ830499-HQ830554). As we had to use general eukaryote primers for the DGGE analyses, we inevitably also picked up numerous sequences belonging to Metazoa and Fungi. The results below however only focus on the micro-eukaryotes. Nineteen sequences showed 100% homology to those of named identified eukaryotic organisms, mostly metazoans and diatoms. Other sequences often most closely matched uncultured organisms, which confirms that marine benthic protists are still understudied. Three phylogenetic groups accounted for 63% of the total sequences (TABLE 2): Stramenopiles (mainly diatoms), Metazoa and Fungi. Surprisingly, diatom bands were recovered from the top (0-1 cm) but also from the deeper (9-10 cm) anoxic sediment layers (not shown). Protozoan sequences (Cercozoa, Foraminifera and other Rhizaria, and Amoebozoa) accounted for only 13% of all retrieved sequences. Sequences matching with Chlorophyta, Marine Alveolates Group II and Dinophyceae were also found. One sequence could not be assigned to any known eukaryotic group ('uncultured') and five sequences gave ambiguous BLAST results ('various'); these groups may comprise further protozoan diversity.

TABLE 2. Phylogenetic affiliation of DGGE bands of micro-eukaryotes (primers Van Hannen 1998) for 2007 (54 seq) and 2008 (44 seq).

|                            | 2007      |      | 2008      |      |
|----------------------------|-----------|------|-----------|------|
|                            | Nb        | %    | Nb        | %    |
| Stramenopila               | 17        | 31,5 | 14        | 31,8 |
| Alveolata                  | 0         | 0,0  | 1         | 2,3  |
| Dinophyceae                | 2         | 3,7  | 4         | 9,1  |
| Marine Alveolates GROUP II | 2         | 3,7  | 0         | 0,0  |
| Amoebozoa                  | 1         | 1,9  | 1         | 2,3  |
| ciliates                   | 0         | 0,0  | 3         | 6,8  |
| Cercozoa                   | 3         | 5,6  | 7         | 15,9 |
| Acantharea                 | 1         | 1,9  | 2         | 4,5  |
| Foraminifera               | 2         | 3,7  | 2         | 4,5  |
| Chlorophyta                | 2         | 3,7  | 2         | 4,5  |
| Fungi                      | 7         | 13,0 | 3         | 6,8  |
| Metazoa                    | 10        | 18,5 | 5         | 11,4 |
| various eukaryote          | 6         | 11,1 | 0         | 0,0  |
| uncultured eukaryote       | 1         | 1,9  | 0         | 0,0  |
|                            | <b>54</b> |      | <b>44</b> |      |

For the two silty stations sampled in 2008 (130 and 700), DGGE analyses again revealed a high eukaryotic species richness (between 35 and 70 bands per sample). As we can see in the depth profiles (Figure 5) which shows the Shannon index for both stations during the whole sampling period (February-July), an increase in species richness was detected from May-June onwards for station 700, while for station 130 species richness was highest in February, decreased in March and increased again slightly in May-June.

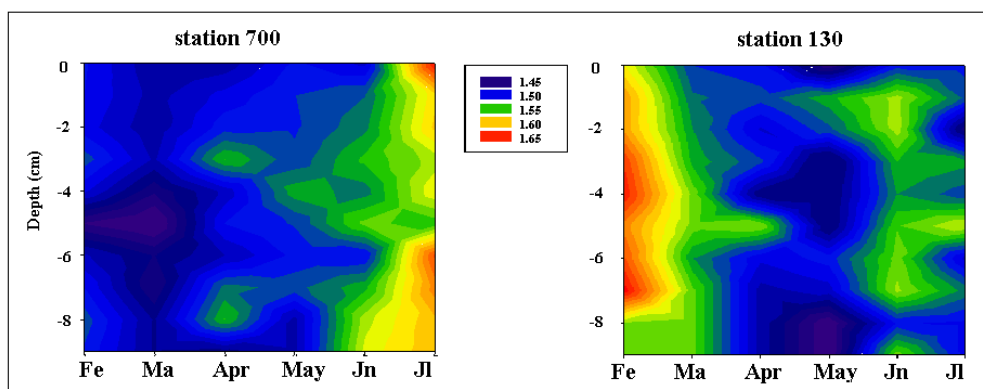


Figure 5. Depth-seasonal representation of Shannon index for microeukaryotic species richness in station 130 and 700 (2008).

For 2008, 240 bands have been excised, of which so far 77 have been sequenced. BLAST analyses and alignments revealed 44 unique sequences. Stramenopila (mainly diatoms), Metazoa (Nematoda, Nemertea, Gastrotricha) and Fungi again accounted for most (50%) of these sequences. Protozoan sequences (Alveolata, Ciliata, Cercozoa, Foraminifera, Acantharea and Amoebozoa) were relatively more abundant (36%) than in 2007. In addition sequences matching Dinophyceae and Chlorophyta were found (TABLE 2). Some of the sequences (13) found in 2008, corresponded with those found in 2007.

The predominance of DGGE bands affiliating with diatoms in the dark subtidal sediments is surprising, especially in the 2007 samples, since the sediments were anoxic and aphotic. The molecular data however are confirmed by microscopic analyses (not shown) which reveal the presence of live diatom cells in almost all samples.

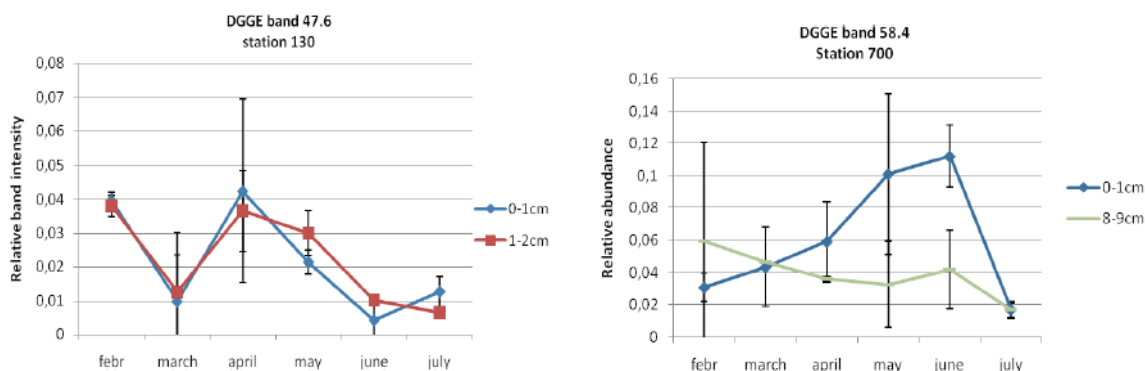


Figure 6. Relative band intensities of a Ciliate (DGGE band 47.6-left) and a Cercozoa (DGGE band 58.4-right) according to months for 2 sediment horizons in station 130 (left) and station 700 (right). N=2;  $\pm$ stdev.

Distinct changes in seasonal and depth distribution have been detected for the relative abundance of selected phylotypes (see e.g. Figure 6). An example of a profile of a ciliate (*Acineta* sp-DGGE band 47.6) is given for two depths (0-1 cm and 1-2 cm) for station 130 and of a cercozoan species (*Protaspis* sp – DGGE band 58.4) for two depths for station 700. The relative abundance of *Protaspis* increases from February onwards with a peak in June in the top sediment layer, while a decrease is seen in a deeper layer (8-9 cm). The June peak in the top layer is also present in station 130 (not shown) and could be related to an increase in organic matter deposition (< algal blooms) in early summer.

In addition to the DGGE analyses with the Van Hannen primers, we also tested the Diez et al. (2001) DGGE primer set. These primers amplify a larger DNA fragment and thus contain more phylogenetic information. After fine-tuning of the protocol, preliminary DGGE runs revealed a molecular diversity which is even higher than the one observed with the Van Hannen primers. The high amount of band classes however made both band excision and alignment problematic. For our analyses we therefore opted for a combination of DGGE using the Van Hannen primer set combined with a clone library approach.

To exclude the possibility that the diversity of certain important protozoan groups is underestimated due to the predominance of diatom DNA in the samples (or PCR bias for this DNA) (cf. Shimeta et al. 2007), we also developed and tested a nested PCR – DGGE approach for three primer-sets which are specific for important benthic protozoan groups, viz. ciliates, Cercozoa and Kinetoplastida. The primers were tested on 16 samples from 4 stations (435, ZG, 130 and 700, both February and July). About 40 bands of each DGGE were excised, of which so far respectively 11 'ciliate', 14 'kinetoplastid' and 8 'cercozoan' bands have been sequenced and analyzed using BLAST. The Cercozoa-specific primers proved to be 100% Cercozoa-specific, whereas ciliate- and kinetoplastida-specific primers revealed a majority of sequences belonging to various other groups of microbial eukaryotes (Stramenopila, Fungi, Dinophyceae, etc.). A possible explanation is that PCR conditions are not optimal (annealing temperature too low). Comparison of the primers with the sequences showed that one to two mismatches could be found between the 'aspecific' sequences and the primers. Due to this aspecific amplification we did not further use the group-specific DGGE approach. The group-specific primers sets were however used for construction of the clone libraries (see below).

A PCO ordination analysis of the fully aligned micro-eukaryote DGGE data set of 2007 is shown in Figure 7A; only environmental variables that correlated significantly with the first of second axis and with a correlation coefficient > 0.5 are shown in the diagram as supplementary (passive) variables (Primer 6; Clarke & Gorley 2006). Along the first, most important principal component, samples are separated along a gradient of sediment composition, with silty stations on the right, sandy on the left and mixed stations taking an intermediate position (see 2.2.1.4 for more information on granulometry of the stations). Sandy stations are characterized by higher salinity (due to their more offshore position) and higher bacterial species diversity; silty stations have higher Chl a and bacterial biomass. Variation along the second axis is related to seasonality (Feb vs July). Grain size, either directly or through modification of the chemical and physical environment (including the presence of pollutants, cf. above and below) thus strongly influences eukaryotic community structure. No significant differentiation was observed between the top and bottom sediment layers.

Differences in community composition between the sediment types can be attributed to various groups (e.g. alveolates 'ALV' and Fungi 'FUNG'), but also diatoms. This may reflect the existence in the BCZ of an on-offshore gradient in phytoplankton species composition (M'Harzi, *et al.*, 1998) or species-specific mineralization and/or preservation of diatom cells in silty and sandy sediments (cf. Kristensen, *et al.*, 1995, Boon, *et al.*, 1999, Harnstrom, *et al.*, 2011). We also performed a separate PCO analysis on those samples for which DGT/DET data were available (Figure 7B). This analysis showed that silty sediments had significantly higher values for especially Mn (both DGT and DET) and DGTAs.

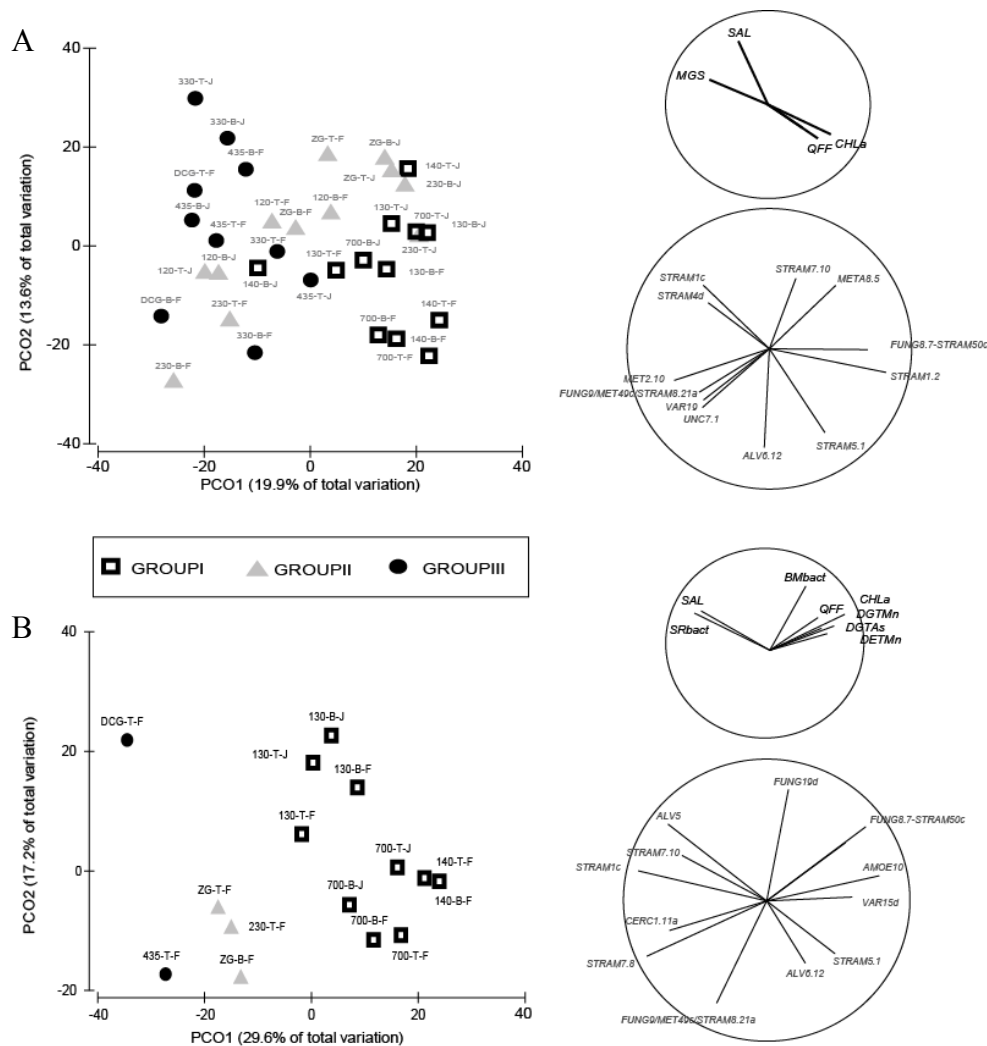


Figure 7. PCO correlation biplots of 97 eukaryotic OTUs using 34 samples (A) (DCG July is not included in the analyses as it took an outlier position), and 15 samples (B) (only those for which DET and/or DGT metal concentrations were measured). CHL *a*, chlorophyll *a*; QFF, quantity of fine fraction; BMbact, biomass bacteria; MGS, median grain size; SAL, salinity; SRbact, species richness bacteria; T, top (0-1 cm), and B (9-10 cm) sediment layer; F, February; J, July.

PCO ordinations were also performed on the fully aligned 2008 DGGE data for stations 130 and 700 (see Figure 8, only shown for station 130). The 2008 data show that within a single sediment type (silty) there are pronounced changes in eukaryotic community composition with season and depth. Microeukaryotic community composition changed with from February to July, with especially May and July being

distinct, probably related to seasonal and in-depth variation in redox potential, pH and sulphides in the sediment (Fig. 8). The latter was probably mainly related to the deposition of phytoplankton-derived detritus, evident from the high number of diatoms ('BACI') in May (and July) and the increase in chlorophyll *a* during that period (see below). Interestingly, variation partitioning showed that an independent effect of metals was observed explaining variation in microeukaryotic communities (not shown). More details about these results can be found in Pede *et al.* (in prep. b).

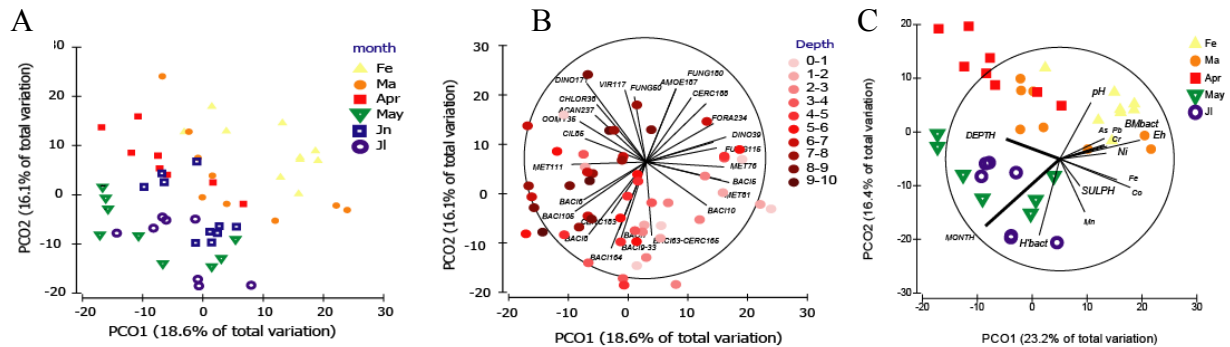


Figure 8. Principal Coordinate Analysis (PCO) based on the 2008 microeukaryote data set for station 130. A/B, for the total data set (with A showing month and B depth for the same ordination), and C, for the data set for which metal data were available (all except June). In B, only OTUs with significant ( $p < 0.05$ ) and correlation coefficients  $> 0.5$  with at least one of the axes are shown. In C, Vectors DEPTH and MONTH (in bold) are based on ordinal variables,  $0 \rightarrow 10$  cm and Julian date respectively. SULPH, dissolved sulphides;  $H'_{bact}$ , bacterial diversity; BMbact, bacterial biomass.

### SSU rRNA clone libraries and sequencing of Bacteria

In 2007, eight DNA libraries were obtained (4 stations, 2 sediment horizons). The stations were DCG, 435, 700 & 130. The universal primers 8F and 1492R were used. A total of 288 sequences of about 600 bp were obtained (TABLE 3). Sequences were identified using BLAST. As shown in TABLE 3, the number of bacterial groups varied between 5 and 10 in the sediments analysed [500 mg of sediments (ww) were used in the analyses; this corresponds to a surface of  $0.4 \text{ m}^2$  for stations DCG & 435 and  $2.9\text{-}3.2 \text{ m}^2$  for stations 130 & 700]. Gamma- and delta-Proteobacteria, as well as CFB bacteria, were observed in all the DNA libraries.

TABLE 3. Number (Nb) and percentage (%) of clones obtained in each of the 4 stations analysed. H, 0-1 cm sediments; B, 9-10 cm sediments.

|                            | DCG-H |      | DCG-B |      | 435-H |      | 435-B |      | 130-H |      | 130-B |      | 700-H |      | 700-B |      |   |     |
|----------------------------|-------|------|-------|------|-------|------|-------|------|-------|------|-------|------|-------|------|-------|------|---|-----|
|                            | Nb    | %    |   |     |
| $\alpha$ -Proteobacteria   | 1     | 2.4  |       |      |       |      | 2     | 4.9  |       |      |       |      |       |      |       |      | 3 | 7.9 |
| $\beta$ -Proteobacteria    | 1     | 2.4  |       |      | 2     | 5.3  |       |      |       |      |       |      |       |      |       |      |   |     |
| $\gamma$ -Proteobacteria   | 18    | 43.9 | 13    | 34.2 | 12    | 31.6 | 18    | 43.9 | 10    | 37   | 10    | 30.3 | 13    | 40.6 | 12    | 31.6 |   |     |
| $\delta$ -Proteobacteria   | 5     | 12.2 | 6     | 15.8 | 11    | 28.9 | 3     | 7.3  | 9     | 33.3 | 10    | 30.3 | 5     | 15.6 | 11    | 28.9 |   |     |
| $\epsilon$ -Proteobacteria |       |      |       |      |       |      |       |      |       |      |       |      |       |      |       |      |   |     |
| Actinobacteria             | 6     | 14.6 | 3     | 7.9  | 4     | 10.5 | 2     | 4.9  |       |      | 1     | 3.03 | 1     | 3.13 |       |      |   |     |
| Acidobacteria              | 3     | 7.3  | 5     | 13.2 | 1     | 2.6  | 6     | 14.6 | 1     | 3.7  | 3     | 9.09 |       |      |       |      | 3 | 7.9 |
| CFB bacteria               | 2     | 4.9  | 4     | 10.5 | 4     | 10.5 | 1     | 2.4  | 5     | 18.5 | 6     | 18.2 | 8     | 25   | 7     | 18.4 |   |     |
| Planctomycetes             | 3     | 7.3  | 3     | 7.9  |       |      | 3     | 7.3  |       |      | 1     | 3.03 | 1     | 3.13 |       |      |   |     |
| Nitrospirales              | 1     | 2.4  | 1     | 2.6  |       |      | 4     | 9.8  |       |      |       |      |       |      |       |      |   |     |
| Verrucomicrobia            |       |      | 2     | 5.3  |       |      | 1     | 2.4  |       |      |       |      |       |      |       |      |   |     |
| Chlorobi                   |       |      |       |      |       |      |       |      |       |      |       |      | 1     | 3.13 | 1     | 2.6  |   |     |
| Chloroplastes              |       |      |       |      |       |      |       |      |       |      |       |      | 1     | 3.13 | 1     | 2.6  |   |     |
| OD1                        |       |      |       |      |       |      | 1     | 2.4  |       |      |       |      |       |      |       |      |   |     |
| WS3                        |       |      |       |      |       |      |       |      |       |      | 1     | 3.03 |       |      |       |      |   |     |
| TG3                        |       |      |       |      |       |      |       |      |       |      | 1     | 3.03 |       |      |       |      |   |     |
| OP8                        |       |      |       |      |       |      |       |      |       |      |       |      | 1     | 3.13 |       |      |   |     |
| Spirochaetes               |       |      | 1     | 2.6  |       |      |       |      |       |      |       |      |       |      |       |      |   |     |
| Unknown                    | 1     | 2.4  |       |      | 4     | 10.5 |       |      | 2     | 7.41 |       |      | 1     | 3.13 |       |      |   |     |
| Nb of clones               |       | 41   |       | 38   |       | 38   |       | 41   |       | 27   |       | 33   |       | 32   |       |      |   | 38  |
| Nb of groups               |       | 10   |       | 9    |       | 7    |       | 10   |       | 5    |       | 8    |       | 9    |       |      |   | 7   |

### SSU rRNA clone libraries and sequencing of Archaea

A total of 17 16S rDNA sequences were obtained in station DCG (in the two sediment horizons considered; sediments of February 2007). 10 of these sequences are complete ( $\pm$  1500 bp). The majority of these sequences cluster in the Marine Group 1 Crenarchaeota (Gillan & Danis 2007). These new BCP archaeal sequences were aligned to other similar sequences in the GenBank database and were then used to adapt the existing PCR primers for DGGE. The PCR amplifications were not successful in the other BCP stations considered.

### SSU rRNA clone libraries and sequencing of Micro-Eukaryotes

We first made two clone libraries (250 clones each), one for the upper sediment horizon (combination of top cm's of stations DCG and 700) and one for the lower sediment horizon (combination of bottom cm's of stations 130 and 700) using the general eukaryotic primers 1427f and 1637r (Van Hannen et al., 1998). These clones were also used for the construction of a set of markers that were used in the DGGE analyses.

We also made 3 group-specific clone libraries with protozoan primers for ciliates, Cercozoa and Kinetoplastida (cf. above); the kinetoplastid-specific clone library however was not successful (no positive clones). CL were made with lumped PCR products of PCR reactions performed with template DNA of both stations 130 and 700, different months and different depths. Eighty-six positive ciliate-clones and 37 Cercozoa-clones (positive clones after screening) were found. After sequencing (69 clones for Ciliates, 27 clones for Cercozoa) and BLAST analysis, 47% and 95% respectively of the sequences could be assigned to the correct taxonomic group. The remaining sequences were related to Bacillariophyta (Diatoms) and uncultured eukaryotes, despite the specificity of the primers. For ciliates, 15 unique sequences,

representing 5 different taxonomic ciliate classes were identified. Sequences related to *Acineta* sp. (class Phyllopharyngea) and representatives of the class Spirotrichea (*Strombidium*, *Trachelostyla*, *Holosticha*, *Tintinnopsis*) dominated the clone library. In addition representatives related to other important ciliate groups were found (Oligohymenophorea, Litostomatea, Karyorelictea). These five ciliate groups have previously been reported from subtidal marine sediments (Shimeta et al 2007).

For Cercozoa, 5 unique sequences were found; representing only one cercozoan clade, the Cryomonadida clade – as recently described in Chantangsi & Leander (2010). BLAST analyses of obtained sequences were all most closely related to *Protaspis* sp (Thaumatomonadida) and *Cryothecomonas* sp, 2 closely related species (Hoppenrath & Leander 2006). Members of the genus *Protaspis* are a group of cercozoan biflagellates that glide along substrates with heterodynamic flagella and are common predators in marine benthic habitats (Chantangsi & Leander, 2010, Hoppenrath & Leander, 2006, Luo, et al., 2009). *Cryothecomonas* is a parasite of phytoplankton (Tillmann, et al., 1999) or a free-living predator (Thomson et al 1991). Maximum Likelihood phylogenetic analyses (not shown) reveal that our sequences fall within a diverse cluster of as yet largely unidentified cercozoan representatives, within the Cryomonadida clade.

When comparing the diversity observed with the clone libraries with that observed in the DGGE sequence analyses (cf. above), we note that 3 ciliate sequences (one *Strombidium* and two *Acineta*) are identical. Rarer clones were not observed amongst the sequences obtained with the DGGE approach. For Cercozoa on the other hand, a higher diversity is found using the DGGE approach with the general eukaryotic primers (4 Thaumatomonadida, 1 Cercomonadida, 1 Vampyrellidae and 1 uncultured Cercozoa) than in the CL approach with the group-specific primers. Our presumption that by using the general eukaryotic primers, protozoan diversity is underestimated, is thus correct for ciliates (and probably other protozoan), but not for Cercozoa.

### Isolation of microorganisms

To date, a total of 11 pure cultures have been obtained in the aerobic medium (medium I) and 23 cultures in the anaerobic media (media II-IV). No cultures were obtained in medium V. The pure cultures will be transferred to the BCCM culture collection.

### **2.2.1.3. Determination of microbial biomass**

#### Bacteria

MPN counts were obtained with 4 types of media in BCP sediments collected in February 2007 (medium V was unsuccessful). For medium I (oxic conditions) the MPN counts varied between  $4.9 \times 10^2$  to  $7.0 \times 10^7$  per gram of sediments (ww) and counts were similar in the two sediment horizons considered. In anaerobic medium II, counts varied between  $4.6 \times 10^2$  to  $2.0 \times 10^6$  per gram of sediments (ww); counts were always significantly higher in the 9-10 cm horizon for sediments of station 130, 140, 230 & 700. In anaerobic medium III, counts varied between  $2.3 \times 10^2$  to  $1.0 \times 10^6$  per gram of sediments (ww). Except in stations 120, 330 & DCG, counts were always significantly higher in the 9-10 cm horizon. Finally, in medium IV, counts

varied between  $4.5 \times 10^1$  to  $1.7 \times 10^6$  per gram of sediments (ww). No MPN counts were obtained for station 435.

DAPI counts were obtained in all stations in February and July 2007 (n=4) (TABLE 4). The DAPI-counts varied between  $5.3 \times 10^5$  and  $7.5 \times 10^8$  bacteria in 500 mg of sediments (ww). For the surface sediments (0-1 cm) in February, DAPI-counts were significantly higher in stations 130/700 than in stations DCG/435 (up to 2 orders of magnitude); the same situation was observed in July although the difference was not significant for station DCG. For the 9-10 cm layer of the sediments in February, DAPI-counts were significantly higher in stations 130/700 than in stations 435 (not significant for DCG); in July, the DAPI-counts were significantly higher in stations 130 than in stations 435 and DCG (not significant for 700).

TABLE 4. DAPI-counts (range for 500 mg -ww- of sediments, n=4); Feb, February; Jul, July. Two sediment sections were considered (0-1 cm and 9-10 cm). Letters (a, b) refer to comparisons between stations (within one sediment layer); stations are not significantly different if at least one letter is shared (Dunn's test,  $P < 0.05$ ).

|             | 120     | 130     | 140     | 230     | 330     | 435     | 700      | DCG     | ZG03    |
|-------------|---------|---------|---------|---------|---------|---------|----------|---------|---------|
| Feb 0-1 cm  | 4.2E+07 | 3.7E+08 | 1.1E+08 | 9.4E+06 | 3.5E+06 | 2.1E+06 | 2.6E+08  | 1.6E+06 | 7.1E+06 |
|             | 1.2E+08 | 5.2E+08 | 7.5E+08 | 9.5E+07 | 1.0E+07 | 7.9E+06 | 8.9E+08  | 2.5E+06 | 5.8E+07 |
|             | ab      | a       | ab      | ab      | ab      | b       | a        | b       | ab      |
| Feb 9-10 cm | 6.9E+07 | 4.9E+08 | 1.9E+07 | 7.9E+06 | 2.3E+07 | 4.5E+06 | 3.9E+08  | 3.6E+06 | 3.6E+06 |
|             | 1.6E+08 | 7.1E+08 | 2.7E+08 | 2.4E+08 | 1.6E+08 | 7.9E+06 | 6.8E+08  | 4.4E+07 | 4.8E+07 |
|             | ab      | a       | ab      | ab      | ab      | b       | a        | ab      | ab      |
| Jul 0-1 cm  | 1.6E+08 | 2.8E+08 | 4.6E+07 | 7.7E+07 | 5.8E+07 | 5.3E+05 | 1.68E+08 | 5.8E+06 | 8.4E+07 |
|             | 3.2E+08 | 3.2E+08 | 8.1E+07 | 2.1E+08 | 1.3E+08 | 3.7E+06 | 5.2E+08  | 1.5E+07 | 2.0E+08 |
|             | a       | a       | ab      | ab      | ab      | b       | a        | ab      | ab      |
| Jul 9-10 cm | 5.8E+07 | 1.8E+08 | 2.9E+08 | 8.3E+07 | 2.8E+07 | 8.2E+06 | 7.4E+07  | 9.6E+06 | 8.0E+07 |
|             | 1.6E+08 | 3.4E+08 | 6.3E+08 | 1.9E+08 | 9.2E+07 | 1.4E+07 | 2.8E+08  | 4.5E+07 | 2.3E+08 |
|             | ab      | a       | a       | ab      | ab      | b       | ab       | b       | ab      |

Significant differences of bacterial biomass were thus found among the BCP stations considered in this study. Muddy sediments (e.g., 130, 140, 700) featured the highest numbers of bacteria and sandy stations (e.g., DCG, 435) the lowest. This is not surprising because aquatic bacteria are almost inevitably associated to surfaces (Cooksey & Wigglesworth-Cooksey 1995) and available surfaces are elevated in muddy stations (see below, point 2.2.1.4.).

In 2008, DAPI-counts were obtained for sediments of stations 130 & 700 between February and July. An example of profile is shown in Figure 9. As for the DGGE profiles, reproducibility was good and DAPI-count profiles were used in ordination approaches (see below).

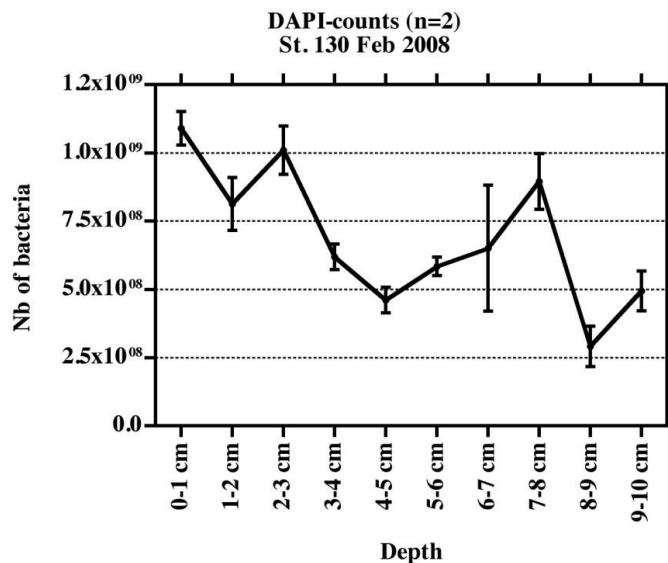


Figure 9. Example of a DAPI-count profile obtained in February 2008 in station 130 (n=2).

### Micro-eukaryotes

No biomass counts could be obtained for the February 2007 samples. However, preparations have been successfully made for the July 2007 (except stations DCG, 330 and 435) and all 2008 samples. The July 2007 counts (n=3-4) yielded values ranging between  $8,25 \times 10^5$  to  $5,19 \times 10^6$  cells per ml sediment. These values are in the same order of magnitude as those reported in the literature for subtidal sediments (e.g. Shimeta et al. 2007). Cell numbers tended to be on average higher in the deeper sediment layers. Unfortunately, no data are available for the sandiest stations, which have the lowest prokaryote counts. Heterotrophic nanoflagellates were most abundant in all samples (> 90 % of cell count; not shown).

### **2.2.1.4. Geochemical properties of the sediments**

#### Laser granulometry.

Sediments sampled in 2007 in the 9 stations were studied using a Malvern Mastersizer 2000 laser granulometer. They have been classified in three groups. In Group I (stations DCG, 435 and 330), sediments have a MGS of 400  $\mu\text{m}$  (Figure 10). In Group II (stations 120, 230 0-1 cm, ZG03) sediments have a MGS of 200  $\mu\text{m}$ . In Group III (130, 140, 700, 230 9-10 cm), sediments are very muddy, with a MGS of 12.5  $\mu\text{m}$ . The shape of curves appear very similar whatever the depth or the season, except in station 230 which features sand at the surface and mud at 9-10 cm. Stations 130, 140 and 700, located close to the coast, are dominated by clays and silt particles. Particle size distribution from stations 120, 230 and ZG03 display variable contents of clays (0-76%) mixed with sandy particles smaller than those present in the open sea. Station 140 showed very heterogeneous sediments and reproducibility between different cores was bad.

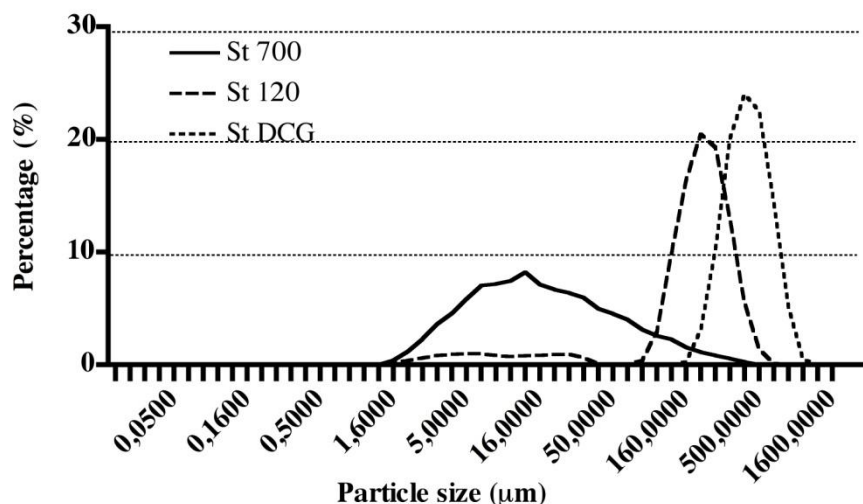


Figure 10. Particles size distribution as measured with a laser granulometer.

#### Specific area measurements and porosity.

Granulometric data have been completed by specific surface area (SSA) measurements. Sediments from stations 130, 140 & 700 (fine fraction < 63 µm higher than 80 %), displayed SSA values of 13.6 (130), 10 (140), and 11 (700) m<sup>2</sup> g<sup>-1</sup>. A mesoporosity characterizes also the surface of these particles, with a main size at 30 nm. Sediments from stations 120 and ZG03 displayed lower SSA values, between 1.2 and 1.5 m<sup>2</sup> g<sup>-1</sup>. All the other stations displayed SSA values inferior to 1 m<sup>2</sup>.g<sup>-1</sup>, which is the detection limit of the technique.

#### Dissolved sulfide as determined by the DGT approach.

For stations 140 and 700 in 2007, results indicate clearly a sulfate-reducing bacterial activity just below the water-interface characterized by a strong S(-II) gradient of about 40 µmol L<sup>-1</sup> in the first cm (Figure 11). Under this level, sulfides concentration did not evolve quantitatively, which means that organic matter and/or sulfates are the limiting factor of the bacterial activities. In addition, the high contents of sulfides in the porewaters suggest, that all the labile iron and other heavy metals should be trapped at least in the solid phase, and probably in AVS compounds. Increase of dissolved sulfides in the station 230 is more regular in the first 8 cm, then the same concentration level as for the two previous stations is reached. It seems that microbial activity in this station occurs with a lower kinetic. Station 130, with very muddy sediment, should be however considered as a heterogeneous site, since the presence of dissolved sulfides is quantitatively detected between 6-12 cm depth. In that station, sulfate-reducing microbial activity takes place in well defined zones, suggesting for instance a discontinuous organic supply in these sediments. This behaviour has already been observed and partly explained using lipid compounds as a biomarker (Billon et al., 2007). In sandy sediments (DCG, 435 & 330, ZG03), the concentration of dissolved sulfides is under the detection limit, probably due to the fact that sediments remain oxic all along the core. This could be explained by a low supply of organic matter whatever the season.

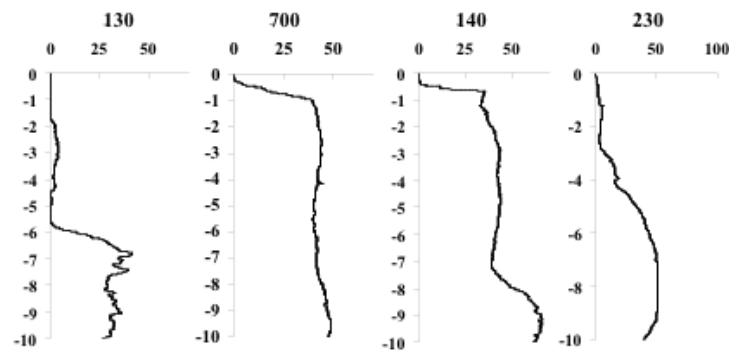


Figure 11. Dissolved sulfide concentration profiles (in  $\mu\text{mol.L}^{-1}$ ) in function of depth (cm) determined by AgI DGT in 4 sediment cores from stations 130, 700, 140 and 230 sampled in February 2007.

In 2008, several other profiles have been measured only for the stations 130 and 700. In station 130 (Figure 12), the concentrations of dissolved sulfides in the winter and spring are low in the 4 first cm ( $< 1 \mu\text{mol L}^{-1}$ ). Below 5 cm, sulfides contents increased to reach variable maxima, that range from 15 to  $80 \mu\text{mol L}^{-1}$ . In June and July, the supply of organic matter due to the organism degradation at the surface of the sediments did increase the activity of sulfate reducing bacteria, close to the water-sediment interface. Profiles exhibits therefore high maxima at around 3-4 cm depth with dissolved sulfide values at around  $400 \mu\text{mol.L}^{-1}$  in the porewaters. According to these profiles, the bioturbation seems not sufficient enough to get also high concentrations of sulphides below 8 cm and below this depth the concentrations are comparable to those obtained in the other seasons. Thus, the active production of dissolved S(-II) in the sediment porewaters in summer should trap efficiently the trace metals in the solid sulfide pool. In the other periods studied, metal availability in the surface sediments should be higher.

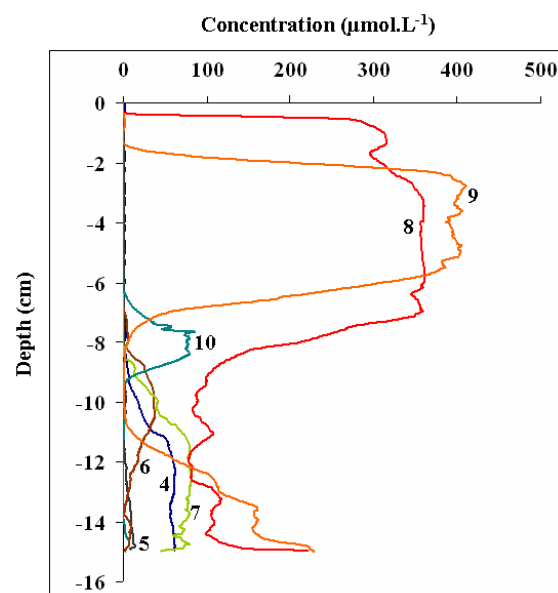


Figure 12 (previous page). Dissolved sulfide concentration profiles (in  $\mu\text{mol L}^{-1}$ ) in function of depth (cm) determined by AgI DGT in station 130 for the following sampling dates: Feb-08 (4); Mar-08 (5); April-08 (6); May-08 (7), June-08 (8), July-08 (9) and November-08 (10).

Acid Volatile Sulfides (AVS) and Chromium Reducible Sulfur (CRS).

Results presented in Figure 13 indicate the absence of AVS in sandy sediments (DCG, 435), because they are either not produced or quickly reoxidized, for producing CRS for instance. Low contents of CRS were also found in these stations. For the other sites, AVS are generally present at lower concentrations than the CRS. One surprising feature is the higher concentrations of AVS in the surface sediments than in the bottom, suggesting that a transformation of AVS occurs in function of the burial of the particles. However, this trend is not necessarily bound to an increase of CRS with depth, suggesting a more complex pathway of production of CRS, not only based on the partial reoxidation of the AVS.

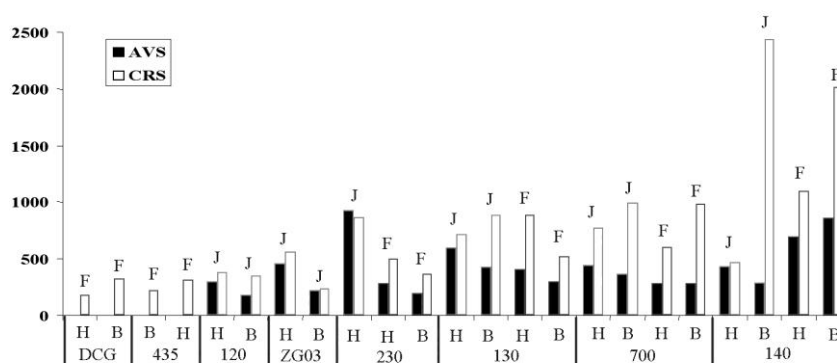


Figure 13. AVS and CRS contents in the sediments sampled from the stations DCG, 435, 120, ZG03, 230, 130, 700 and 140 in February 2007 (F) and July 2007 (J). H, surface sediments (0-2 cm); B, bottom sediments (8-10 cm).

More analyses of AVS and CRS contents have been performed in 2008 in the stations 130 and 700. For station 130, concentrations indicate large scattering of the data. For instance, in the surface sediments  $[S-AVS] = 660 \pm 1700$  ppm (for 8 campaigns between Feb-07 and July-08). Differences in bacterial activity, partial reoxidation of surface sediments and heterogeneity of the sediments are probably the main reasons of such a high standard deviation. Profiles of AVS and CRS have also been measured in station 700 and indicated slightly lower concentrations than in the station 130. In both cases, a slow increase of CRS contents occur in the sediments as a function of depth, whereas no such tendency has been pointed out for AVS, indicating that most of the sulfidization process takes place in the first centimeter of the sedimentary column. Generally, the AVS/CRS ratio is lower than 1. That means the transformation of AVS into CRS is effective in our sediments. The results pointed also out that the sulfidization process in sediment is fully achieved and labile iron is still in excess. It is therefore surprising to notice no relevant production of AVS and/or CRS in surface sediments of the station 130 in June and July 08. Several explanations may be proposed: (i) the solubility product of FeS is not achieved in these porewaters; (ii) although concentrations of sulfides are high, reoxidation processes occurs and do not permit a quantitative production of inorganic sulfide precipitates and; (iii) the remaining labile iron fraction is not quickly reactive to a kinetically point of view. To sum up, sulfidization processes occur mainly in the surface of the sediments. In deeper depths, the lack of biodegradable organic matter is a limiting factor to subsequent production of AVS and CRS.

### Simultaneously Extracted Metals (SEM) and Toxicity Index (TI).

According to the results obtained in 2007 and 2008 (Figures 14 & 15), we can assume that AVS are in excess compared to the labile metals Cu, Zn and Pb (generally more than 10 time higher), which are thereby trapped in sulfides under anoxic conditions. Consequently, sediments should not be toxic towards Cu, Zn and Pb. For the sites DCG and 435 the TI has not been calculated because AVS were not detected. However, concentrations of SEM in these samples remain low (about ten times lower than in muddy sediments), mainly due to the very low quantity of fine fraction. In addition, for the station 130, no seasonal effect has been observed on the TI; the values remain very negative whatever the sampling date, with always a large excess of AVS.

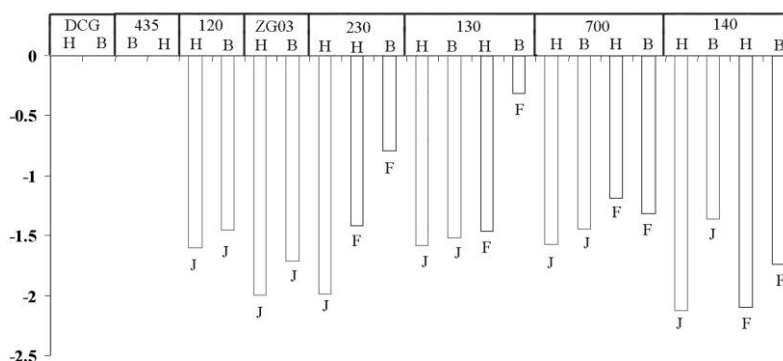


Figure 14. Logarithm of TI calculated for the sediments sampled in February 2007 (F) and July 2007 (J), in stations DCG, 435, 120, ZG03, 230, 130, 700 and 140.

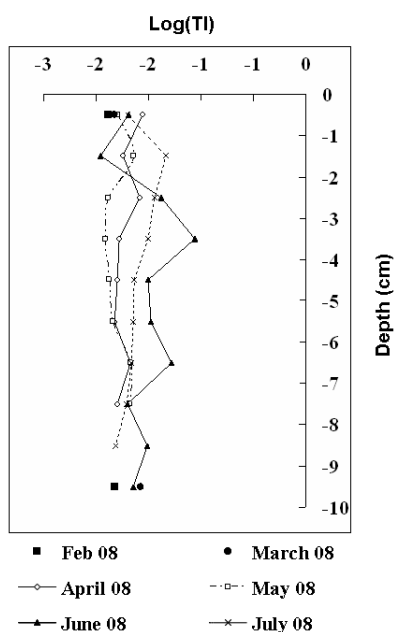


Figure 15. Logarithm of the Toxicity index (TI) calculated for sediments of station 130 sampled in February (Feb), March, April, May, June and July 2008.

## Pigment analyses

The 2007 chlorophyll *a* concentrations in sediments are shown in Figure 16. Chlorophyll *a* levels are very low in the sandy (DCG, 435 and 330) and mixed (230, 120 and ZG) sediments, both in February and in July. The silty stations (700, 130 and 140) however show much higher values. For the silty stations 700 and 130, chlorophyll *a* concentrations in winter were on average higher at depth than at the sediment surface (but SD are big); the opposite appears in summer.

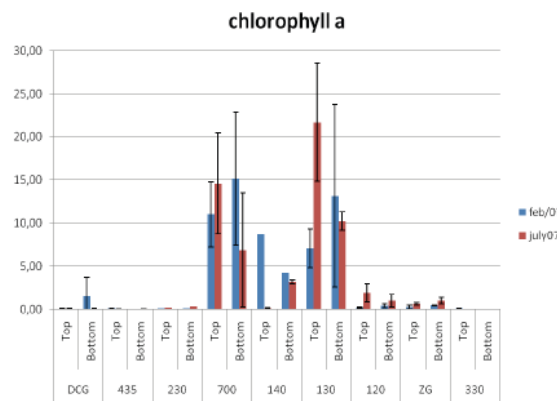


Figure 16. Chl *a* concentrations ( $\mu\text{g g}^{-1}$  SDW) (mean  $\pm$  SD) at the 2 depths at the 9 sampling stations for February and July 2007 (n=2-3). Top= 0-2cm; bottom= 8-10cm.

In 2008, the main spring bloom occurred in late April-early May (Figure 17, A). Pigment analyses were done for all depths (0-10cm) for the silty stations 130 and 700 (Figure 17, B). Again (cfr 2007), February shows higher chlorophyll *a* concentrations at higher depth than in the top sediment, especially in station 130. Chlorophyll *a* concentrations in the surface layers, derived from the spring phytoplankton bloom, mainly increase from May onwards. Note that in all months chlorophyll *a* concentrations can be high in deeper layers.

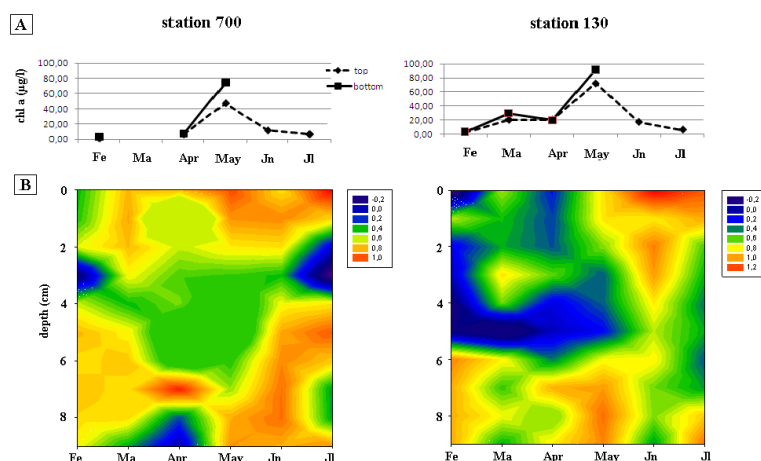


Figure 17. Chlorophyll *a* concentrations in the water column ( $\mu\text{g/l}$ ) in the upper water-layers ('top') and near the sediment surface ('bottom'), and B: two-dimensional representation of chl *a* concentrations in the sediment ( $\mu\text{g/g}$  DW-values are log-transformed), at the 2 silty sampling stations (700 and 130) in spring 2008; X-axis, month; Y-axis, depth (cm). Fe, February; Ma, March; Apr, April; Jn, June; Jl, July

## DET/DGT analysis

### A. Spatial variability.

Sediments of the sandy stations 435, ZG03 and DCG contain low amounts of organic matter (OM) and consequently associated trace metals. Dissolved oxygen and other oxidants are abundantly present. As a result, the vertical profiles of trace elements Mn, Fe, Co and As assessed by DET and DGT did not present major concentration variations with the depth (data not shown).

High resolution profiles of trace elements were assessed by DET and DGT in muddy sediments of stations 130, 140 and 700. Generally good correspondence between DET and centrifuge data were observed at the 3 stations. The trace element profiles at those three stations show more pronounced differences (Figures 18–19). The remobilization zones of the trace elements appear at specific depths for the different stations. The trace elements at station 700 show much higher concentrations than at the two other ones. High concentrations have been observed for As (at the 3 stations) and further research should be carried out on this element.

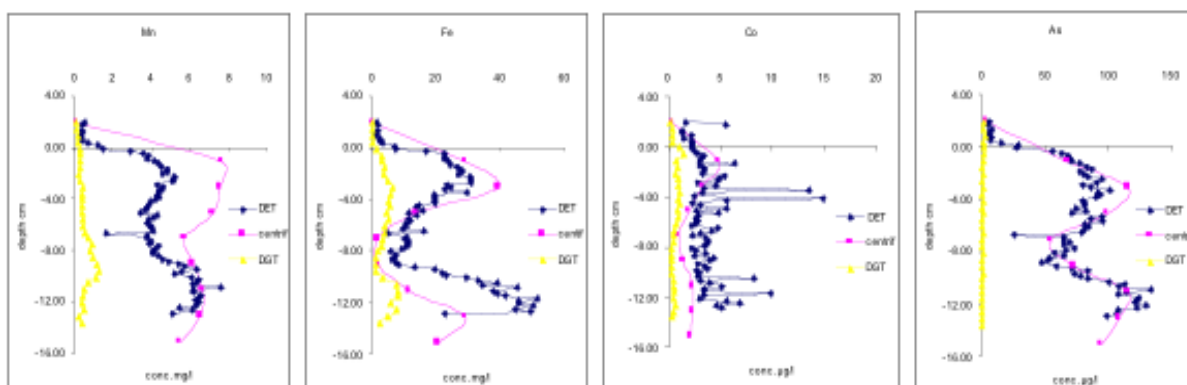


Figure 18. Vertical profiles of Mn, Fe, Co and As assessed by DET, DGT and centrifuge at station 130 in February 2007.

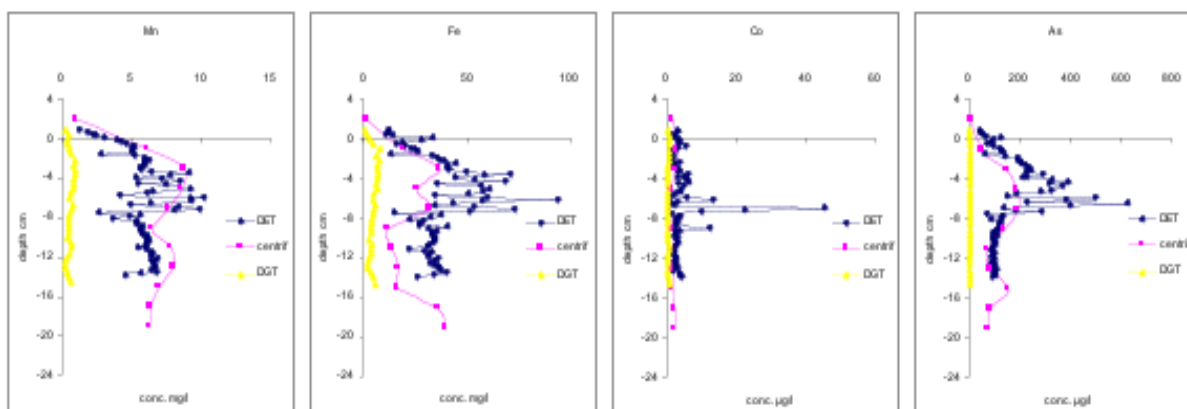


Figure 19. Vertical profiles of Mn, Fe, Co and As assessed by DET, DGT and centrifuge at station 700 in February 2007.

## B. Seasonal variability.

### B.1 Seasonal variation of POC, $\delta^{13}\text{C}$ and $\delta^{15}\text{N}$ at station 130.

Dissolved oxygen profiles indicate highest concentration during the winter months of February and March 2008 in overlying bottom waters and sediment pore waters. At 0.3 cm of depth the sediment becomes anoxic. This depth rises to 0.1 cm in the spring months of April and May. These results suggest an increased microbial activity in the sediment surface layer in the spring months, probably due to a supply of freshly produced organic matter. The POC varied between 1.4 and 2.3 % between February and May 2008 (TABLE 5). This can be explained by a variable input of organic matter from the Scheldt estuary and by the spatial heterogeneity of the sediments. The lower percentage of POC during February to March is not a result of bacterial degradation because bacteria preferentially use the lighter isotopes, which would result in more positive  $\delta^{13}\text{C}$  values of POC instead of lower ones as observed for March. On the contrary, the isotope ratios of organic carbon suggest an input of freshly produced POC in March because the  $\delta^{13}\text{C}$  values decreased, in agreement with the lower  $\delta^{13}\text{C}$  values of marine phytoplankton (Michener & Schell, 1994). The  $\delta^{15}\text{N}$  values in sedimentary POC also decreased, but the interpretation of the values is more difficult. The degradation of the organic matter in the following months is corroborated by a decrease in dissolved oxygen levels in the surface sediment layer and by a progressive increase in  $\delta^{13}\text{C}$  and  $\delta^{15}\text{N}$  because the lighter isotopes are preferentially assimilated by the microbial community (Blair et al. 1985). This progressive increase in the isotopic ratios is in fact a balance between POC degradation and input of freshly produced organic matter, with the former process dominating the latter.

The redox profiles corroborate the results obtained on dissolved oxygen, with lowest values in spring ( $-135$  mV at the SWI and  $-372$  mV at 10 cm of depth). During March 2008, pH values were at the lowest and most variable and dissolved sulfide levels remained always very low compared to other months. In February, sulfide concentrations rapidly increased from  $5 \mu\text{M}$  at 8 cm to  $63 \mu\text{M}$  at 12.3 cm; values remained stable until the bottom of the sediment cores (see above). Measurable amounts of  $\text{S}^{2-}$  were not detected during April and May in the upper 6.5 cm of the sediments. In April, sulfides increased to  $40 \mu\text{M}$  between 8 and 11 cm of depth and dropped again below  $5 \mu\text{M}$  below 14 cm. In May, sulfide levels increased to a stable concentration of  $40\text{-}80 \mu\text{M}$  between 8 and 12 cm of depth. Seasonal variations of these parameters induce temporal variation in some of the trace metals as we will see further in this report.

TABLE 5.  $\delta^{15}\text{N}$ ,  $\delta^{13}\text{C}$  and POC values in the sediment top layers.

| Month | $\delta^{15}\text{N} \text{ ‰}$ | $\delta^{13}\text{C} \text{ ‰}$ | POC % |
|-------|---------------------------------|---------------------------------|-------|
| Feb   | 9.93                            | - 23.00                         | 2.3   |
| Mar   | 7.95                            | - 23.41                         | 1.4   |
| Apr   | 8.46                            | - 23.03                         | 1.6   |
| May   | 8.22                            | - 22.62                         | 1.7   |

## B.2 Seasonal variation of trace elements assessed by DET and DGT probes.

Subsurface DET profiles (Figure 20) displayed a range of concentrations from detection limits in deep layers to a maximum of 94  $\mu\text{M}$  of Mn, 720  $\mu\text{M}$  of Fe and 3.8  $\mu\text{M}$  of As indicating a typical redox pattern for coastal marine sediments. Iron presented a typical pattern in relationship to the redox conditions (oxic, sub-oxic and anoxic). In the suboxic pore water layers (between 2 - 6 cm of depth), Fe oxides were reduced and total dissolved Fe levels (DET) reached concentrations of about 700  $\mu\text{M}$  during all surveys, except in April 2008 where the maximum was 160  $\mu\text{M}$  (Fig. 20B).

In February and May 2008, when sulfide levels were important in the sediments below 8 cm of depth, low total dissolved Fe levels (DET) were observed, while during the other months Fe levels reached 340  $\mu\text{M}$ . The seasonal variability of the Mn profiles (DET) is much less pronounced (Fig. 20A). In the deepest sediment layers, even with dissolved sulfide levels above 5  $\mu\text{M}$ , dissolved Mn levels were still relatively high. This is not surprising as the affinity of Mn for sulfides is relatively low. Several studies have indeed shown that MnS is not observed in most pore waters (Canavan et al. 2007; Huerta-Diaz et al. 1998; Morse & Luther 1999; Billon et al. 2001). For arsenic, an important suboxic maximum was observed in February 2008 (DET) (Fig. 20C).

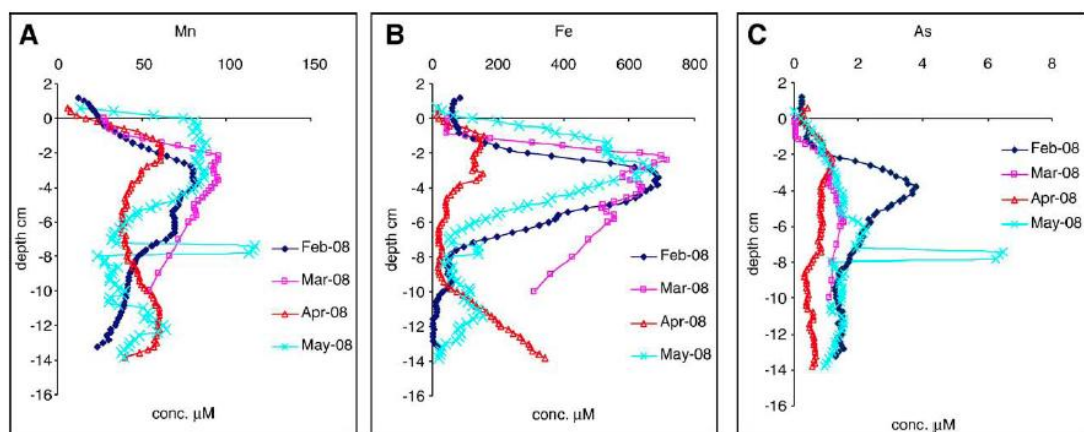


Figure 20. Vertical profiles of Mn (A), Fe (B) and As (C) assessed by DET from February to May 2008.

The DGT approach gives a direct measurement of time averaged fluxes (mass of metal ( $M$ )/ $\text{cm}^2 \cdot \text{s}$ ) rather than concentrations. Concentrations can however, be estimated when (1) a constant pore water flux is maintained and (2) all compounds binding onto the resin have the same diffusion coefficient in the gel layer. If the flux is constant (no depletion in concentration or rapid re-supply from the solid phase), the concentration ( $C_b$ ) can be calculated by the following formula :

$$M = \frac{C_b D A t}{\Delta g} \quad (1)$$

If, for different gel thicknesses ( $\Delta g$ ), the calculated  $C_b$  is constant then the flux is constant during the exposure period.

In 2008, a couple of DGT probes (thickness of the diffusive gels : 0.80 and 0.12 mm) arranged back to back was inserted into one large sediment core (7 cm) at stations 130 and 700. Another couple of probes (one DET and one DGT-Agl probe), arranged back to back, was inserted into the same core. No systematic differences were observed between the two DGT probes with different thicknesses of diffusive gel, neither in sediment porewaters at station 130 or at station 700 (data not shown). The random differences between the two profiles corresponding to the thinner and the thicker gel layers can be explained by sample heterogeneity. In order to validate this hypothesis of heterogeneity, twin DGT probes (with the same thickness of diffusive gel and arranged back to back), were inserted into one sediment core at station 130. Since two similar DGT probes were inserted into exactly the same sediment area, vertical profiles of trace elements should almost be identical. Actually good comparable results were obtained for the twin DGT probes. No systematic differences were observed between the concentrations found in the two DGT probes. The random differences between the two profiles were within the error due to sample heterogeneity.

The second condition mentioned above (i.e., the same diffusion coefficient for all compounds within the gel) is much more difficult to prove *in situ*. In fact, free ions diffuse faster than complexes (Zhang, 2004) but the percentage of free ions, inorganic and organic complexes is difficult to determine in the sediments as well as their diffusion rate. Since the overall diffusion coefficient used in our pore water concentration calculations (equation 1) is overestimated, the pore water concentration and hence the exchange fluxes are underestimated causing our reported fluxes to be minimum.

The labile Fe, Mn and As levels (DGT approach) displayed profiles similar to those observed with the DET approach except for Fe in March (Figure 21). For Co and Ni suboxic maxima were observed, while the Pb and Cr profiles presented several high peaks at various depths in March (for Cu this was observed for all sampling periods). These peaks may be explained by local heterogeneities and/or analytical artifacts (Figure 21). In the  $<63 \mu\text{m}$  fraction of the solid phase in the surface sediment the following concentrations were observed (all concentrations are in  $\mu\text{g g}^{-1}$  dw) : 20,000-23,000 (Fe), 620-780 (Mn), 55-65 (Cr), 26-33 (Ni), 13-16 (Cu), 25-32 (Pb), 7-10 (As), 0.36-0.48 (Cd) and 28,000-31,000 (Al). This means that all elements are enriched versus Fe, the enrichment factor ranging from 1.5 to 2.5 for Cr, Cu, Mn, Ni and Pb, and up to 6 for As and Co. Trace elements are known to be associated with Fe oxides (adsorption or coprecipitation) and can thus be released in the pore water together with Fe, during suboxic conditions. The vertical profiles of Mn, Fe and As assessed by DET and DGT in this study indicate that the remobilization zone and subsurface maximum of these elements shifts upwards, closer to the sediment-water interface (SWI), from winter to spring, corresponding with a decrease in oxygen concentrations and redox potential (Figures 20–21).

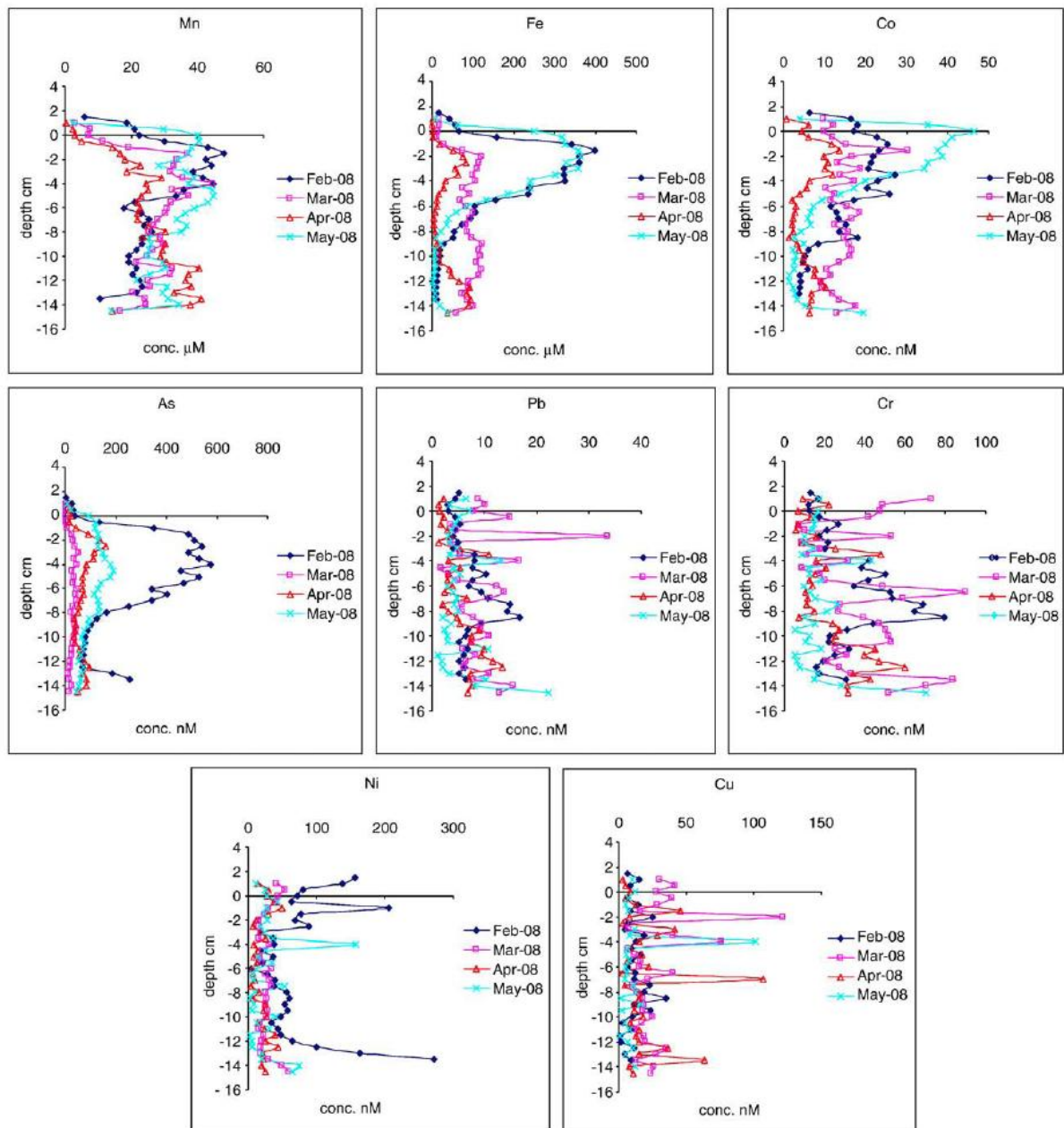


Figure 21. Vertical profiles of Mn (A), Fe (B), Co (C), As (D), Pb (E), Cr (F), Ni (G) and Cu (H) assessed by DGT from February to May 2008.

It is worthwhile to investigate seasonal effects of phytoplankton blooms (in surface sediment) and sulfide in the deepest sediment layer, on the trace metal profiles in the pore waters. The phytoplankton biomass at station 130 is mainly composed of diatoms (De Bock & Sabbe, unpubl. data) and was  $< 1.5 \mu\text{g}$  chlorophyll  $\text{a L}^{-1}$  until March, then gradually increased to approximately  $16 \mu\text{g chl a L}^{-1}$  by mid April. Based on the chl-a in the water column and the  $\delta^{13}\text{C}$  - POC levels in sediments, we can assume that pore waters became enriched in newly supplied DOC (dissolved organic carbon) / POC (particulate organic carbon) in March – April potentially forming large Fe organic complexes which are incapable of diffusing into the small pores of the DET and DGT gels (Davison and Zhang, 1994 & Zhang and Davison, 1999), explaining the lower subsurface concentrations of Fe in April. The behavior of

Mn and As is similar to Fe but less pronounced. For labile dissolved Fe (DGT), this is also valid in March. Another possible reason for low Fe could be the introduction of oxygen during DET and DGT deployment in April (the oxygen concentration at the SWI is then very low), but this should normally result in small colloidal Fe and Mn oxhydroxides. Such small colloids are measured with the DET probe, but not with the DGT unless these colloids are very unstable. However, for Fe both the subsurface DET and DGT profiles are strongly reduced in April, suggesting that oxygen is not the key parameter causing the subsurface suppression in April.

In the deep sediment layers dissolved sulfide clearly controls the level of dissolved trace metals. In March, the elevated concentrations of Fe, Mn and several other trace metals may be explained by the absence of dissolved sulfide. On the contrary, DET and DGT analyses in February and May have revealed low levels of trace metals with high levels of dissolved sulfide. It is interesting to compare the solubility product of iron-sulfide compounds (FeS) reported in literature (Davison, 1991, Rickard and Morse, 2005) with our results. Iron sulfide solubility ( $pK_s$ ) decreases as follows in marine systems : amorphous ferrous sulfide ( $2.95 \pm 0.1$ ), mackinawite ( $3.6 \pm 0.2$ ), greigite ( $4.4 \pm 0.1$ ), pyrrhotite ( $5.25 \pm 0.2$ ) and pyrite ( $16.4 \pm 1.2$ ) (Davison, 1991). The concentration levels of  $Fe^{2+}$ , dissolved sulfide and pH observed in our study are comparable to those reported by Davison (1980 & 1991). The solubility of FeS in a marine waters (pH>7) is not well defined (e.g., Rickard and Morse, 2005). Using the equations reported by Davison (1991), which define the ionic activity product (IAP),

$$IAP = [Fe^{2+}] [HS^-] \gamma_{Fe^{2+}} \gamma_{HS^-} (H^+)^{-1} \quad (2)$$

$$K_1 = a [HS^-] a [H^+] / a [H_2S] \quad (3)$$

we attempted to predict the presence and the nature of the FeS compounds. Equation (3) was used to derive the concentration of  $HS^-$  from the total soluble sulfide, i.e.  $H_2S + HS^-$  ( $S^{2-}$  being negligible) levels. Values of  $\gamma_{Fe^{2+}}$  and  $\gamma_{HS^-}$  in seawater were taken from Davison (1980). In the case of high  $Fe^{2+}$  (about 700  $\mu M$  for DET, 100  $\mu M$  for DGT) and low dissolved sulfide concentrations (about 1.5  $\mu M$ ) (observed at 3 - 4 cm of depth in the month of February), the  $-\log(IAP)$  values was 2.83, using DET values for  $Fe^{2+}$ , and 3.67, using DGT values for  $Fe^{2+}$ , which are in the range of amorphous ferrous sulfide and mackinawite. In the case of low  $Fe^{2+}$  (about 70  $\mu M$  for DET and 5  $\mu M$  for DGT) and high dissolved sulfide concentrations (about 80  $\mu M$ ) (deeper sediment layers in the month of May), similar  $-\log(IAP)$  values were obtained. The calculated  $-\log(IAP)$  value based on the DET Fe concentrations is perhaps overestimated because not all DET-Fe is labile. In order to corroborate the above findings, the Visual MINTEQ software was used to calculate the saturation index (SI) of metals (see section 2.4.5 Numerical modeling)

#### 2.2.1.5. Data integration

The proposed data analyses are aimed at describing the observed variation patterns in biomass, biodiversity and (molecular) community composition of the microbial assemblages present in BCP sediments, but are also crucial for integrating the results of both the microbiological and geochemical analyses. They allow to

evaluate the importance of the main biogeochemical drivers of microbial diversity and biomass in these sediments (including the metal pollutants), and more specifically to identify microbial phylotypes which are strongly related to the presence of metals.

In 2007, 26 variables (DGT: Pb, Cr, Mn, Fe, Co, Ni, Cu, As; DET: Ag, Cd, Sn, Pb, Al, V, Cr, Mn, Fe, Co, Ni, As; QFF; SAA; DAPI; DGGE; O<sub>2</sub>; pH) were analyzed in 9 stations of the BCP taking two sediment sections into account (0-1 cm and 9-10 cm) and two different periods (February and July). As most of the data was non-parametric, a Spearman's rank correlation global analysis was first used to identify main trends in our data (February and July were grouped in the same analysis). To study the relationship between all the variables the principal component analysis method (PCA) was also used. As metals were measured every mm for DET (or every 0.5 cm for DGT) a mean concentration was first calculated for the two selected horizons (0–1 and 9–10 cm). For bacterial diversity, significant negative correlations were only observed between the number of DGGE bands and levels of Co (–0.65 for DGT, –0.68 for DET) (TABLE 6).

TABLE 6. Spearman correlation coefficients between metal concentrations as measured by DET and DGT, total bacterial biomass (DAPI), and total bacterial biodiversity (DGGE). Only significant correlations are indicated. ns, not significant; /, not measured.

|     |      | Ag | Al | As   | Cd | Co    | Cr | Cu | Fe   | Mo | Mn   | Ni | Pb | Sn | V  | Zn |
|-----|------|----|----|------|----|-------|----|----|------|----|------|----|----|----|----|----|
| DET | DAPI | ns | ns | 0.73 | ns | 0.63  | ns | /  | 0.76 | /  | 0.87 | ns | ns | ns | ns | /  |
|     | DGGE | ns | ns | ns   | ns | –0.68 | ns | /  | ns   | /  | ns   | ns | ns | ns | ns | /  |
| DGT | DAPI | /  | /  | 0.65 | /  | 0.54  | ns | ns | 0.74 | /  | 0.69 | ns | ns | /  | /  | /  |
|     | DGGE | /  | /  | ns   | /  | –0.65 | ns | ns | ns   | /  | ns   | ns | ns | /  | /  | /  |

For bacterial biomass, significant positive correlations were observed between DAPI-counts and four metals : Mn (DET: 0.87; DGT: 0.69), Fe (DET: 0.76; DGT: 0.74), Co (DET: 0.63, DGT: 0.54), and As (DET: 0.73, DGT: 0.65). DAPI-counts were also positively correlated to SSA (0.80) and QFF (0.89). No other relevant correlations were observed between DAPI-counts and other variables (correlation values not significant and/or < 0.6) except for pH (–0.79).

The biomass of heterotrophic nanoflagellates could only be studied in 6 stations in July 2007. It was significantly correlated to Fe (0.83) as determined with DET analysis, and also to pH (-0.90) and SSA (0.88).

A principal component analysis is presented in Figure 25. Three groups of variables are evident. In the first group, it can be seen that the vector for total bacterial biomass (DAPI) points in the same direction as vectors for Fe (DGT & DET), Mn (DET), As (DET & DGT) and Co (DGT). No other trace metals are associated with the biomass vector. Vectors for QFF and SSA point also in the same direction. This means that all these variables are positively correlated. In this first group, vectors for DAPI, As (DET & DGT) and QFF are almost superimposed ( $\pm$  same length,  $\pm$  same direction) and are therefore very well correlated. The second group of variables, with vectors orthogonal to the first group (i.e., not correlated to the first group), is only composed of trace metals. The elements Cr, Al, Ni, Sn, V, and Ag are only found in that group (measured by DET and/or DGT), whereas Co, Mn, Ni, and Pb are also represented in other groups. Of the 11 variables of this group 9 elements were measured by the DET approach (Figure 22).

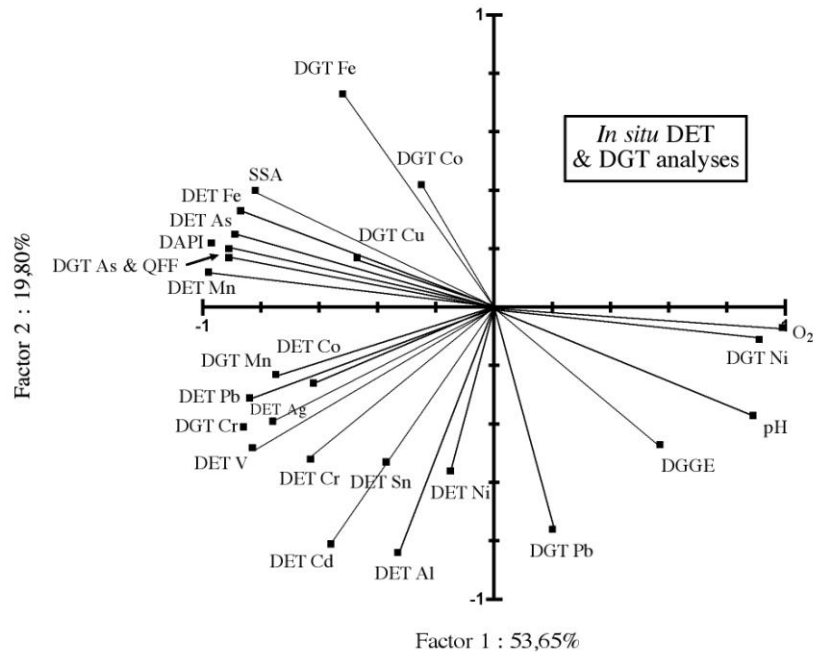


Figure 22. Relationships between 26 variables in porewaters of marine sediments of the BCP. The two first factors of the principal components analysis explain 73.45 % of the variance.

Finally, the third group of variables contains vectors pointing in the same direction as the variable for bacterial diversity (DGGE). These vectors are DGT Pb, DGT Ni, pH and O<sub>2</sub> (Figure 25). However, none of these vectors were closely associated with the DGGE vector meaning that correlations are not really relevant. The vector for DGGE points almost in the opposite direction as vectors for DGT Co, DGT Fe and SSA, which suggests the existence of a negative correlation between biodiversity and these variables (as already suggested by the Spearman's correlations).

Various biogeochemical variables were, as expected, correlated to each other. For instance when DET results are considered, levels of Fe were significantly correlated to Mn (0.94) and As (0.93) levels. Similarly, levels of Pb were significantly correlated to levels of V (0.73) and Ag (0.71).

In 2008, 43 variables were analyzed in 2 stations of the BCP (130 and 700) taking 10 sediment sections into account (0-10 cm) and 6 different periods (February to July). As for 2007, most of the data was non-parametric and a Spearman's rank correlation global analysis was first used to identify main trends in the data. These analyses were performed separately in station 130 and 700. In station 130 the situation for bacterial biomass and biodiversity was different from the trend observed in 2007. Indeed, bacterial biomass in 2008 did not correlate well to any variable in station 130. However, bacterial biodiversity as determined by the maximum number of DGGE bands was significantly correlated to Zn levels as determined by DGT (0.70). For micro-eukaryotes no good correlations to any geochemical variable was observed in station 130. In station 700 the situation for bacterial biomass and biodiversity was also different from the trend observed in 2007. No good correlations were observed for biomass and the only good correlation observed was between DGGE and DET-Fe (0.63).

Results may also be analyzed on a monthly basis. As an example, we here show the results of a redundancy analysis (RDA) of the eubacterial DGGE data of station

130 for February 2008, using forward selection of environmental variables and significance testing using Monte Carlo permutation tests (Figure 23).

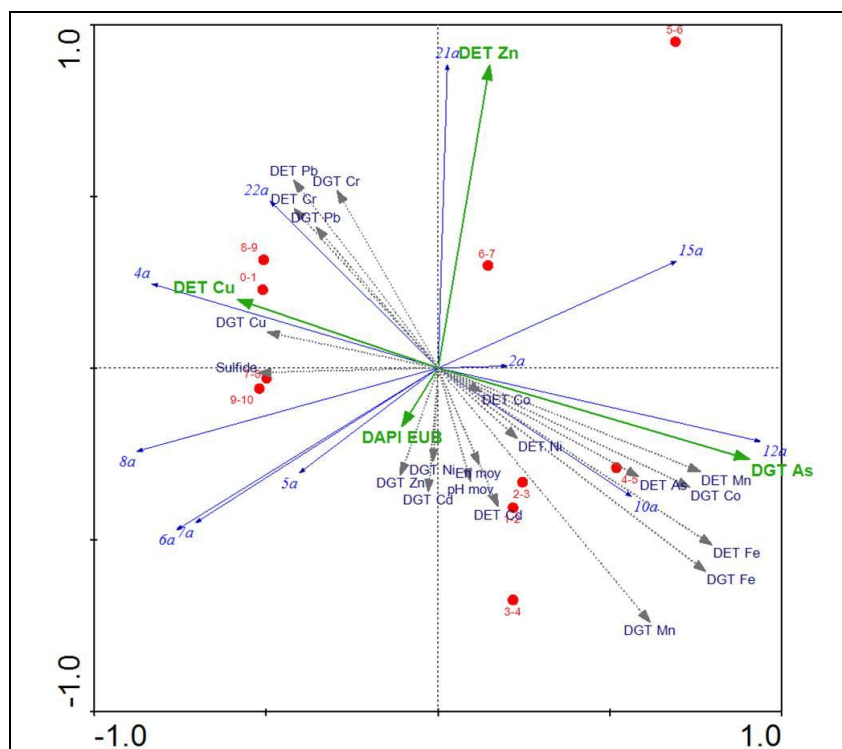


Figure 23. RDA analyses of eubacterial DGGE data (Feb. 2008, core A, st. 130), with significant environmental variables (green), supplementary environmental variables (dotted arrows), phylotype numbers (blue arrows) and samples (depth horizons, red).

This analysis (Figure 23) shows that there are pronounced changes in phylotype composition with depth (cf. also Figs 4 & 6), and that these changes can be significantly related to specific geochemical (i.c. DET Cu, DGT As, DET Zn) and biological variables (DAPI Eub). Bearing in mind that these relations are purely regressions between the biological and geochemical data, they do allow to identify specific phylotypes that vary with metal variables (e.g. note the strong correlation between phylotype 12a and As, or phylotype 21a and Zn).

Likewise, multivariate analyses (PCO, correlation, variation partitioning) were performed using the microeukaryotic data-set (see above), and these showed that variations in the communities were mainly related to the changes in Eh and pH, but trace metals as well had a significant independent impact on microbial community structure (see Pede *et al.*, in prep. b, for more details).

The DGT profiles for Mn, Fe, Co, As and Cu at station 130 in February and April (Cr only in February) displayed increasing concentrations with depth (Figure 24). Ni presented a reversed trend in February, while Pb (in February and April) and Cr (in April) had more or less constant concentrations in the water column and porewater layers adjacent to the SWI (Figure 24). We calculated concentration gradients and exchange fluxes over 2 cm of depth (TABLE 7), and as mentioned above, for each element at the SWI using a diffusion coefficient of  $10^{-5} \text{ cm}^2 \text{ s}^{-1}$  (Baeyens *et al.*, 1986), which was corrected for a porosity value of 0.9 (the ratio of the fluid volume to the total volume of sediment). Exchange fluxes of trace metals in February can be

slightly higher due to diagenetic processes, than in April. Oxygen and redox values, as well as Fe and Mn concentrations, were lower in April than in February. As suggested earlier, freshly produced organic matter (POM) entering the sediment porewaters can bind dissolved Fe and Mn compounds, reducing their porewater concentrations. Fe and Mn effluxes (from sediments to overlying water) are higher ( $0.063\text{--}1.6 \text{ mmol m}^{-2} \text{ d}^{-1}$ ) compared to the other elements (Co, As, Cu :  $4.2 \times 10^{-5}$  to  $1.6 \times 10^{-3} \text{ mmol m}^{-2} \text{ d}^{-1}$ ). Also the Ni influx in February is of the order of the outfluxes of the latter elements (TABLE 7).

TABLE 7. Exchange fluxes of trace elements at the Sediment Water Interface (SWI) in station 130 (calculated from vertical pore water profiles).

| <i>Element</i> | <i>Calculated flux in February<br/>(mmol·m<sup>-2</sup>·d<sup>-1</sup>)</i> | <i>Calculated flux in April<br/>(mmol·m<sup>-2</sup>·d<sup>-1</sup>)</i> |
|----------------|---|--|
| Mn             | 0.10  | 0.063  |
| Fe             | 1.6   | 0.26   |
| Co             | 5.7E-05   | 4.2E-05  |
| As             | 1.6E-03   | 4.4E-04  |
| Cr             | 6.2E-05   | 0  |
| Ni             | -1.2E-03  | 1.6E-04  |
| Cu             | 8.6E-05   | 5.4E-05  |
| Pb             | 0   | 0  |

Remobilization fluxes of trace metals at the SWI, estimated by “DGT pistons” placed at the SWI, were used to calculate fluxes based on the element concentrations in the DGT resin and on the DGT equation (equation 1). We estimated minimal fluxes with the assumption that all solutes moved with the speed of free ions through the DGT gel layer, while metal complexes move slower (Zhang, 2004). The fluxes correspond to the trace elements that can be mobilized in the sediment (including the labile fraction in the solid sediment phase) and that is vertically transported to the probe (TABLE 8).

TABLE 8. Remobilization fluxes of trace elements at the Sediment Water Interface in April 2008, calculated from pore water profiles and estimated by DGT pistons. The DGT piston values are average values obtained from 3 different deployment times: 2, 4 and 6 hours in different sediment cores. For most elements, Relative Standard Deviation is about 100% due to sample heterogeneity.

| <i>Element</i> | <i>Calculated flux<br/>(mmol·m<sup>-2</sup>·d<sup>-1</sup>)</i> | <i>DGT piston<br/>(mmol·m<sup>-2</sup>·d<sup>-1</sup>)</i> |
|----------------|---|--|
| Mn             | 0.063   | 0.10   |
| Fe             | 0.26  | 0.095  |
| Co             | 4.2E-05   | 4.4E-05  |
| As             | 4.4E-04   | 3.7E-04  |
| Cr             | 0   | 2.8E-04  |
| Ni             | 1.6E-04   | 3.0E-03  |
| Cu             | 5.4E-05   | 9.5E-04  |
| Pb             | 0   | 7.0E-05  |

The “DGT piston” fluxes and those calculated via the concentration gradients for Mn, Fe, Co As are within the same order of magnitude. For Cr, Ni, Cu and Pb fluxes are at least 10 times more elevated. In fact, the DGT piston acts as a “pump”

at the SWI and trace element concentrations may be directly measured. As the trace element concentrations at the SWI and the overlying water are zero (the "DGT piston" is placed at the SWI), the concentration gradient is maximized which is not always accomplished when exchange fluxes are calculated based on the vertical concentration profiles. For Mn, Fe, Co and As both fluxes are rather similar (Table 8) which can be explained by the fact that their dissolved phase concentrations are very low in the overlying water as a result of rapid oxidation and precipitation.

## 2.2.2. Field campaigns conclusions

The BCP sampling stations followed in the MICROMET project may be classified in three groups: sandy stations with a mean grain size (MGS) of 400  $\mu\text{m}$  (group I: DCG, 330 and 435), sandy stations with a MGS of 200  $\mu\text{m}$  (group II: 120, 230 [except 0-1 cm], ZG03), and muddy stations with a MGS of 12.5  $\mu\text{m}$  (group III: 130, 140 and 700). In group I sediments the consumption of oxidants does not occur efficiently (i.e., the oxygen penetration depth is important), probably due to the low quantity and bioavailability of organic matter at the water-sediment interface. In addition, the low specific area of the sediments does not encourage adsorption of bacteria (that are mostly restricted to the fine fraction in all stations). Oxygen and sulphates are not significantly reduced and only small quantities of CRS are detected. Low amounts of SEM have been measured (about 10 times lower than in the other sites) but the low contents of AVS may result in a positive toxicity index.

In group III sediments, oxygen is completely consumed within the first mm and the Eh values drop to about -200 mV within the first cm. Production of dissolved and solid sulfides confirms sulfate-reducing activities, mostly in the first cm. Concentrations of Pb, Cu and Zn in SEM are generally more than 10 times lower compared to the AVS, which means that sulfides might act as a sink for the metals present. However, as demonstrated by the DET/DGT analyses, metallic pollutants are nevertheless present in the pore waters of these stations and may therefore be released in the water column. In group II sediments, oxygen is consumed in the first cm and Eh values decrease more slowly than in the muddy stations.

The February 2007 data suggested that bacterial diversity increased from the coast (group III sediments) to the open sea (group I sediments). Indeed, the raw diversity DGGE values were never low in offshore stations DCG and 435 (always >16 DGGE bands) and the lowest values (6 DGGE bands) were always observed in coastal stations. In addition, no Archaea could be obtained by PCR in coastal stations; on the contrary, many archaeobacterial sequences were obtained offshore, in sediments of stations DCG and 435. Reduced diversity in sediments from coastal areas on the BCP was also observed in other studies for Metazoa such as Nematods and harpacticoid copepods (e.g., Vincx 1990). However, a reduced bacterial diversity may also be explained by the inhibition of the PCR by contaminants (this is very frequent with contaminated sediments). It should also be noted that bacterial diversity may be elevated in coastal stations (e.g., the sandy station 120 in February 2007 and the metal contaminated station 130 in July 2007). This means that the situation is much more complex than initially thought and that the observed trend is not valid for all sediment types and/or only valid for some periods of the year. Other methods of DNA extractions must also be tested in the future.

Multivariate analyses of the eukaryotic DGGE data of 2007 also show pronounced changes in community (phylotype) composition with sediment type

(group I-III). No strong shifts in diversity between the group I and group III sediments were observed. This may be due to the fact that deposited diatom cells are preserved in the group III sediments which increases diversity.

In 2008, eubacterial and eukaryotic taxon richness and relative DGGE band intensities were followed monthly in two stations (130 & 700) from the sediment/water interface up to -10 cm of depth, from February to July. Results show that the relative DGGE band intensities change with sediment depth and that reproducibility was good between the replicate cores. Ordination analyses reveal pronounced changes in both bacterial and eukaryotic community composition with season and depth. Eh and pH were the dominant factors structuring the communities, but interestingly the metals as well had a significant, independent impact on the microeukaryotic community structure. Of course, we cannot completely rule out that other, unmeasured factors, which correlate with the metals, actually caused the structural changes observed.

From the 2007 and 2008 data we can conclude that microbial diversity, as measured with DGGE, is not a variable that can be easily related to the environmental variables considered in this study. This might be a result of methodological biases (i.e., DGGE biases) but also to the fact that the studied communities are probably adapted to elevated metal concentrations. Indeed, high diversity values were observed in contaminated sediments of station 130 in July. High diversities in metal contaminated sediments were also observed in other parts of the world (e.g., Gillan et al. 2005). In addition, organic contaminants are also abundant on the BCP. For instance, sediments on the BCP have PCB levels ranging from 0.23 to 10.6  $\mu\text{g g}^{-1}$  (sum of 6 PCBs, Danis et al. 2004). To sum up, bacterial diversity cannot be simply related to metal contamination in the field. Future studies should concentrate on metal bioavailability (not determined in this study), metal resistance, and other methods of biodiversity measurement should be tested.

Contrary to biodiversity, bacterial biomass (DAPI counts) is a variable that displayed elevated and significant correlations to some environmental variables, particularly to dissolved Mn, Fe and As. This is not surprising as these metals may serve as electron donors or acceptors depending on their oxidation state (Canfield et al. 2005). With the exception of arsenic, these metals are also essential components of metalloenzymes and electron transport systems (Beinert et al. 1997, Kendrick et al. 1992). Bacterial biomass was also significantly correlated to chlorophyll *a*. This may be explained by the proliferation of bacteria on decaying phototrophic micro-eukaryotes such as diatoms and *Phaeocystis*.

Bacterial rRNA sequencing (February 2007 samples) has shown that 5 to 10 major bacterial groups are present in the BCP sediments examined (DCG, 435, 130, 700). Three major groups were present in all the four stations examined ( $\gamma$ -Proteobacteria,  $\delta$ -Proteobacteria and CFB bacteria). Acidobacteria represent 2.6–14.6% of the clones in most of the stations. For micro-eukaryotes, 18S rDNA based DGGE of February 2007 samples revealed a surprisingly high diversity of microbial eukaryotes, mainly comprising Stramenopiles (diatoms), as yet unidentified (or ambiguously identified) marine eukaryotes and Fungi, but also Protozoa and microalgae belonging to other groups. The DGGE procedure also picked up many Metazoan sequences. In 2008, the use of Protozoa-specific primer sets (for Cercozoa and Ciliates) in combination with full length 18S rDNA CL allowed a more detailed identification of the protozoan communities present.

With the DET/DGT approaches, high resolution profiles of trace metals in the sediments were obtained. The general good correspondence between the DET and

centrifuge technique proved that reliable data are produced with our sampling approach. Trace elements present a variable geochemical behavior in the sediments, confirming that remobilization is occurring at specific depths. Seasonal variations of elements (Mn, Fe, As) have been observed during the cruises in 2007 and 2008. Although variations in the oxygen concentration and redox potential may explain most of the patterns obtained, microorganisms are important as well (see results of the LABOSI-4 experiment). There is apparently no depletion of trace elements in the sediment porewaters at station 130 and 700. The flux calculations based on DGT profiles show that elements such as Mn, Fe, Co, As and Ni might diffuse out of the sediment into the overlying water column at least for station 130. Flux calculations based on the DGT piston experiments confirm that metallic toxicants may reach the SWI and be released in the seawater. This might be detrimental for the benthic ecosystem. Other metallic toxicants such as Cu, Zn, and Cd will diffuse inside the sediments in station 130.

### **2.2.3. Laboratory simulation approaches**

#### **2.2.3.1. LABOSI-1 experiment**

In this experiment, the effect of sediment mixing was evaluated. 72h after hand mixing of the sediments, the Eh profiles of the incubated sediments were very different from those observed in the field (i.e., undisturbed sediments). The same situation was observed after 7 days of incubation (data not shown).

Before hand mixing of the sediments, the composition of the bacterial community varied with depth (i.e., the 0-1 cm section was different from the 4-5 cm section). After mixing, the composition of the sediments was clearly affected with new bands appearing in the 0-1 cm section. These bands were still present 168h after homogenization of the sediments. For micro-eukaryotes, DNA extractions were performed at Day 0 (before mixing) and at Day 7 (7 days after mixing of the sediments). DGGE was performed on all sediment horizons. Seven days after homogenization of the sediments diversity was not significantly different from the diversity of the controls (presence/absence of DGGE bands). Shifts were nevertheless observed in the vertical distribution of the DGGE bands (intensity of DGGE bands). This means that mixing of the sediment leads to changes in community composition (and so to an artificial situation) and that the sediments do not recover after 7 days of incubation.

Some DET/DGT measurements were performed in the field using intact sediment cores and other measurements were performed in the laboratory after mixing of the sediments (3, 5 and 7 days after mixing). After mixing, metal profiles did not recover after 7 days of incubation at 11°C (when compared to the field situation). Concentration values observed at the seawater-sediment interface (SWI) after 7 days were also very different from the field situation. The same conclusions may be drawn for DGT measurements.

For LABOSI-1, the effect of sediment mixing was thus clearly visible for metals assessed by DET. When compared to the field situation, the maximum concentrations were lower after mixing. In the field, the reduction zone of the oxygen-sensitive elements appeared beneath the SWI (-1 cm for Mn and Co, -3 cm for Fe

and As). This reduction zone disappeared after mixing of the sediments and trace metal profiles did not recover.

### 2.2.3.2. LABOSI-2 experiment

For this experiment undisturbed sediments were exposed to a culture of early spring diatoms during 14 days. The exposure had no significant effects on the Eh and pH (not shown). The bacterial communities living at the interface (0-3 mm) were analysed and 11 DGGE bands were followed. No significant differences were observed between controls and experimental microcosms (data not shown). The eukaryotic microbial communities living in the upper sediment layer (0-1 cm) were analyzed. The composition of the communities was not affected by the different treatments (not shown).

The bacterial biomass was significantly affected at Day-0 (from  $1 \times 10^9$  to  $0.4 \times 10^9 \text{ mL}^{-1}$ ) and Day-5 (from  $0.6 \times 10^9$  to  $0.2 \times 10^9 \text{ mL}^{-1}$ ), with significantly less bacteria in experimental microcosms (not shown). All other changes were not significant, and biomass was maintained between  $0.2 \times 10^9$  and  $0.6 \times 10^9 \text{ mL}^{-1}$  up to Day-15. For nanoflagellate counts, no significant differences were observed during LABOSI-2 (Figure 24). Biomass was maintained at ca.  $1 \times 10^6 \text{ mL}^{-1}$ .

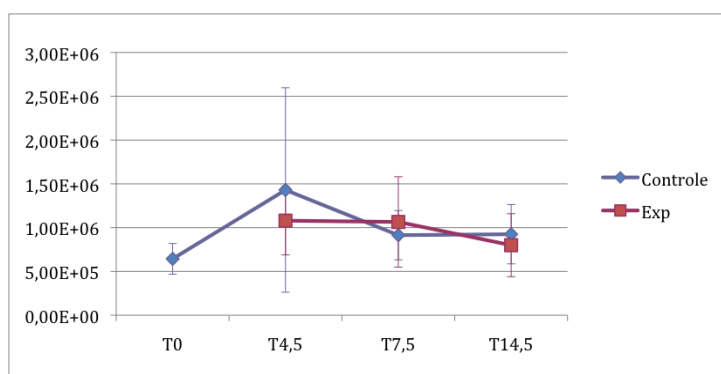


Figure 24. DAPI-counts for nanoflagellates during LABOSI-2, at day 0 (T0), day 4,5 (T4,5), day 7,5 (T7,5) and day 14,5 (T14,5).

Sulfides were  $<0.5 \mu\text{mol L}^{-1}$  in the first 6 cm of each microcosm. No differences were observed between control and experimental microcosms. During LABOSI-2, DET/DGT measurements were only performed in the microcosms (not in the field). No differences have been observed between control and experimental sediments after the incubation period (results not shown). DOC was measured during the 14 days of incubation. No significant differences were observed between controls and experimental microcosms and a general decrease of the DOC was observed during the incubation, from 30 to 10 ppm (not shown). Chlorophyll a values were higher in the top layer (0-1cm) of the microcosms where the diatoms were accumulated by sedimentation (Figure 25).

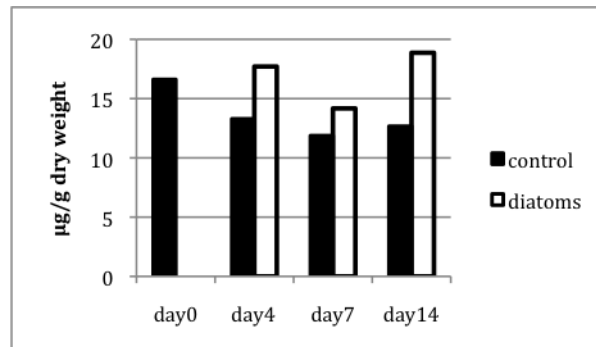


Figure 25. Chlorophyll a values ( $\mu\text{g g}^{-1}$  dw) in LABOSI-2.

During LABOSI-2, benthic fluxes were also measured using 4 sediment cores ( $\varnothing$  9 cm) maintained in an incubator (Figure 26). Two sediment cores received the diatom culture mix (4 cm of overlying water with diatoms corresponding to  $0.39 \mu\text{g chlorophyll a cm}^{-2}$ ), whereas the two remaining cores were used as controls. The 4 cores were kept during 2 weeks in the dark at  $4^\circ\text{C}$  in an incubation chamber at the Lille-1 University. Incubation experiments were carried out during 8 hours at days 0, 5, 7 and 15. The values of the benthic fluxes are summarized in TABLE 9.

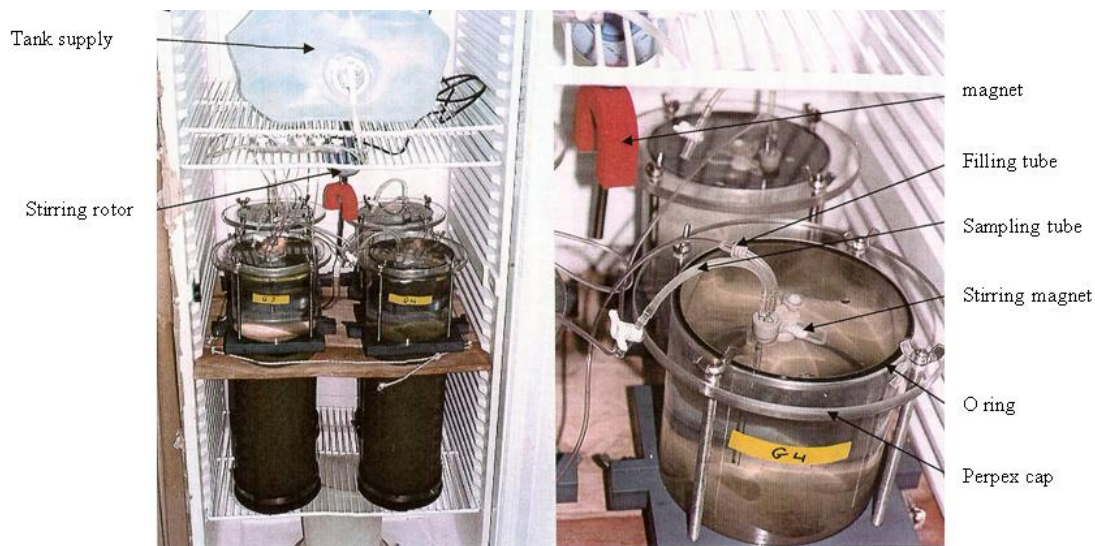


Figure 26. LABOSI assembly installed in a cooled incubator, from Denis (1999).

A summary of the fluxes obtained during the LABOSI-2 experiment are presented in TABLE 10. Overall, a general good agreement between diffusive and benthic fluxes was observed. However, the presence of the diatoms did not affect metal fluxes through the water-sediment interface.

Before and after the incubation procedure, several cores were cut every cm under nitrogen in order to extract porewater by centrifugation. Alkalinity and trace metals concentrations have then been measured (Figure 27).

TABLE 9. Values of the benthic fluxes (expressed in  $\text{nmol.m}^{-2}.\text{h}^{-1}$ ) estimated for the LABOSI-2 experiment. OM, organic matter.

| LABOSI II      |                    |                |            |          |
|----------------|--------------------|----------------|------------|----------|
| Element        | nature of the flux | averaged value | confidence | remark   |
| O <sub>2</sub> | negative           | -40000         | high       | -        |
| Alk            | positive           | 2000000        | high       | -        |
| As             | positive           | 200            | low        | -        |
| Cd             | positive           | 2              | medium     | -        |
| Co             | positive           | 5              | high       | if no OM |
| Cr             | positive           | 50             | medium     | if OM    |
| Cu             | -                  | -              | -          | -        |
| Fe             | positive           | 3000           | high       | -        |
| Mn             | positive           | 4000           | medium     | -        |
| Ni             | -                  | -              | -          | -        |
| Pb             | -                  | -              | -          | -        |
| V              | negative           | -60            | high       | if no OM |
| Zn             | negative           | -600           | high       | if no OM |

TABLE 10. Summary of the fluxes obtained during the LABOSI-2 experiment.

| LABOSI II |                    |                    |                         |
|-----------|--------------------|--------------------|-------------------------|
| Element   | Incubation         | Profiles           | Profile shape           |
|           | nature of the flux | nature of the flux |                         |
| As        | <b>positive</b>    | <b>positive</b>    | interface dissolution   |
| Cd        | <b>positive</b>    | -                  | no trend                |
| Co        | <b>positive</b>    | <b>positive</b>    | interface dissolution   |
| Cr        | <b>positive</b>    | -                  | progressive dissolution |
| Cu        | -                  | -                  | no trend                |
| Fe        | <b>positive</b>    | <b>positive</b>    | interface dissolution   |
| Mn        | <b>positive</b>    | <b>positive</b>    | interface dissolution   |
| Ni        | -                  | <b>positive</b>    | interface dissolution   |
| Pb        | -                  | -                  | no trend                |
| V         | <b>negative</b>    | <b>negative</b>    | progressive dissolution |
| Zn        | <b>negative</b>    | <b>negative</b>    | interface dissolution   |

### 2.2.3.3. LABOSI-3 experiment

In this experiment sediments were exposed to an experimental *Phaeocystis* bloom during 7 days. Sediments were undisturbed. The exposure had no significant effect on the Eh and pH of the sediments and the composition of the bacterial communities living at the interface (0-3 mm) was not affected by the treatment. A DGGE band corresponding to *Phaeocystis* was present at Day-7 in the experimental microcosms. This band was absent from the controls indicating that *Phaeocystis* was successfully accumulated at the interface. Similarly, the composition of the eukaryotic communities was not affected by the treatments (not shown). The microbial biomass (bacteria and micro-eukaryotes) was not significantly affected by the treatments after 7 days of incubation (data not shown).

Sulfides were  $<0.5 \mu\text{mol L}^{-1}$  in the first 6 cm of each microcosm. No differences were observed between control and experimental microcosms. The

concentrations profiles of Mn and Co assessed by DET and DGT were significantly increased in the overlying water of the microcosms containing *Phaeocystis* (Figures 27–28). This was not the case for other elements. No effects were observed in the sediments for these metals.

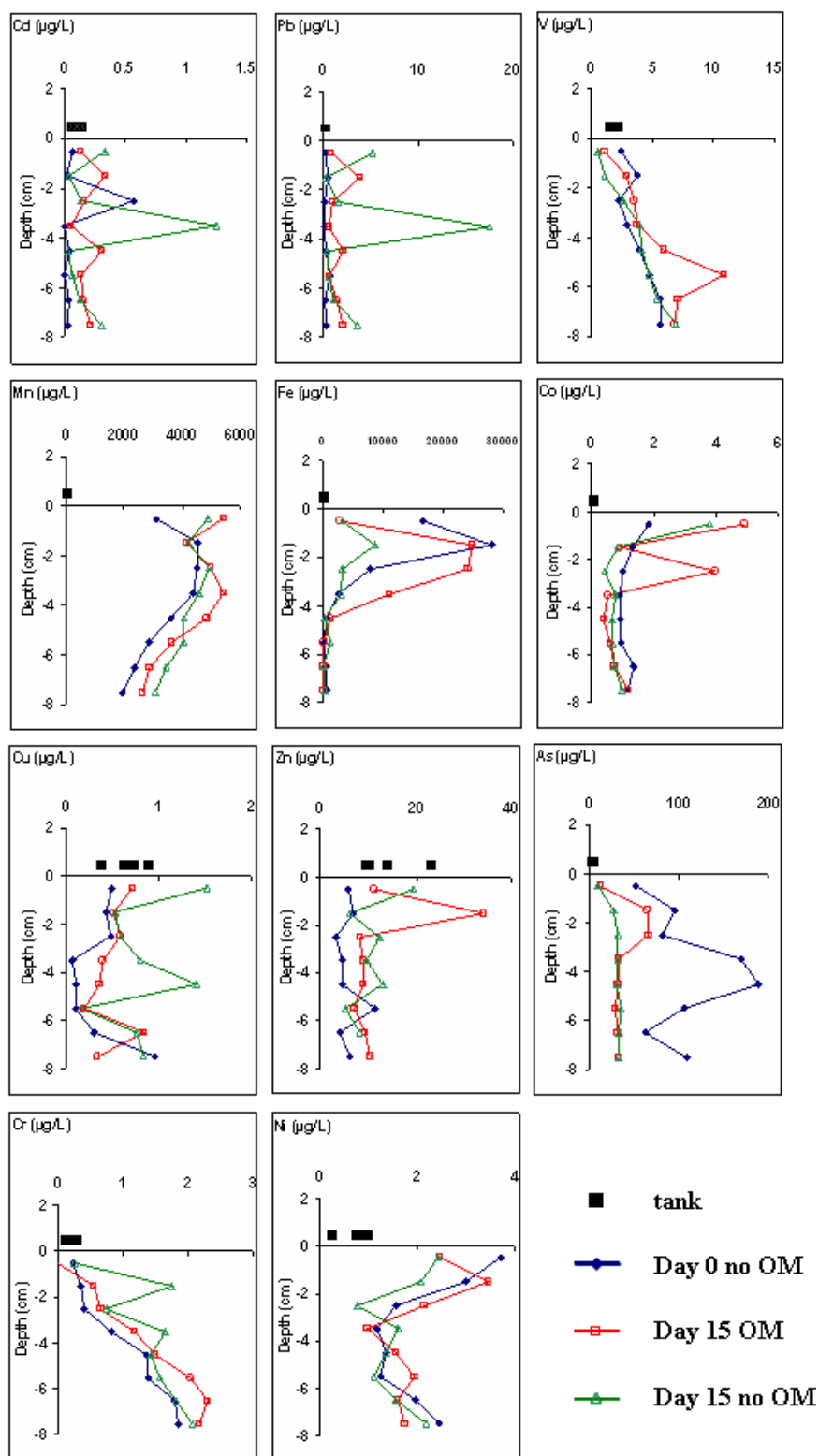


Figure 27. Concentration profiles of Cd, Pb, V, Mn, Fe, Co, Cu, Zn, As, Cr and Ni in porewaters of sediments that have been used for the incubation experiments during LABOSI-2 (except for the profile Day 0 : no organic matter, OM).

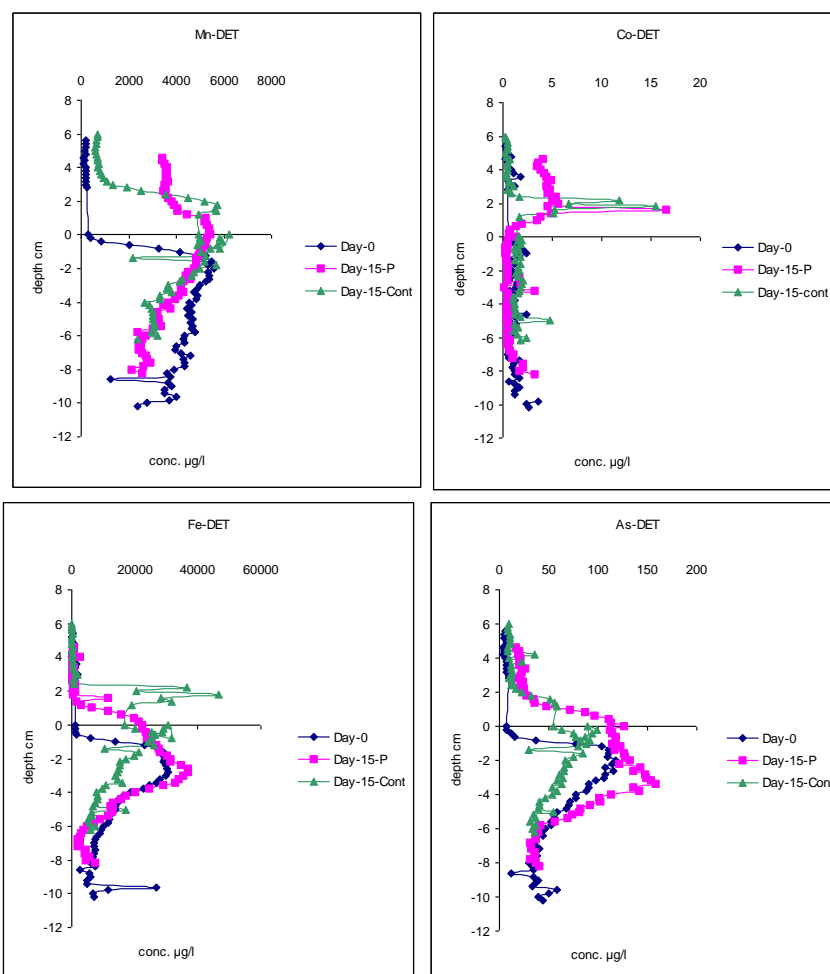


Figure 27. Mn, Fe, Co As profiles assessed by DET technique during the LABOSI-3 experiment. Blue line (diamonds) represents the DET profiles of trace metal assessed at Day-0 before *Phaeocystis* deposition on the sediments; pink line (squares) represents the DET profiles 7 days after *Phaeocystis* deposition; green line (triangles) displays the DET profiles for the controls.

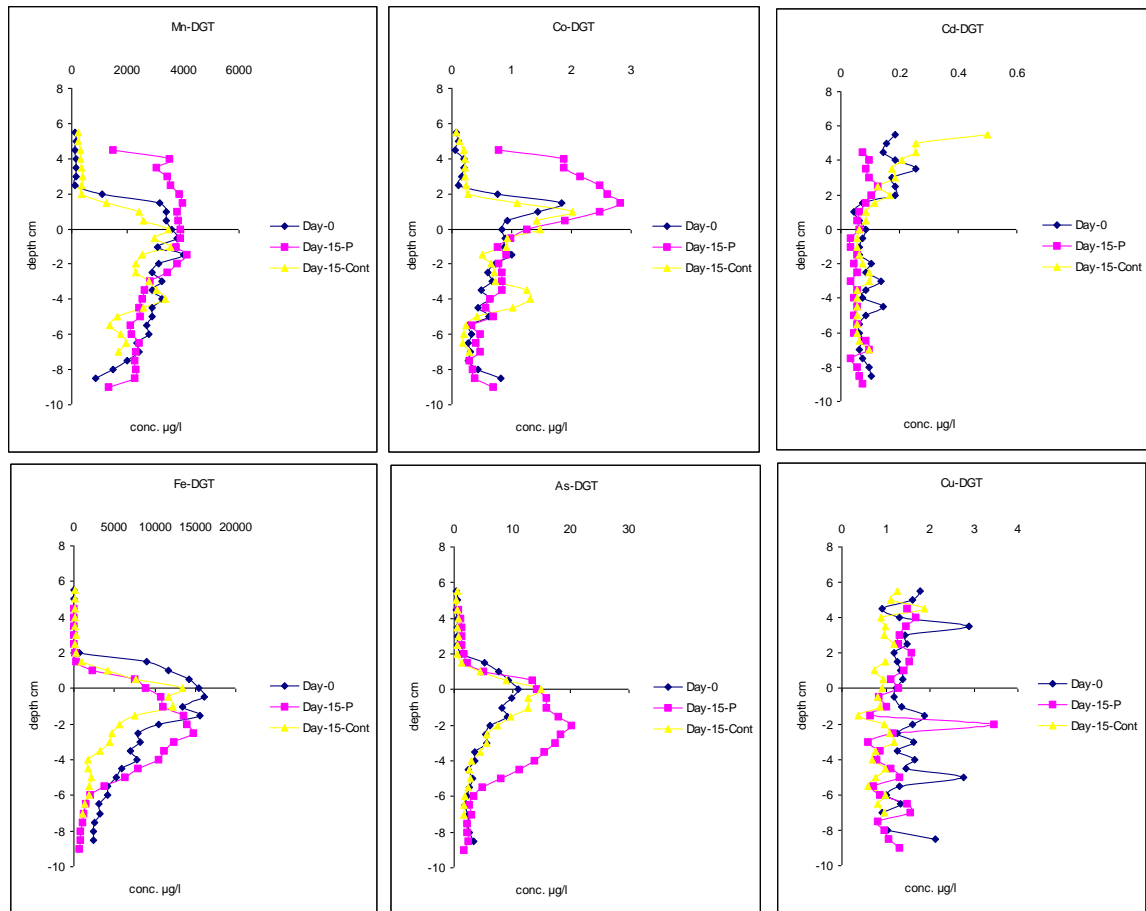


Figure 28. Mn, Co, Fe, As, Cd and Cu profiles assessed by DGT technique during the LABOSI-3 experiment. Blue line (diamonds) represents the DET profiles of trace metal assessed at Day-0 before *Phaeocystis* deposition on the sediments; pink line (squares) represents the DET profiles 7 days after *Phaeocystis* deposition; yellow line (triangles) displays the DET profiles for the controls.

DOC was measured during the 7 days of incubation. Values were < 50 ppm in all microcosms. A significant increase (mean: 180 ppm) was observed at Day-7 only in experimental microcosms.

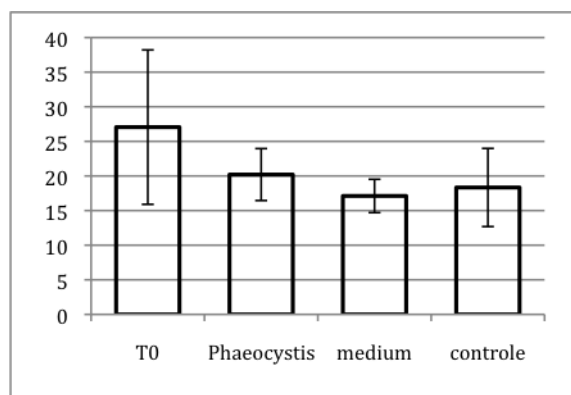


Figure 29. Chlorophyll a values (µg/g dw) in LABOSI-3 (right). Bars indicate standard deviation (n=3).

Chlorophyll *a* values (Figure 29) were highest at the start of the experiment ( $T_0$ ) (but standard deviation was high), and were decreased at Day-7. No significant difference were observed between microcosms treated with *Phaeocystis*, the medium and the control (=seawater). This is surprising because in the microcosms treated with *Phaeocystis*, higher chlorophyll *a* (or phaeopigments) values were expected.

Compared to LABOSI-2, the rate of oxygen consumption was about two times higher. The impact of *Phaeocystis* was not significant. The biological oxygen demand (BOD) is related to the temperature and probably to the quantity of bioavailable organic matter in the sediments. Particulate organic carbon (POC) should be measured to check this latter hypothesis. Alkalinity fluxes displayed high positive values, especially in the core treated with *Phaeocystis* (Figure 30). This finding has been confirmed by the alkalinity profiles obtained in the porewaters of the sediments: at the interface, the value of alkalinity in the core was about 10 times higher than in the controls.

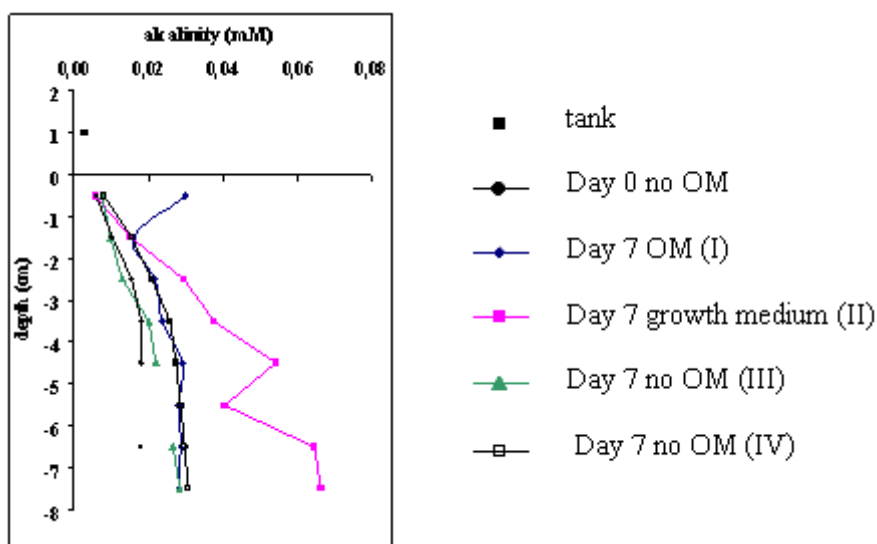


Figure 30. Alkalinity profiles in the cores during LABOSI-3 experiment.

Metal fluxes for LABOSI-3 were also calculated. Fluxes values were comparable to those obtained during the LABOSI-2 experiment. Fluxes were generally higher except for Mn where the averages were similar. For Ni, some fluxes were measurable and were positive (average located at  $100 \text{ nmol m}^{-2} \text{ h}^{-1}$ ). In comparison to LABOSI-2, only a few values were significant because less incubation experiments could be performed. A summary of the fluxes obtained during the LABOSI-3 experiment are presented in TABLE 11. Overall, a general good agreement between diffusive and benthic fluxes was observed. However, the presence of *Phaeocystis* did not affect metal fluxes through the water-sediment interface.

TABLE 11. Summary of the fluxes obtained during the LABOSI-3 experiments.

| LABOSI III |                    |                    |                         |
|------------|--------------------|--------------------|-------------------------|
| Element    | Incubation         | Profiles           | Profile shape           |
|            | nature of the flux | nature of the flux |                         |
| As         | positive           | positive           | interface dissolution   |
| Cd         | positive           | -                  | no trend                |
| Co         | positive           | positive           | interface dissolution   |
| Cr         | positive           | -                  | progressive dissolution |
| Cu         | -                  | -                  | no trend                |
| Fe         | positive           | positive           | interface dissolution   |
| Mn         | positive           | positive           | interface dissolution   |
| Ni         | positive           | positive           | interface dissolution   |
| Pb         | -                  | -                  | no trend                |
| V          | negative           | -                  | progressive dissolution |
| Zn         | -                  | -                  | no trend                |

Profile of metal concentrations were also determined in the sediments for LABOSI-3 (Figure 31). For Cd, Cu, Pb and Zn, several values were completely different than the others, probably because of contamination problems and/or problems of detection. For the other profiles, the shapes found for the 5 cores were quite similar: V and Cr exhibited a slow increase all along the cores, whereas Ni got the opposite trend. Co and Mn were released in the first millimetres of the sediments and were strongly reabsorbed and/or (co)precipitated just below at 1-2 cm of depth. Finally, As was released in the pore waters at the same depth that Fe, but Fe precipitated, probably with sulfides just below, whereas As concentration decreased slowly or raised a plateau at about  $100 \mu\text{g L}^{-1}$  at the bottom of the sediment core. Overall, the shapes of these profiles were quite similar to those obtained during the LABOSI-2 experiment (similar directions have been obtained for the fluxes). Finally, addition of organic matter (*Phaeocystis*) at the surface of the sediments did not result in any change of the metal fluxes at the water-sediment interface.

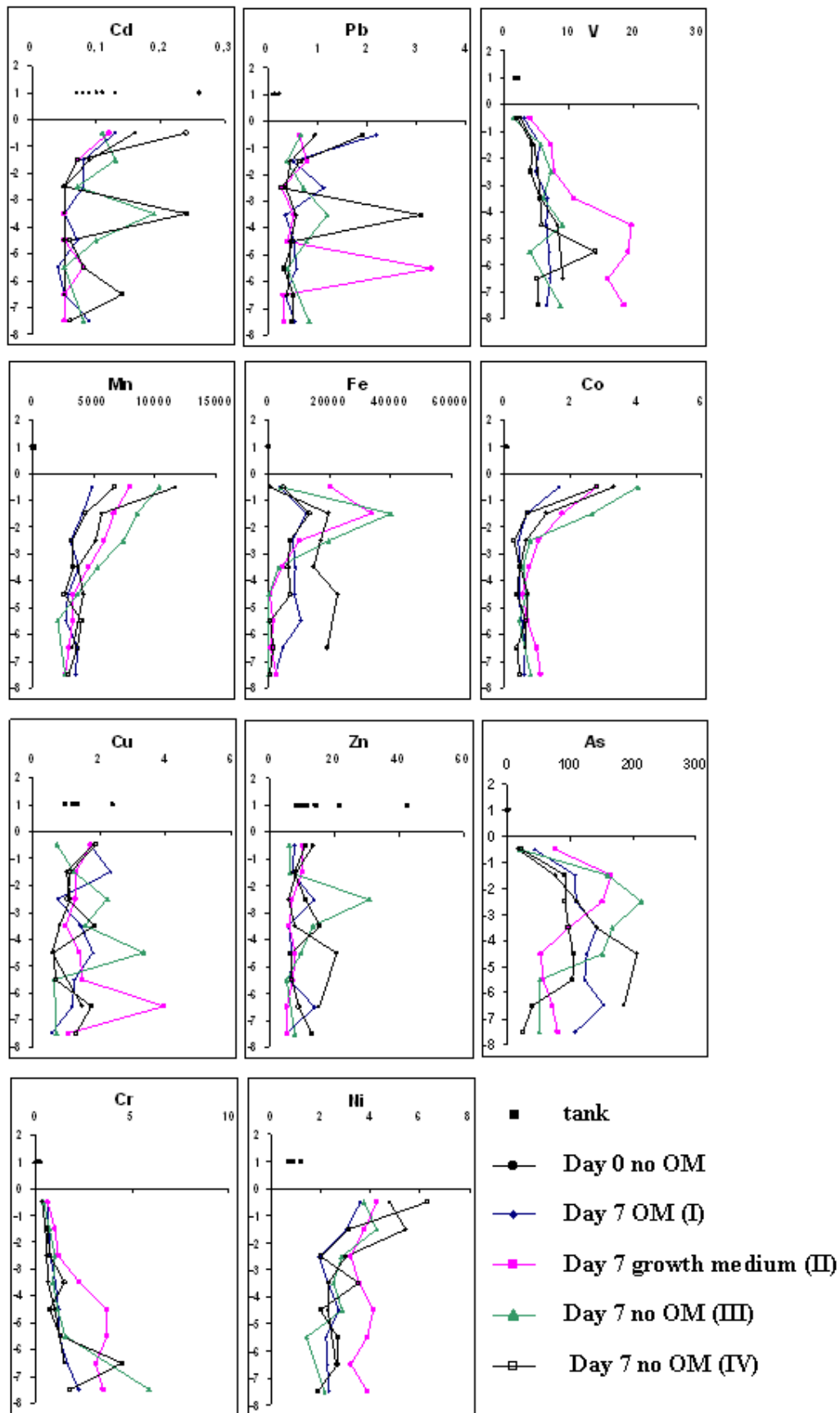


Figure 31. Concentration profiles of Cd, Pb, V, Mn, Fe, Co, Cu, Zn, As, Cr and Ni in the porewaters of sediments that have been used for the incubation experiments during LABOSI-3 (except for the profile Day 0 : no organic matter, OM).

#### 2.2.3.4. LABOSI-4 experiment

The algal suspension was added on Day-0 in half of the microcosms and samples were taken after 2h (Day-0), 2 days (Day-2) and 7 days (Day-7). A slight but significant acidification was observed at the sediment-seawater interface on Day-2 and Day-7 in the microcosms that received algae: the initial pH values were 7.9 at the beginning of the incubation and dropped down to 7.7-7.8 after one week (data not shown). No effects of algae addition were noticed on the redox potential or on the oxygen levels of the overlying waters: Eh values around 200 mV were observed up to -0.5 cm into the sediments for all microcosms, and values dropped to -130 mV at -1.5 cm of depth (not shown). Oxygen levels, measured at 5 mm above the sediments, were maintained at an average of 5 mg L<sup>-1</sup> throughout the experiment with no significant differences between experimental and control microcosms. Similarly, salinity was stable, with values of 30.0 ± 0.5‰ in all microcosms.

The chlorophyll a content of the sediments was measured at the seawater-sediment interface (TABLE 12). All sediment cores presented a background chlorophyll a concentration around 20 µg g<sup>-1</sup> (dw). The introduction of phytodetritus into the experimental microcosms was clearly visible; after 2h values of chlorophyll a significantly increased to 30 µg g<sup>-1</sup>. After 2 and 7 days, chlorophyll a values were respectively 1.8 and 1.6 more elevated in the experimental microcosms than in the controls.

TABLE 12. Chlorophyll a in 0-5 mm sediments (mean ± SD; µg g<sup>-1</sup> dw). Different letters (a, b) indicate significant differences between controls and treatment (Student t-test, α = 0.05).

|                 | 2h           | Day-2        | Day-7        |
|-----------------|--------------|--------------|--------------|
| <b>Controls</b> | 19.7 ± 1.4 a | 22.4 ± 3.6 a | 21.9 ± 2.2 a |
| <b>Algae</b>    | 30.3 ± 3.1 b | 41.6 ± 1.3 b | 35.2 ± 4.0 b |

Values of DOC in the 0-5 mm porewaters are shown in TABLE 13. Although mean DOC values of the experimental microcosms clearly increased with the incubation time, which is indicative of a mineralization process, no significant differences were found (variability between replicate microcosms was particularly high on Day-7).

TABLE 13. DOC in 0-5 mm sediments (mean ± SD; mg L<sup>-1</sup>). Different letters (a, b) indicate significant differences between controls and treatment (Student t-test, α= 0.05).

|                 | 2h           | Day-2        | Day-7        |
|-----------------|--------------|--------------|--------------|
| <b>Controls</b> | 17.3 ± 5.2 a | 14.6 ± 2.8 a | 17.2 ± 1.3 a |
| <b>Algae</b>    | 16.8 ± 0.5 a | 18.1 ± 1.5 a | 24.1 ± 5.4 a |

Bacterial DAPI counts are listed in TABLE 14. Bacterial counts did not evolve during 48h (the differences between controls and experimental microcosms were not significant). At Day-7 bacterial counts were significantly higher (1.3 times) in the experimental microcosms. DAPI counts of nanoflagellates are shown in TABLE 15.

Only on Day-2 these counts were significantly higher (1.4 times) in the experimental microcosms.

TABLE 14. Bacterial DAPI counts ( $\times 10^9$ ) in 0-5 mm sediments (mean  $\pm$  SD; cells  $\text{g}^{-1}$  dw). Different letters (a, b) indicate significant differences (t-test,  $\alpha = 0.05$ )

|                 | 2h               | Day-2            | Day-7            |
|-----------------|------------------|------------------|------------------|
| <b>Controls</b> | 4.0 $\pm$ 0.73 a | 3.0 $\pm$ 0.27 a | 2.9 $\pm$ 0.31 a |
| <b>Algae</b>    | 5.1 $\pm$ 1.6 a  | 4.1 $\pm$ 0.85 a | 3.8 $\pm$ 0.44 b |

TABLE 15. DAPI counts of nanoflagellates ( $\times 10^6$ ) in 0-5 mm sediments (mean  $\pm$  SD; cells  $\text{mL}^{-1}$ ). Different letters (a, b) indicate significant differences (t-test,  $\alpha = 0.05$ ).

|                 | 2h              | Day-2           | Day-7           |
|-----------------|-----------------|-----------------|-----------------|
| <b>Controls</b> | 8.4 $\pm$ 2.7 a | 4.5 $\pm$ 0.2 a | 6.1 $\pm$ 1.1 a |
| <b>Algae</b>    | 5.6 $\pm$ 2.4 a | 6.2 $\pm$ 0.7 b | 5.7 $\pm$ 1.4 a |

Metals released into the overlying waters were monitored by HR-ICP-MS throughout the experiment (Figure 32). After two hours of exposure to the algal suspension a significant increase of the metal concentration was observed for Cd, Co and As. After two days of exposure (Day-2) the concentrations of four metals were significantly higher in the overlying water of the experimental microcosms when compared to the controls: Cd ( $\times 2.7$ ), Co ( $\times 5.6$ ), Mn ( $\times 13.8$ ), and As ( $\times 1.8$ ). After 7 days of exposure no differences were observed in the overlying waters between controls and experimental microcosms (Figure 32).

Exchange fluxes (in  $\text{mol m}^{-2} \text{d}^{-1}$ ) were calculated and are presented in TABLE 16. During the first 48 hours, 4 measured metals in experimental microcosms (As, Cd, Co and Mn) presented fluxes that differed significantly from those observed in the control microcosms. For As, Co and Mn, large negative fluxes (i.e., effluxes, from sediments to overlying water) were observed in the experimental microcosms. These negative fluxes reached  $-1084 \text{ nmol m}^{-2} \text{d}^{-1}$  for As,  $-512 \text{ nmol m}^{-2} \text{d}^{-1}$  for Co, and  $-755 \text{ } \mu\text{mol m}^{-2} \text{d}^{-1}$  for Mn. A positive flux was noticed for Cd (i.e., towards the sediments). For the other metals (Pb, Fe, Ni, Cu and Zn) no differences were observed between control and experimental microcosms and fluxes were either negative or positive (TABLE 16A). During the last 5 days (Day-2 to Day-7) only 2 measured metals in experimental microcosms (As and Cd) presented fluxes that differed significantly from those measured in the control microcosms (TABLE 16B). For As in the experimental microcosms, fluxes were less negative than during the first 48 hours and some microcosms displayed large positive fluxes ( $+262 \text{ nmol m}^{-2} \text{d}^{-1}$ ). For Cd, fluxes were still positive but less elevated than during the first 48 hours.

The mineralization activity of the microbial community was first assessed using the Biolog EcoPlate system (CLPP approach). Mineralization was clearly visible, with a total of 15 enzymatic activities that differed significantly between control and experimental microcosms (Figure 33). The majority of these activities (13 over 15) were more elevated in the experimental microcosms by a factor 1.3 to 15.1 and occurred on Day-2 and Day-7. Only two activities were significantly reduced (on Day-2, by a factor 0.6-0.8). Microbial mineralization already started after 2h of incubation as indicated by the significant increase of three enzymatic activities (Figure 33). The

mineralization activity of the microbial community was also studied using the FDA approach. The FDA approach indicated that the esterase activity progressively increased from Day-0 to Day-7 (Figure 34) with an esterase activity that was 1.9 times more elevated at Day-7 in the experimental microcosms than in the controls.

Finally, bacterial production during the incubation of the microcosms was evaluated by the incorporation of tritiated thymidine. Values were stable in the control microcosms and ranged between 0.2 and 0.8 mg C m<sup>-2</sup> d<sup>-1</sup> (Figure 35). In the experimental microcosms values were significantly more elevated, especially on Day-2 when a maximum was observed at 8.7 mg C m<sup>-2</sup> d<sup>-1</sup>. This value was at least 10 times more elevated than in the controls.

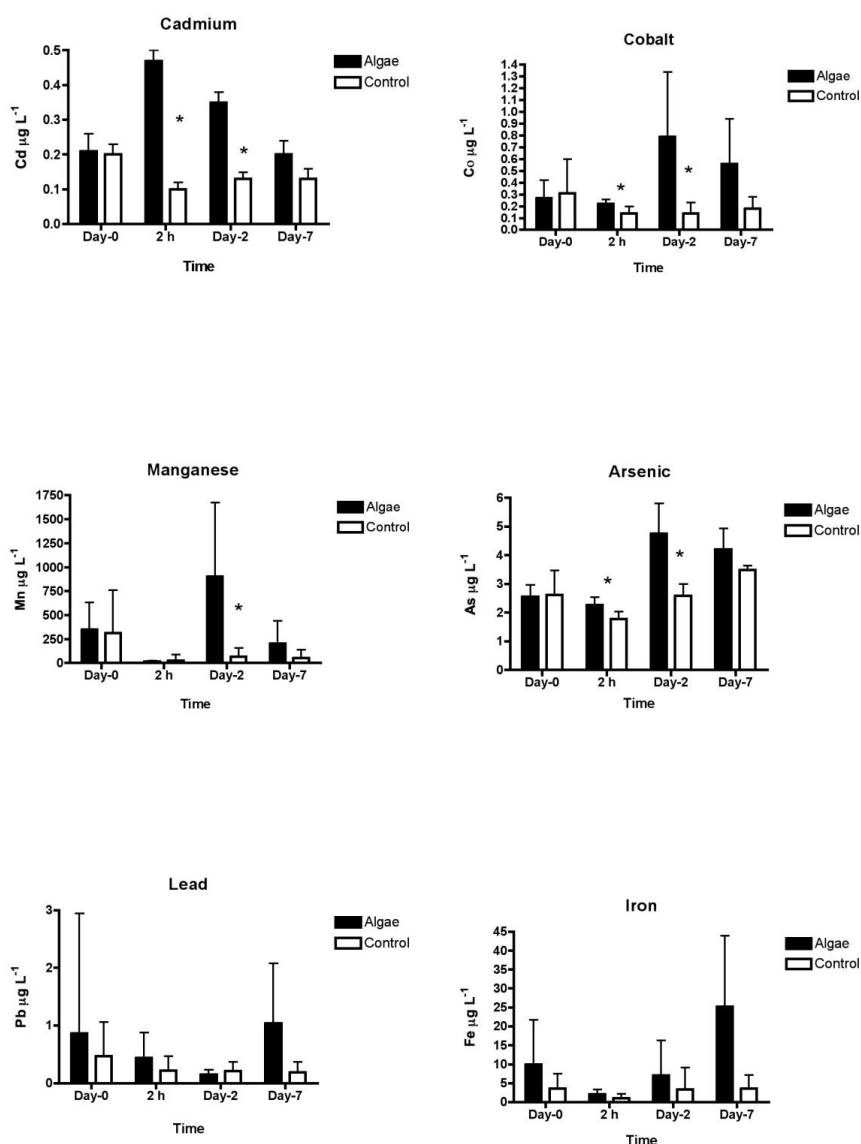


Figure 32. Metals in the overlying water as measured by ICP-MS (mean  $\pm$  SD). Significant differences are indicated by an asterisk (Student t-test,  $\alpha = 0.05$ ). Day-0 represents the overlying water at the end of the 10-days stabilization period, i.e. before the start of the experiment; this overlying water was then eliminated and replaced by the algal suspension or fresh seawater for controls.

TABLE 16 Exchange fluxes (negative values are from sediments to overlying water) in mol m<sup>-2</sup> d<sup>-1</sup> calculated using metal concentrations in overlying waters. Minimum and maximum values obtained from 6 microcosms (A) or 3 microcosms (B) are indicated. Significant differences between algae and controls are indicated in boldface (Mann-Whitney U test, two-tailed,  $\alpha=0.05$ ).

| <b>A. Between Day-0 and Day-2</b> |                                |                                |                                |                                |
|-----------------------------------|--------------------------------|--------------------------------|--------------------------------|--------------------------------|
|                                   | Algae                          |                                | Controls                       |                                |
|                                   | Min                            | Max                            | Min                            | Max                            |
| <b>As</b>                         | <b>-1084 x 10<sup>-9</sup></b> | <b>-349 x 10<sup>-9</sup></b>  | <b>-266 x 10<sup>-9</sup></b>  | <b>+ 115 x 10<sup>-9</sup></b> |
| <b>Cd</b>                         | <b>+11 x 10<sup>-9</sup></b>   | <b>+30 x 10<sup>-9</sup></b>   | <b>-12 x 10<sup>-9</sup></b>   | <b>-3.5 x 10<sup>-9</sup></b>  |
| <b>Co</b>                         | <b>-512 x 10<sup>-9</sup></b>  | <b>-34 x 10<sup>-9</sup></b>   | <b>-47 x 10<sup>-9</sup></b>   | <b>+51 x 10<sup>-9</sup></b>   |
| <b>Mn</b>                         | <b>-755 x 10<sup>-6</sup></b>  | <b>-89.1 x 10<sup>-6</sup></b> | <b>-77.4 x 10<sup>-6</sup></b> | <b>+46.2 x 10<sup>-6</sup></b> |
| Pb                                | -1.9 x 10 <sup>-9</sup>        | +123 x 10 <sup>-9</sup>        | -36 x 10 <sup>-9</sup>         | +8.7 x 10 <sup>-9</sup>        |
| Fe                                | -7.1 x 10 <sup>-6</sup>        | +0.5 x 10 <sup>-6</sup>        | -4.7 x 10 <sup>-6</sup>        | +0.1 x 10 <sup>-6</sup>        |
| Ni                                | -1.0 x 10 <sup>-6</sup>        | +0.2 x 10 <sup>-6</sup>        | -0.2 x 10 <sup>-6</sup>        | -0.1 x 10 <sup>-6</sup>        |
| Cu                                | -130 x 10 <sup>-9</sup>        | +848 x 10 <sup>-9</sup>        | -225 x 10 <sup>-9</sup>        | +746 x 10 <sup>-9</sup>        |
| Zn                                | -19 x 10 <sup>-6</sup>         | +1.9 x 10 <sup>-6</sup>        | -10 x 10 <sup>-6</sup>         | +7.0 x 10 <sup>-6</sup>        |

| <b>B. Between Day-2 and Day-7</b> |                               |                               |                               |                               |
|-----------------------------------|-------------------------------|-------------------------------|-------------------------------|-------------------------------|
|                                   | Algae                         |                               | Controls                      |                               |
|                                   | Min                           | Max                           | Min                           | Max                           |
| <b>As</b>                         | <b>-45 x 10<sup>-9</sup></b>  | <b>+262 x 10<sup>-9</sup></b> | <b>-189 x 10<sup>-9</sup></b> | <b>-114 x 10<sup>-9</sup></b> |
| <b>Cd</b>                         | <b>+7.8 x 10<sup>-9</sup></b> | <b>+16 x 10<sup>-9</sup></b>  | <b>-5.0 x 10<sup>-9</sup></b> | <b>+0.7 x 10<sup>-9</sup></b> |
| Co                                | -96 x 10 <sup>-9</sup>        | +188 x 10 <sup>-9</sup>       | -10 x 10 <sup>-9</sup>        | -1.3 x 10 <sup>-9</sup>       |
| Mn                                | -22 x 10 <sup>-6</sup>        | +295 x 10 <sup>-6</sup>       | +5.7 x 10 <sup>-6</sup>       | +14 x 10 <sup>-6</sup>        |
| Pb                                | -79 x 10 <sup>-9</sup>        | +1.9 x 10 <sup>-9</sup>       | -13 x 10 <sup>-9</sup>        | +10 x 10 <sup>-9</sup>        |
| Fe                                | -6.1 x 10 <sup>-6</sup>       | -0.3 x 10 <sup>-6</sup>       | -0.4 x 10 <sup>-6</sup>       | +1.0 x 10 <sup>-6</sup>       |
| Ni                                | -0.2 x 10 <sup>-6</sup>       | -86 x 10 <sup>-9</sup>        | -0.1 x 10 <sup>-6</sup>       | +1.3 x 10 <sup>-9</sup>       |
| Cu                                | -614 x 10 <sup>-9</sup>       | -281 x 10 <sup>-9</sup>       | -759 x 10 <sup>-9</sup>       | -49 x 10 <sup>-9</sup>        |
| Zn                                | -1.4 x 10 <sup>-6</sup>       | -0.05 x 10 <sup>-6</sup>      | -3.1 x 10 <sup>-6</sup>       | +1.1 x 10 <sup>-6</sup>       |

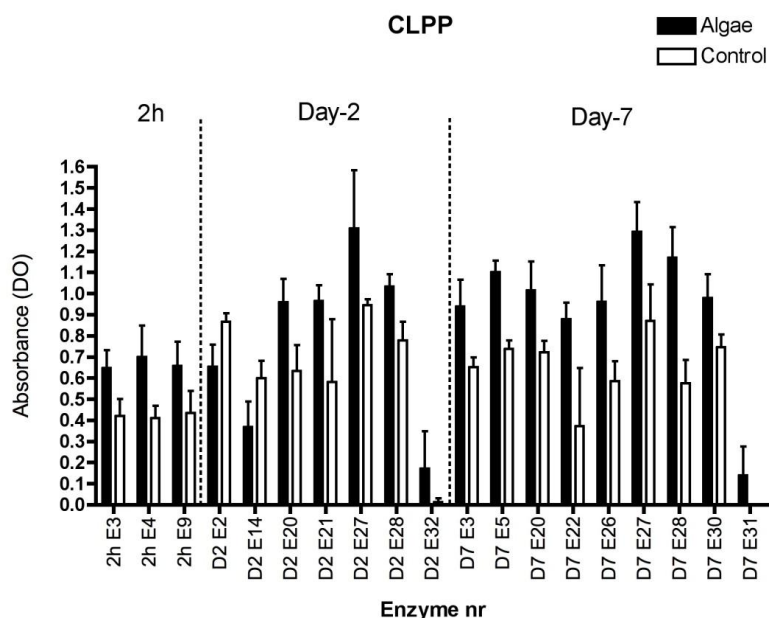


Figure 33. Bacterial activity as measured using CLPP. The EcoPlate™ system of Biolog was used, which measures the use of 31 carbon sources. Only the carbon sources which produced significant differences between controls and experimental microcosms (Algae) are indicated (Mann-Whitney U test). E2 to E31 refer to the type of carbon source.

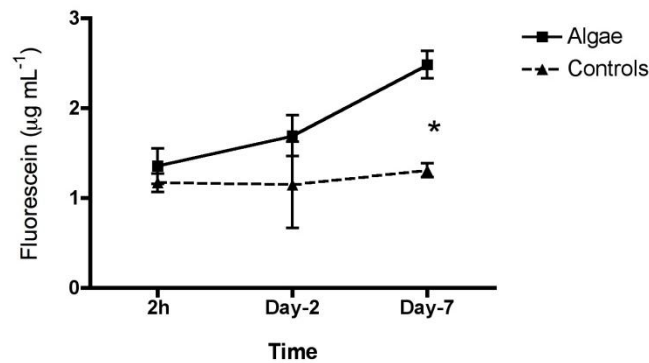


Figure 34. Fluorescein Diacetate Analysis (FDA) which estimates the total esterase activity of the microbial community as the quantity of released fluorescein according to time (mean  $\pm$  SD). Significant differences are indicated by an asterisk (Student T test,  $\alpha = 0.05$ ).

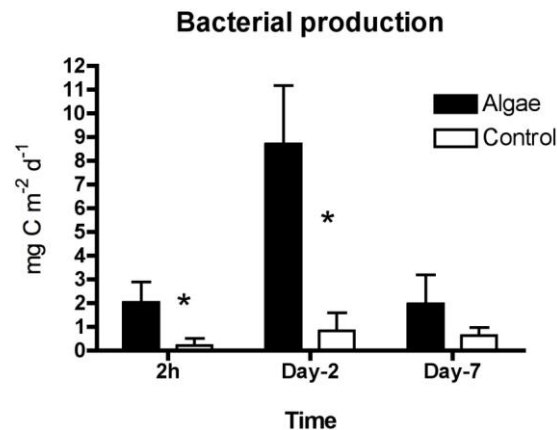


Figure 35. Bacterial production in the surface sediments (at the interface) during the incubation of the microcosms as measured by incorporation of tritiated thymidine (mean  $\pm$  SD). Significant differences are indicated by an asterisk (Student T-test,  $\alpha = 0.05$ ).

### Microeukaryotic and bacterial community composition

Microeukaryotic and bacterial diversity (DGGE band/phyloptype richness) was calculated for the entire community (DNA-based) and for the active community (RNA-based) (Figure 36). Bacterial diversity was constant throughout the experiment in both the total and active communities, except for a small but significant (between Day-0 and Day-7) decrease in the active communities of the control microcosms (Fig. 36). For microeukaryotes, values were more or less stable in the control microcosms for DNA. In the experimental microcosms however, an increase can be seen at Day-2 (significantly higher than in the control, 2h and Day-7). This increase corresponds with an increase in heterotrophic nanoflagellate biomass at day-2 (see above). RNA-based species richness on the other hand decreased during the experiment for the controls, and was significantly lower than the experimental microcosm on Day-7. A

decrease was also measured for the algal treatment at Day-2, but this was not significant. By analogy with the DNA data, we would have expected an increase in diversity of the active community at Day-2. Our data suggest that while total diversity initially increased due to the addition of algal organic matter, some organisms became dominant in the active community, thereby obscuring the signal from rare taxa.

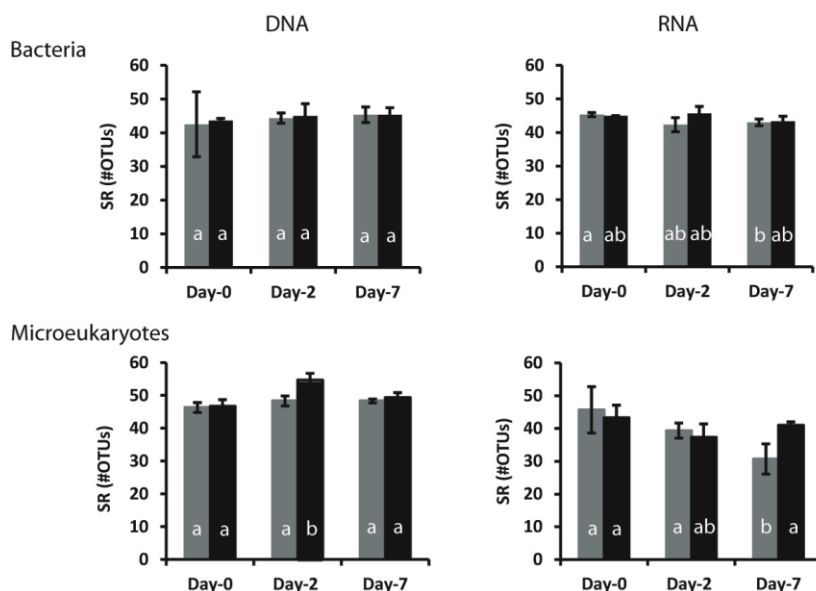


Figure 36. Bacterial and microeukaryotic OTU richness (SR; mean  $\pm$ SD; n=3) as obtained by DGGE fingerprint analyses of ribosomal DNA and RNA extracted from the surface sediments. Grey, control; black, algae-enriched microcosms. Different letters (a, b) indicate significant differences between SR within each community (Student t-test,  $\alpha = 0.05$ ).

When considering community composition as obtained by DNA/DGGE (relative species abundance matrix), addition of the algae to the sediments has a significant effect ( $p < 0.05$ ) both for bacteria and microeukaryotes (with focus on protozoa), viz. the separation between control (black) and treated (red) microcosms in the ordination (Figure 37). Method of extraction (DNA vs RNA) did appear to have a strong effect ( $p < 0.001$ ); this means that the difference between the total community and the active community is significant. Overall, patterns (treatment & time) in the composition of the active (RNA-based) community were less distinct, and not significant for protozoa ( $p > 0.05$ ).

Bacterial community composition showed a distinct change two hours after the addition of the algal suspension, but the bacterial response was most distinct after two days, and communities shifted back towards control composition on Day-7. The effect of algal enrichment on total and active protozoan community structure was most pronounced on Day-7, especially clear in the DNA-based PCO. Identification of the DGGE bands, in combination with the multivariate analyses of the DGGE data revealed that especially many ciliates together with smaller heterotrophic flagellates were active at Day-7 in the sediments (not shown). In addition, various metazoans (MET; a.o. Nematoda, Platyhelminthes, Gastrotricha) were related to the algal addition (not shown). Benthic nematodes have been reported to graze on settled *Phaeocystis* and *Skeletonema* and/or associated micro-organisms (Vanaverbeke *et al*, 2004).

A time- shift, irrespective of the treatment is also visible in the ordination diagrams, probably related to pH, salinity, oxygen levels, etc. Fig. 37 also shows that changes in total bacterial and active protozoan community composition could be significantly related to many of the measured trace metals (Cd, Fe, As, Co, Zn and Pb). However, it remains unclear to what degree the released trace metals have a structuring impact on the communities.

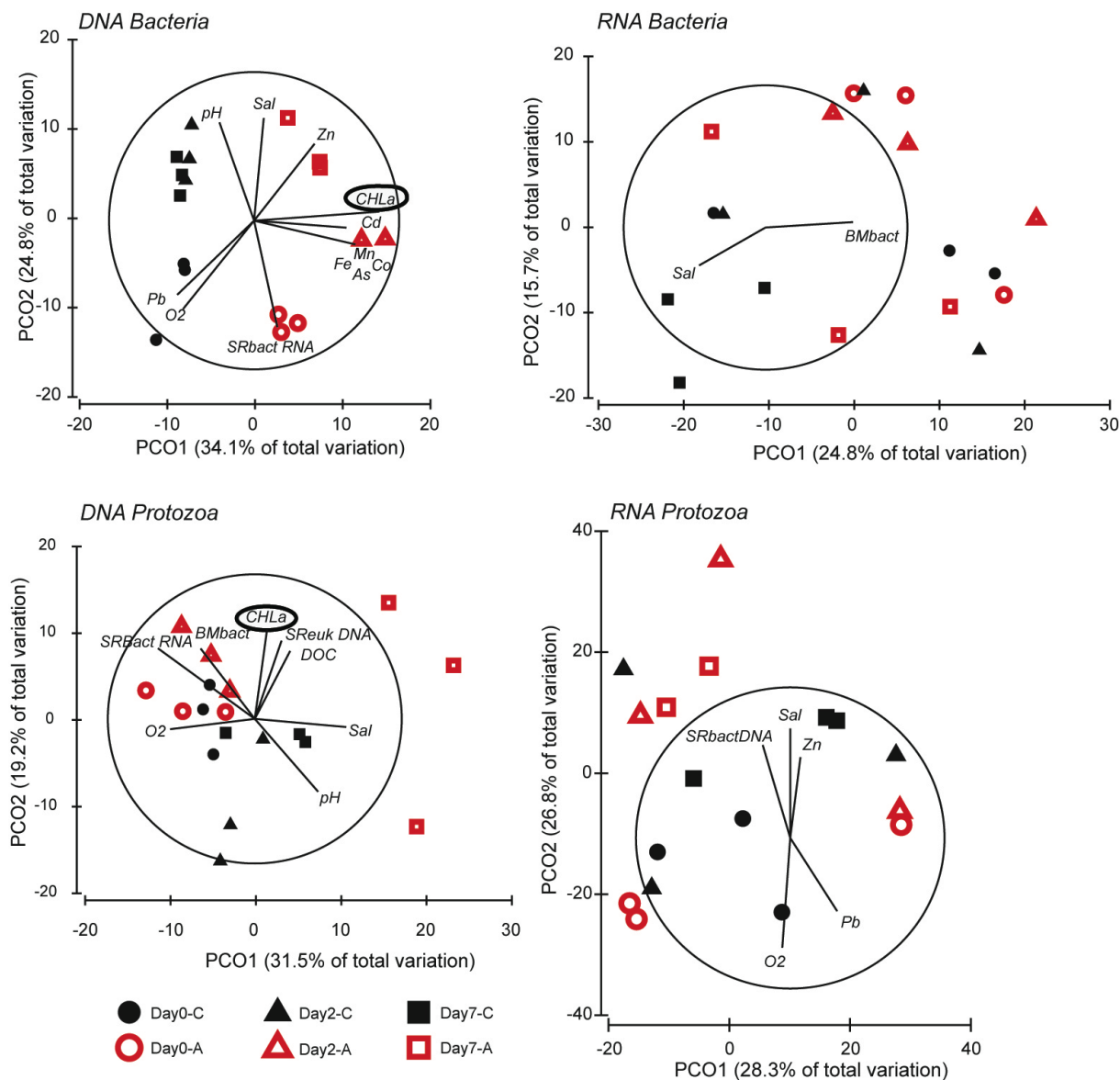


Figure 37. Principal Coordinates Analysis (PCO) for total (DNA) and metabolically active (RNA) bacterial and protozoan community compositions as obtained by DGGE fingerprint analyses, after 2 hours (Day-0), 2 days (Day-2) and 7 days (Day-7). Environmental variables significantly correlated ( $p < 0.05$ ) to one of both axes with  $R > 0.5$  are displayed as supplementary variables. Percentages of variation explained by each axis is indicated, C, control (no algae addition); A, algae-enriched sediments; SAL, salinity; DOC, dissolved organic carbon; SR, species richness; BMbact, bacterial biomass; metals = DGT metals

### 2.2.3.5. LABOSI-5

For this experiment, only the microeukaryotic community was assessed by DGGE. We used microcosms to evaluate the impact of a series of arsenic contamination levels (0=control, 60, 120, 240, 480 and 960  $\mu\text{g/L}$ ) on the active microeukaryotic community of two different stations; station 130 with silty sediments and high metal concentrations, and station 230 with mixed sediments and low metal concentrations (see results phase I). The changes in community composition were analyzed using rRNA-based DGGE. Each concentration was tested in triplicate ( $n=3$ ), except for station 230 - control (0  $\mu\text{g/L}$  As;  $n=2$ ), due to the failing of the extraction of one replicate.

The initial concentrations of arsenic in the sediment from the top layer of station 130 were measured, and amounted to 14.58  $\mu\text{g/g}$  As in the solid phase, and 67.33  $\mu\text{g/L}$  in the pore water. These values are similar to the As concentrations determined for station 130 during phase I (see above). For station 230, arsenic concentrations were not measured. However, concentrations of 12.88  $\mu\text{g/L}$  and 5.77  $\mu\text{g/L}$  (DET; average of first cm-values;  $n=6$ ) were found in February and July 2007 respectively.

Microeukaryotic species richness (number of DGGE bands) varied between 29 and 60 (Figure 38). We detected distinct effects of As contamination on the diversity and composition of these communities. Diversity ( $\sim$ number of DGGE bands) significantly decreased at contamination levels  $\geq 480$   $\mu\text{g As L}^{-1}$  in both sediment types, but the decrease was more pronounced in the sandy (43%) than in the silty sediment (32%), suggesting higher tolerance to As contamination in the silty sediment.

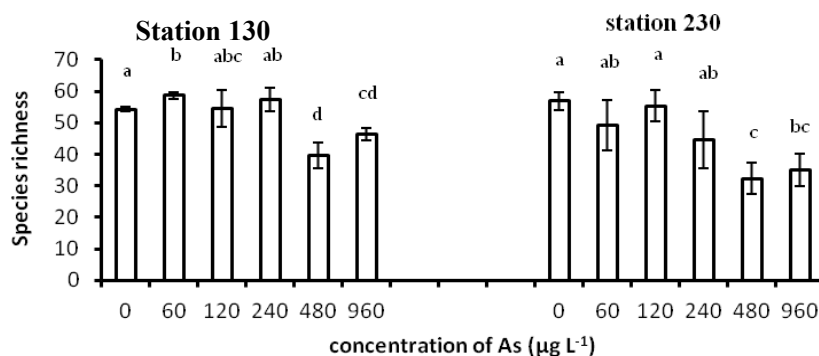


Figure 38. Microeukaryotic species richness (Nb of DGGE bands) as obtained by DGGE fingerprint analyses of ribosomal RNA extracted from the surface sediments (mean  $\pm$ SD;  $n=3$ ). Different letters (a, b, c, d) indicate significant differences between different treatment (arsenic concentrations) within each station (Student t-test,  $\alpha = 0.05$ ).

The stations seemed to have significantly different community compositions ( $F= 29.81$ ;  $p<0.001$ ; see also Fig. 39-A). This confirms our previous results (PHASE I) that microeukaryotic communities were different in silty (station 130) and mixed (station 230) sediments. The treatment (series of arsenic levels) also had a strong effect, reflected in the PCO analyses (Fig. 39). In the separate PCO plots (B & C), the samples grouped together according to their contamination level, and arranging

themselves into three (0-60, 120-240, 480-960) and two (0-240, 480-960) groups in station 130 and 230 respectively. Note that differences between replicates in station 230 were more dissimilar (especially replicate a) -this was also seen during Phase I- what might explain why the treatment effect was not significant ( $p>0.05$ ) in station 230.

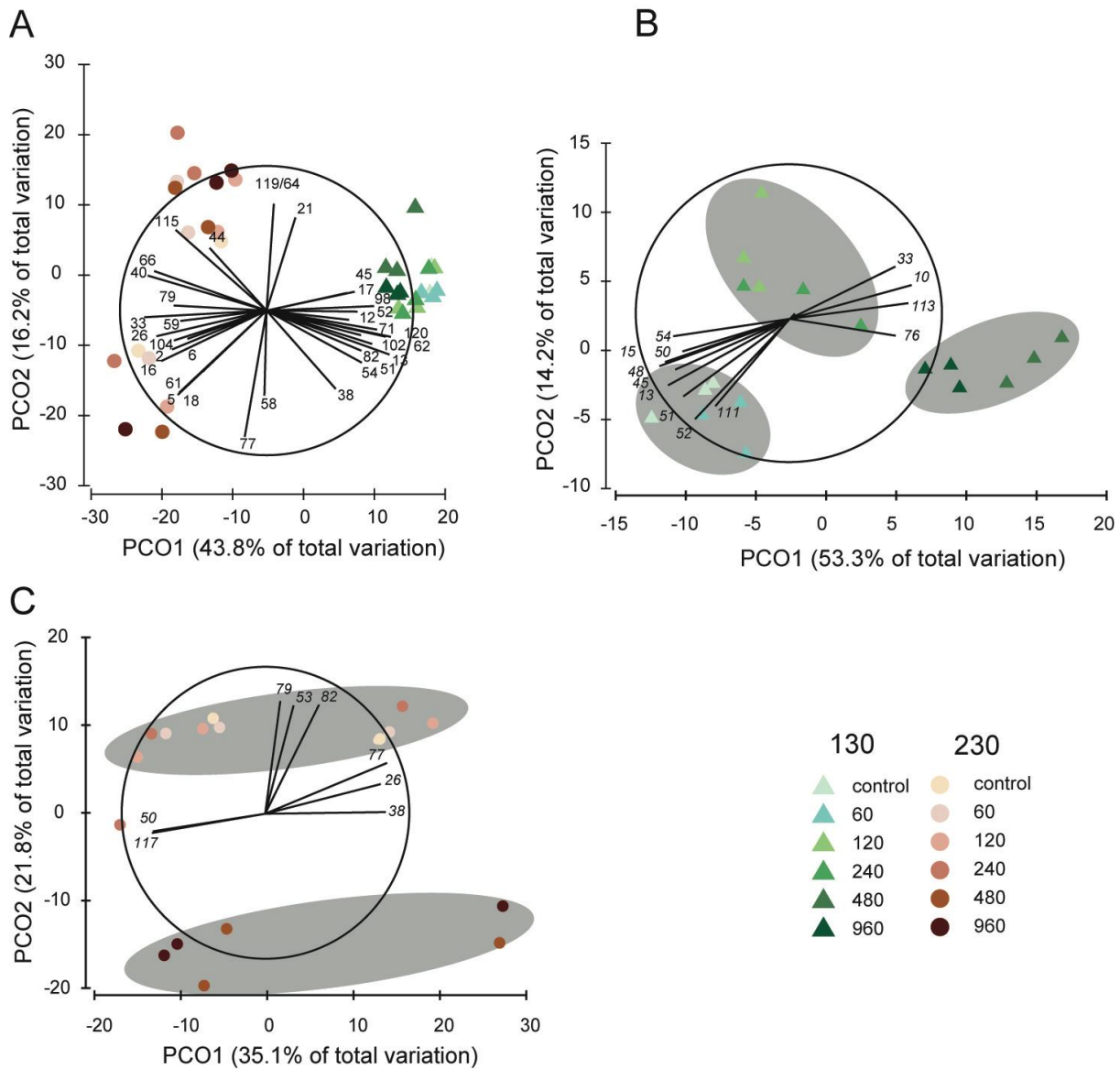


Figure 39. Principal Coordinates Analyses (PCO) based on Bray-Curtis similarities for all samples (A), and samples from station 130 (B) and station 230 (C) separately. Species (DGGE band nr –for identification see Pede et al., in prep. d) with a correlation  $>0.5$  and significantly correlated ( $p<0.001$ ) to one of both axes are given in the diagram (Spearman correlation type). Percentage of variation explained by the individual axes is given. Replicate C for the control is excluded for station 230 due to an outlier position.

More details of this study can be found in Pede et al. (in prep., d). It was e.g. also shown that the response to As contamination was most pronounced in Fungi and ciliates. Fungi responded most sensitively to high As concentrations, while only some ciliates increased in relative abundance with higher As levels.

## 2.2.4. Laboratory simulation approaches conclusions

The experiments performed during the MICROMET project clearly demonstrate that microbial mineralization of phytoplankton-derived phytodetritus accumulated at the surface of contaminated muddy sediments may lead to an increased efflux of trace elements from these sediments. Four LABOSI experiments were conducted with muddy sediments of station 130. Microbiological and geochemical variables were always followed for several days in the sediments (up to 14 days). LABOSI-1 permitted to test all the procedures and equipment and demonstrated that sediments cannot be homogenized for short microcosm incubations and that fresh intact cores must be sampled in the field.

### LABOSI-2 & LABOSI-3

During LABOSI-2 and LABOSI-3 phytodetritus were added on the sediments. Diatoms and *Phaeocystis* cells were efficiently accumulated at the SWI, as indicated by (i) color changes of the sediments (for the diatom exposure), (ii) DGGE analysis and (iii) DOC measurements. However, this accumulation did not produce any significant change of the microbial communities living at the SWI. This can be explained by several factors. First, the temperature : a low temperature may result in a low biological activity. Indeed, during LABOSI-2 the temperature was fixed at 4°C (the *in situ* temperature in February), and although the temperature was fixed at 15°C during LABOSI-3 (conducted in June) no microbiological effects were recorded. This means that other factors must be invoked. Secondly, it is possible that a large quantity of organic matter was already present in control sediments (i.e., the organic matter added during the experiments would be insignificant). This was clearly the case for LABOSI-2, but not for LABOSI-3 (DOC was increased 4 times). Another possibility is that the number of sampling points was not sufficient and that microbial communities needed more (or less) time to react. Finally, the heterogeneity of the sediments was possibly masking small biological effects. Indeed, large standard deviations were observed for DAPI-counts.

During LABOSI-2 and LABOSI-3, geochemistry, oxygen, alkalinity and metal fluxes were also determined. Oxygen was rapidly consumed in the overlying water (for the closed core experiments, not for the open microcosms) indicating that organic matter was degraded by respiration resulting in an increase of the porewater alkalinity of the sediments. For that reason,  $\text{HCO}_3^-$  was progressively released in the overlying water. Benthic fluxes of trace metals obtained after 8 hours of incubation indicated high positive fluxes for Mn and Fe, moderate positive fluxes for As, Cr and Ni and low positive fluxes for Cd and Co. Conversely, V and Zn were trapped at the surface of the sediments. For Pb and Cu, erratic values were obtained and no conclusions are allowed. Metal diffusive fluxes have not been calculated but their direction agreed quite well with the benthic fluxes trends.

When closed core experiments are considered (LABOSI-2 & 3), the addition of organic matter, either diatoms or *Phaeocystis*, did not change significantly the behaviour of trace metals in the porewaters and their fluxes at the SWI. On the contrary, concentrations profiles for Mn and Co assessed by DET and DGT during open microcosm experiments were significantly increased in the overlying water of the microcosms containing *Phaeocystis* (when compared to controls). This discrepancy between closed core experiments and open microcosm experiments can

be explained by the fact that stagnating seawater was used for the microcosm experiments (the overlying seawater was not renewed) and that fresh seawater was used for the closed core experiments (the water was followed during 8 hours then renewed). It is thus possible that some of the *Phaeocystis* cells were washed away during the closed core experiments. Finally, a large concentration of biodegradable POC is probably present in the sediments. This POC might be much higher than the fresh POC input to the systems at the beginning of the incubation experiments. POC has still to be measured in the sediments.

To conclude on LABOSI-2 & 3, it seems that moderate accumulations of diatoms and *Phaeocystis* do not have major effects on microbial diversities and biomasses in muddy sediments of station 130, at least after 14 days of exposure. However, it seems that these moderate accumulations of *Phaeocystis* do increase the release of Co and Mn from the sediments. This means that metals may continue to diffuse in the water column and that 0.39  $\mu\text{g}$  of chlorophyll *a* per  $\text{cm}^2$  (from an early spring diatom bloom), or 0.82  $\mu\text{g}$  of carbon from *Phaeocystis* (per  $\text{cm}^2$ ), is not sufficient to stop secondary contaminations by metals such as Co, Mn or As.

#### LABOSI-4

The experiments performed in LABOSI-4 clearly demonstrate that microbial mineralization of phytoplankton-derived phytodetritus accumulated at the surface of contaminated muddy sediments may lead to an increased efflux of trace elements from these sediments. Several important points must be considered. First, the quantity of phytodetritus used in this experiment was in the range of what can be observed in the field. Although the algal suspension used here was 21.4 times more concentrated than the maximum values observed in the North Sea during a *Phaeocystis* bloom (chlorophyll *a*: 750  $\mu\text{g L}^{-1}$  versus 35  $\mu\text{g L}^{-1}$ ) (Schoemann et al., 2005), it should be noted that the height of the water column over the microcosms was only 4 cm, and that station 130 is located at ca. 10 m of depth. Consequently, considering that all phytodetritus may reach sediments, the present experiment was equivalent to an 85 cm column of seawater containing 35  $\mu\text{g L}^{-1}$  of chlorophyll *a* (4 cm  $\times$  21.4), or to a 10 m column containing 3  $\mu\text{g L}^{-1}$  of chlorophyll *a* (750  $\times$  0,04  $\times$  10). Such a chlorophyll *a* concentration (3  $\mu\text{g L}^{-1}$ ) is exactly the mean concentration observed in spring in coastal areas such as the Bay of Biscay (France), with peaks at 10  $\mu\text{g L}^{-1}$  (Gohin et al. 2003). On the coastal BCP and the English Channel, mean values are commonly higher than 30  $\mu\text{g L}^{-1}$  (Denis and Desroy 2008). On the BCP, values of ca. 20  $\mu\text{g L}^{-1}$  at station 130 were observed throughout March and April 2008, with values reaching 100  $\mu\text{g L}^{-1}$  in May (unpublished observations). Lancelot et al., 2005 estimated that 24% of the production may reach sediments, the rest being exported or degraded in the water column. As a result, for the period between March and April on the BCP, a quantity of 4.8  $\mu\text{g L}^{-1}$  may potentially reach the sediments (24% of 20  $\mu\text{g L}^{-1}$ ). Although the actual input of phytodetritus in North Sea sediments is hard to determine, as it depends on currents and wind (Van Duyl et al., 1992; Denis and Desroy, 2008), we may consider that the quantity of phytodetritus used in the present experiment (3  $\mu\text{g L}^{-1}$ ) is in the lower range of values that may potentially be observed on sediments during a real phytoplankton bloom.

Another point to consider is the origin of metals appearing in the overlying waters during the experiment. Metals measured after 2h originate mostly from the added algal suspension in itself (clearly our algal suspension was contaminated with

Cd) but also from the disturbance of the WSI. Indeed, it can be seen that the increases observed after 2h are of the same range as the dissolved metal concentrations of the algal suspension (see materials and methods). As a consequence, no conclusions can be drawn about effluxes of metals from sediments after 2h of exposure to phytodetritus. However, this is not the case for Day-2: concentrations of Mn, Co and As in the experimental microcosms were respectively 60 times, 3.6 times and 2.1 times more elevated than the values observed in the same microcosms after 2h. These increases can only be explained by (i) the mineralization of phytodetritus that releases metals directly into the overlying water, and (ii) by an efflux of metals from the sediments. It has been calculated that the complete mineralization of the phytodetritus on Day-2 would only introduce 8.4 (Mn), 0.07 (Co) and 0.58 (As)  $\mu\text{g}$  of metals per liter in the overlying water. This means that the complete mineralization of phytodetritus at the interface only represents a maximum of 0.9% (Mn), 12.4% (Co) and 23.3% (As) of the increases observed on Day-2 in the overlying waters. As a result, 99.1% (Mn), 87.6% (Co) and 76.7% (As) of the metals are coming from the sediments.

A third point is the physico-chemical conditions during the experiment. Like with many approaches, the microcosm experiment presented here is not free from biases: (1) Because stagnating water was used oxygen levels were lower than in the field. Low oxygen levels may promote or impede the flux of metals like  $\text{Fe}^{2+}$ ; (2) In the field, hydrodynamics is known to play an important role in the rate of diffusion as it directly influences the thickness of the DBL, which in turn acts as a diffusion barrier; (3) In the sea, currents and waves may cause water advection and sediment resuspension which may influence metal fluxes. For the first bias (1) it must be noted that microcosms were far from anoxia: oxygen levels at 5 mm above the sediments were about  $5 \text{ mg L}^{-1}$  and increased Fe fluxes were not observed during the experiment. Iron effluxes are frequently observed when anoxia is developing (Petersen et al. 1996). For some metals like  $\text{Mn}^{2+}$  it was shown in other reports that the concentration in porewaters of the top sediment layer (0-5 mm) is not dependent on dissolved oxygen levels of the bottom water, at least on the short term (Pakhomova et al. 2007). Manganese fluxes are therefore not influenced by the redox conditions in the near-bottom water. For the second bias (2) it must be noted that high water flow velocities near the bottom will tend to decrease the DBL thickness and thus increase benthic effluxes (Jørgensen and Des Marais, 1990). Consequently, we may view our measurements in stagnating water as lower estimates of what can be released under high flow velocities. Finally, for the third biases (3), sediment resuspension and water advection are also expected to release more metals into the bottom waters. To sum up, metal fluxes determined in our microcosm approach must be considered as an approximation, probably underestimated, of the real benthic fluxes in muddy sediments of the BCP (they cannot be applied to the whole BCP which also feature coarse and sandy sediments).

Although fluxes determined here are approximations, the most important point of the present research is that mineralization of phytodetritus at the WSI increases effluxes of Mn, Co and As. Flux values obtained in this study are in the range of those observed in situ using benthic chambers deployed on other shallow coastal oxic sediments which may be exposed to phytodetritus (Hunt, 1983; Ciceri et al., 1992; Aller, 1994; Thamdrup et al., 1994; Warnken et al., 2001; Pakhomova et al. 2007). For instance, Mn effluxes were found to vary between  $70\text{--}4450 \mu\text{mol m}^{-2} \text{d}^{-1}$  in the Gulf of Finland and the Vistula Lagoon of the Baltic Sea (Pakhomova et al.

2007), or between 420–2600  $\mu\text{mol m}^{-2} \text{d}^{-1}$  in Galveston Bay, Texas (Warnken et al. 2001). The maximum effluxes obtained here for Mn were only 755  $\mu\text{mol m}^{-2} \text{d}^{-1}$ . Similarly, for As effluxes, other investigators have observed 0.008–2.5  $\mu\text{mol m}^{-2} \text{d}^{-1}$  for Amazon shelf sediments (Sullivan & Aller, 1996) and about 5.1  $\mu\text{mol m}^{-2} \text{d}^{-1}$  for Chesapeake Bay sediments (Riedel et al., 1987). In the present study, As effluxes were 0.045–1.084  $\mu\text{mol m}^{-2} \text{d}^{-1}$ , exactly in the range of the previous observations.

Another point to consider is the role of the benthic microbial communities. It is clear that the onset of mineralization is very fast and starts within 2h of deposition as revealed by CLPP analyses. Benthic microbial communities were shown in other studies to react quickly to fresh inputs of organic carbon (Turley and Lochte, 1990; Meyer-Reil and Köster, 1992). The increased activity of the microbial heterotrophs results in the consumption of the oxygen (Franco et al., 2007; Rauch et al., 2008) which is known to be responsible for >90% of the organic carbon mineralization at the WSI (Bender and Heggie, 1984). As a consequence, the oxic-anoxic interface [usually located at 3-4 mm into the sediments of that station (Gao et al., 2009)] moves upwards and reduced elements like  $\text{Fe}^{2+}$ ,  $\text{Mn}^{2+}$ ,  $\text{Co}^{2+}$  and arsenic species, may diffuse out of the sediments. Fe and Mn oxides are important electron acceptors in anaerobic marine sediments (Thamdrup et al., 1994). Mn oxides are reductively dissolved by the action of bacteria that actively mineralize the phytodetritus thereby releasing  $\text{Mn}^{2+}$  into the porewater (Froelich et al., 1979; Burdige and Gieskes, 1983; van der Zee and van Raaphorst, 2004). This  $\text{Mn}^{2+}$  is then able to diffuse out of the sediments as it is relatively stable to chemical oxidation. In comparison,  $\text{Fe}^{2+}$  ions are more reactive and precipitate at the WSI after its re-oxidation in the contact with oxygen (Pakhomova et al., 2007). Consequently, Fe is not expected to accumulate in oxic seawater as observed in the present microcosm experiment. Increased benthic effluxes of Mn, Co and As from sediments may thus be explained by the development of anaerobic conditions at the WSI which is here a consequence of an increased microbial heterotrophic activity. The effect of anaerobiosis on such metal effluxes was observed in previous microcosm experiments (Petersen et al., 1996) but also in situ (Sundby et al., 1986).

The deposition of fresh phytodetritus at the WSI explains the increased bacterial production observed on Day-2 (ca. 4.3 times, from 2.0 to 8.7  $\text{mg C m}^{-2} \text{d}^{-2}$ ). The fact that this increased bacterial production was not followed by an increased bacterial biomass suggests that biomass development in this group was controlled by grazing, most probably by HNF (increase on Day-2) and ciliates (increase on Day-7), known to be important bacterial grazers (Patterson et al., 1989; Hondeveld et al., 1995). HNF as well did not show a biomass increase, which may be related to enhanced ciliate grazing and/or competition on day 7 (cf. Wey, *et al.*, 2008). As such, the results of LABOSI-4 suggest that the addition of phytodetritus stimulates the development of the microbial loop. The total heterotrophic activity increased (bacteria and nanoflagellates) and this resulted in a consumption of oxygen with a lowering of the pH which in turn promoted the reductive dissolution of Fe/Mn oxyhydroxides that release many metals and metalloids. In addition, large quantities of organic acids were probably generated during the mineralization process. Such organic acids are then able to complex many metallic elements and transport them into the overlying water.

During the last 5 days of mineralization (Day-2 to Day-7) effluxes of trace elements were reduced. This is another indication that effluxes are linked to the mineralization of phytodetritus, as the quantity of phytodetritus is decreasing. Although effluxes of trace elements were reduced, the microbial enzymatic activity

was still intense, as indicated by the esterase activity and the CLPP profiles on Day-7. These increased bacterial activities were not followed by an increased bacterial production: values on Day-7 were at the level of those observed in the controls (ca. 2 mg C m<sup>-2</sup> d<sup>-2</sup>). But the bacterial biomass was now 1.3 times more elevated. This may be explained by a reduced predation by nanoflagellates as these may have been consumed by higher trophic levels (large ciliates, nematodes, etc.). Although the experiment was stopped after 7 days of incubation it is probable that enzymatic activities and bacterial biomass slowly return to pre-exposure values within a few days.

The consequences of arsenic effluxes may be huge in areas covered with contaminated muddy sediments and submitted to an intense rain of phytodetritus. In the microcosm experiment described here the quantity of added phytodetritus was only 5.24 g m<sup>-2</sup> (dw) (0.092726 g / 0,017670 m<sup>2</sup>). It has been calculated that this quantity of deposited phytodetritus has led to the release of 76.4 µg of arsenic per square meter of sediment after only 48h. The Belgian Continental Zone (BCZ) is 3600 km<sup>2</sup> and we may estimate that about 20% of that surface area (720 km<sup>2</sup>) is composed of muddy contaminated sediments located close to the coast between the cities of Oostende and Zeebrugge (Van den Eynde, 2004; Ruddick and Lacroix, 2008; Gao et al., 2009). These muddy sediments have been monitored in various points and results show that the arsenic content is almost unchanged in the area [the monitored stations include contaminated stations 140 and 700 (Gillan and Pernet, 2007)]. If sediments of the area are considered as equivalent, this means that about 55 kg of arsenic may be released into the seawater of the BCZ, in only two days and as a result of the microbial activity alone, when only 5.24 g (dw) of phytodetritus are mineralized on each square meter of this area. As explained before this quantity of phytodetritus is probably a low estimation of what may be deposited on the BCZ during a real phytoplankton bloom (Schoemann et al., 2005). In addition, arsenic effluxes might even be higher because (1) the metal content of the phytodetritus was not taken into account in the above calculations; (2) hydrodynamic effects which lower the DBL and resuspension events were not taken into account.

These large quantities of arsenic released from sediments in the continental zone may then return to the sediments. Indeed positive fluxes (i.e., towards the sediments) up to +262 nmol m<sup>-2</sup> d<sup>-1</sup> have been observed in the present experiment. However, during the stay in the overlying water, arsenic species may be accumulated in the biota. The main arsenic compound in oxic seawater is arsenate (AsO<sub>4</sub><sup>3-</sup>) (Mukhopadhyay et al., 2002). Arsenate is known to be taken up by marine organisms, ranging from phytoplankton, algae, crustaceans, mollusks and fishes (Knowles & Benson, 1983). Fish and marine invertebrates retain 99% of accumulated arsenic in organic form, and crustacean and mollusk tissues are known to contain higher concentrations of arsenic than fishes (Mukhopadhyay et al., 2002). Arsenic, which is now recognized as a carcinogenic element (Pershagen, 1985; Bates et al., 1992), may thus accumulate in marine foodstuffs such as prawns at levels approaching 200 ppm (Nriagu, 1994).

### LABOSI-5

With LABOSI-5 we demonstrated that diversity and composition of micro-eukaryotic communities are significantly influenced by the contamination with arsenic. The decrease in diversity appeared at concentrations of 480 µg As L<sup>-1</sup> and was more pronounced in sandy than in silty sediments, suggesting that communities

from the silty sediments were comprised of less metal-intolerant species at the onset of the experiment (as these were already contaminated by As). A significant shift in community composition occurred at contamination level  $\geq 120 \mu\text{g As L}^{-1}$  and again at  $\geq 480 \mu\text{g As L}^{-1}$  in silty sediment. Surprisingly, the effect of As on protist community composition was not significant in the sandy sediment. Species-specific responses showed that Fungi were most sensitive to high As concentrations. This is surprising, since previous studies indicated that Fungi are quite resistant to metal contamination (e.g. Cernansky, *et al.*, 2009, Vala, 2010). Ciliates on the other hand were the only protists that increased in relative importance with higher As levels, and their metal resistance and bioaccumulation process might be related to the biosynthesis of ciliate metallothioneins (Diaz, *et al.*, 2006), which have unique features compared to metallothioneins from other organisms (Gutierrez, *et al.*, 2009).

### 2.2.5. Numerical modeling

The main chemical equilibrium modelling software used in this work for calculation of metal chemical speciation in surface waters and porewaters under anoxic conditions was VisualMinteq (Gustafsson 2006). JCHESS (Lee *et al.* 2000) was also tested, showing similar results. The main objective of this modelling approach was to detail some major (geo)chemical processes of interest taking place in the sediments of the Station 130 in the North Sea, to better describe them and to assess their implication on pore water chemistry and metal behaviour. Calculations were mostly carried out with experimental data obtained from the field campaigns in 2010. This model results must be taken with caution because: (i) in the calculations, all the (bio)geochemical reactions taking place in the sedimentary medium are assumed to be in thermodynamic equilibrium; and (ii) metal complexation by dissolved organic ligands was taken into account in an approximated manner (Lesven *et al.* 2010).

#### 2.4.5.1. Anions and major species speciation in surface waters and porewaters

Calculations were done in surface waters and porewaters (from  $-1 \text{ cm}$  to  $-6 \text{ cm}$  depth) using the LABOSI-4 data.  $\text{PO}_4^{3-}$  was found, both in overlying waters and porewaters mainly as  $\text{NaHPO}_4^-$  (27%-29%),  $\text{MgHPO}_4$  (23-26%),  $\text{HPO}_4^{2-}$  (23%) and  $\text{H}_2\text{PO}_4^-$  (11%). In the case of  $\text{CO}_3^{2-}$ , it was mostly present as  $\text{HCO}_3^-$  (74%), and to a lesser extent as  $\text{H}_2\text{CO}_3$  (10%),  $\text{NaHCO}_3$  (9%) and  $\text{MgHCO}_3$  (5%).  $\text{Cl}^-$  and  $\text{NO}_3^-$  were found to be mostly as free forms:  $\text{Cl}^-$  (87%), and  $\text{NO}_3^-$  (94%). The three main species existing for  $\text{SO}_4^{2-}$  were:  $\text{SO}_4^{2-}$  (46%),  $\text{NaSO}_4$  (30%-35%) and  $\text{MgSO}_4$  (15%). In porewaters, sulphides were mostly associated with iron ( $\text{FeHS}^+$ ), and with manganese ( $\text{MnHS}^+$ ). Other main species found were  $\text{HS}^-$  and  $\text{H}_2\text{S}$ .

#### 2.4.5.2. Trace metal speciation in surface waters and porewaters

Speciation of trace metals was studied in several samples of surface waters during incubation experiments, and in porewaters of control (Figure 40) and experimental cores of the LABOSI-4 experiment. In the aim to know the influence of different conditions, simulations were done by modifying several parameters such as pH (from 6.5 to 8), temperature (from 5 to 20°C), DOC (from 0 to 100  $\text{mg L}^{-1}$ ) as

seen in Figures 40 and 41, and sulphides (from 0 to 1000  $\mu\text{M}$ ) in Figure 43, in order to know the influence they have in the speciation of trace metals.

Manganese was found, in surface waters and over the whole profile of porewaters of experimental and control cores, mainly in the form of  $\text{Mn}^{2+}$  (~ 65%), and to a lesser extent associated to inorganic complexes such as  $\text{MnCl}_2$ ,  $\text{MnCl}^+$ ,  $\text{MnSO}_4$ ,  $\text{MnHCO}_3^+$  and  $\text{MnCO}_3$  (Figure 40). Speciation of this metal was very poorly affected by changes in temperature and pH, as predicted by Byrne (1988), since this metal is complexed to chloride ions. Manganese was very poorly dependent on DOC contents, but moderately influenced by sulphides; with a S(-II) concentration of 5  $\mu\text{M}$ , more than 65% of Mn is found as  $\text{Mn}^{2+}$ , 10% as  $\text{MnSO}_4$  and only 1% as  $\text{MnSH}^+$ . When S(-II) concentrations are high, for instance of 1000  $\mu\text{M}$ , the speciation evolves in the way of: 4 %  $\text{Mn}^{2+}$ ,  $\text{MnSO}_4$  1% and  $\text{MnSH}^+$  93%.

Iron was found to be mainly as  $\text{Fe}^{2+}$  (40-70% in the control core and 20-70% in the experimental core), with the higher lability between -2 and -3cm (Figure 40), and to a lesser extent as inorganic complexes (10-20 %) and organic complexes (20-40% in the control core and (6-70%) in the experimental core. In surface waters, iron was found to be almost 100% associated to organic matter. Speciation in surface and porewaters was not affected by temperature or pH changes, as previously observed by Byrne (1988), but were found highly dependent on sulphides and DOC concentrations. For surface waters, only when there is no organic matter present in the medium, Fe could be found at 85% as  $\text{Fe}^{2+}$ . In porewaters, Fe is found to be associated with organic matter at 10% when DOC is 10  $\text{mg L}^{-1}$ , and about 70% when DOC concentration is 100  $\text{mg L}^{-1}$ . Sulphides were also found to play an important role for iron, with 90 % of iron complexed to sulphides when sulphides concentration is 1000  $\mu\text{M}$ .

Cobalt speciation observed in surface waters and porewaters along the whole studied profile was similar and in the way of: ~70%  $\text{Co}^{2+}$ , 25 % as inorganic complexes and less than 3 % associated to organic matter (Figure 40). It was very slightly influenced by pH, DOC and temperature changes, but significantly influenced by high sulphide contents (90 % associated to organic matter when sulphide is 1000  $\mu\text{M}$ ).

Nickel speciation was quite stable over the whole depth in all cores, with ~ 55% as  $\text{Ni}^{2+}$ , 35 % as inorganic complexes and 20% as organic complexes (Figure 40). This metal was found to be highly dependent on the concentration of organic matter (with DOC = 100  $\text{mg L}^{-1}$  60 % of nickel was found under Ni-organic complexes) and with sulphide contents (almost 100 % of nickel was associated with sulphides when  $[\text{S(-II)}] = 1000 \mu\text{M}$ ).

Copper was found to be associated with organic matter at almost 100% in all the studied cores (Figure 40). It was not influenced by temperature, pH or sulphides. Only when there is no organic matter present in the medium, copper can be found quantitatively as  $\text{Cu}^{2+}$  (40%).

Zinc speciation studies have shown similar profiles along the whole depth in all cores, with 55% as  $\text{Zn}^{2+}$  and 45% as Zn-inorganic complexes (Figure 40). pH, temperature and organic matter contents didn't have an important role in this case. Conversely, sulphide concentrations played an important role, since almost 100 % of zinc was found to be associated to sulphides when S(-II) concentration was equal to 1000 $\mu\text{M}$ .

Arsenic is a metalloid present in the natural environment under two main oxidation states: As(III) and As(V). Our measurements by ICP-MS did not allow us to distinguish redox species but in anoxic sediments, As(III) has been previously

pointed out (Dowdle et al. 1996). As a consequence, we propose here two separate scenarios: the first one where As is exclusively under As(V) and the second one where As has been completely been reduced under As(III). Further studies should be in the future undertaken to tackle experimentally As redox speciation.

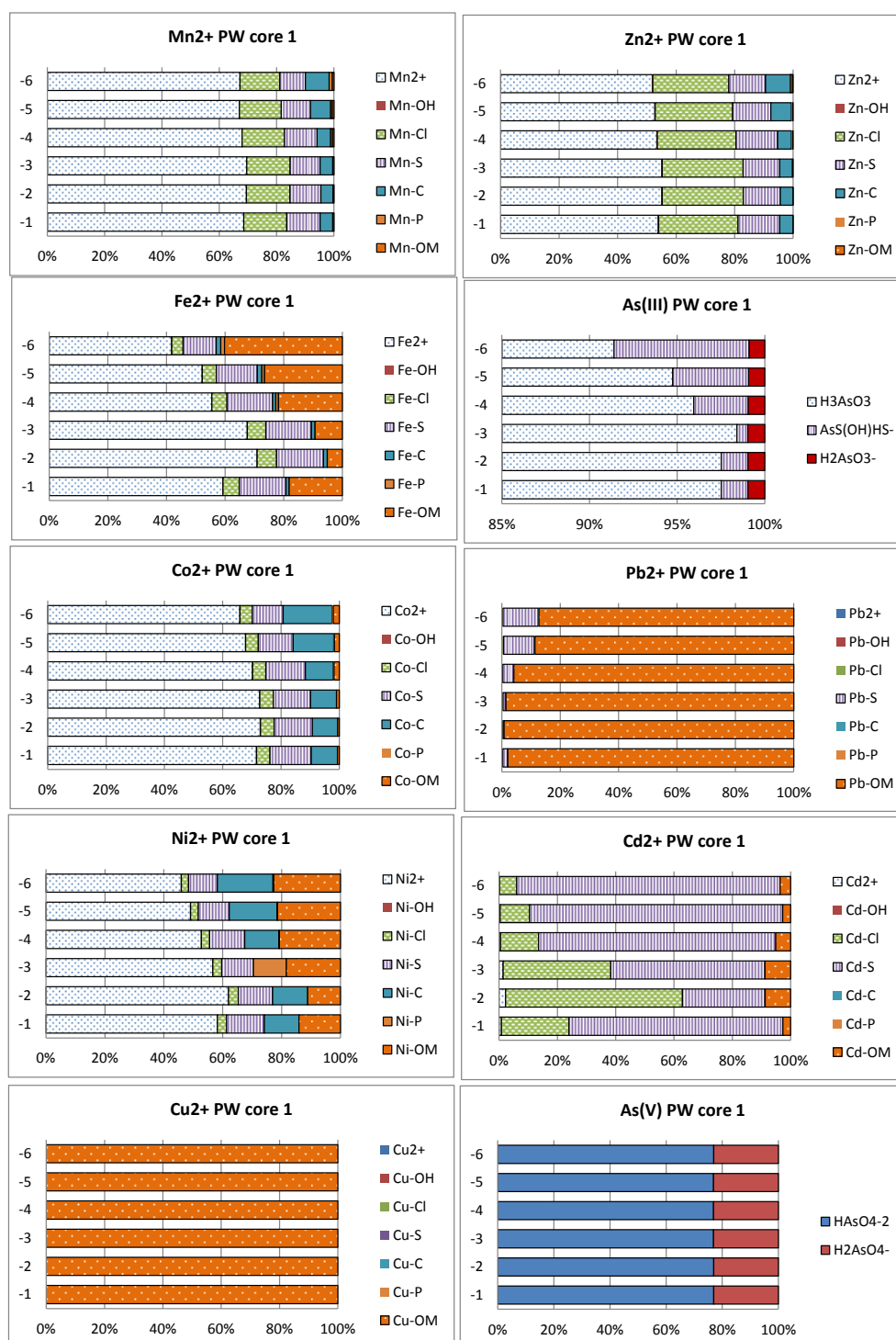


Figure 40. Percentage of free ion, metal-OH (bound to hydroxides), metal-Cl (bound to chlorides), metal-S (bound to sulphur groups), metal-C (bound to carbonates), metal-P (bound to phosphates) and metal-organic matter (OM) complexes calculated with Visual Minteq for Mn, Fe, Co, Cu, Zn, As(III), Pb, Cd and As(V) in porewaters (depth from -1 cm to -6 cm) of a control core (core 1).

Arsenic (V) chemical speciation was found to be very stable in all the studied samples, with ~80% as  $\text{HAsO}_4^{2-}$  and ~20% as  $\text{H}_2\text{AsO}_4^-$  (Figure 40). Its speciation was found to be not dependent on temperature, sulphides and organic matter, but dependent on pH, with almost 100 % as  $\text{HAsO}_4^{2-}$  at pH 8.

Arsenic(III) was found to be almost 100 % as  $\text{H}_3\text{AsO}_3$  in all studied water samples (Figure 40). Organic matter, temperature and pH were found to play a very small role, whereas sulphide concentration highly influenced As (III) speciation, with As (III) found almost as  $\text{AsS(OH)HS}^-$  with sulphide concentrations higher than 100  $\mu\text{M}$ .

Lead was found to be strongly associated with organic matter over the whole depth profile (> 90%) (Figure 40). pH and temperature changes did not affect lead speciation, whereas this metal was found to be highly dependent on sulphides (almost 100% as  $\text{Pb(HS)}_2$  when sulphide concentration is higher than 200  $\mu\text{M}$ ) and organic matter (almost 100 % as Pb-organic complexes when DOC is higher than 10  $\text{mg L}^{-1}$ ).

Cadmium speciation studies revealed that this metal is highly associated to inorganic complexes, especially to sulphides in porewaters (Figure 40), and to chlorides in surface waters. Temperature and pH did not play an important role on its speciation, whereas organic matter contents may affect the speciation of Cd in the surface waters (50% of Cd was found under Cd-organic complexes when DOC is higher than 100  $\text{mg L}^{-1}$ ). Porewaters were highly influenced by sulphide contents, with 100 % of Cd as  $\text{Cd(HS)}_2$  when S(-II) is higher than 50  $\mu\text{M}$ .

Vertical profile of some metals such as Fe, Ni, Co and Cd show a higher release of metals in the interstitial waters between -2 and -3 cm, which can be a consequence of early diagenesis processes (rapid depletion of  $\text{O}_2$ ,  $\text{NO}_3^-$  and  $\text{SO}_4^{2-}$  accompanied with  $\text{HCO}_3^-$  and a sharp decrease of redox potential at the the first centimeters of the surface sediment). Bacterial reductive dissolution of Mn(III and IV) and Fe(III) oxides/hydroxides to Mn(II) and Fe(II) accompanied by microbial degradation of organic matter took place, as resulted in trace metal increases near the sediment water interface. At higher depths, lability of these metals decrease due to the removal of metals from interstitial waters through combination with carbonates and/or sulfides.

According to these results, it is clear that trace metal speciation in the pore and overlying waters is strongly influenced by several parameters, mostly organic matter and sulphides contents. As the free metal cations are generally considered as the the most toxic species for the organisms (Sunda et al. 1978; Allen et al. 1980, Zevenhuizen et al. 1979), the production of sulphides via the sulfatoreduction process (mediated by bacteria and that can be very active in the seawater because of high contents of sulphates), and the recycling of OM in the surface sediments are two main biogeochemical processes that control the bioavailability of dissolved trace metals. Most available metals in this medium (in proportion to their concentrations) are:  $\text{Co}^{2+} > \text{Mn}^{2+} \geq \text{Fe}^{2+} \geq \text{Ni}^{2+} > \text{Zn}^{2+} \gg \text{Cd}^{2+} > \text{Pb}^{2+} > \text{Cu}^{2+}$ . With sulfide production, all metals will be concerned, with a high fraction of metals complexed and consequently less available. With depth, if OM is consumed, some metals can be more labile, such as Fe, Ni and Cu, which were shown to be highly influenced by OM contents (Figure 45 and 46), altering the order of lability as follows:  $\text{Fe}^{2+} \geq \text{Co}^{2+} > \text{Mn}^{2+} \geq \text{Ni}^{2+} > \text{Zn}^{2+} \gg \text{Cu}^{2+} \gg \text{Pb}^{2+} > \text{Cd}^{2+}$ . These calculations help to better understand the fate of trace metals in this medium, showing a higher availability in the first centimeters of the sediment.

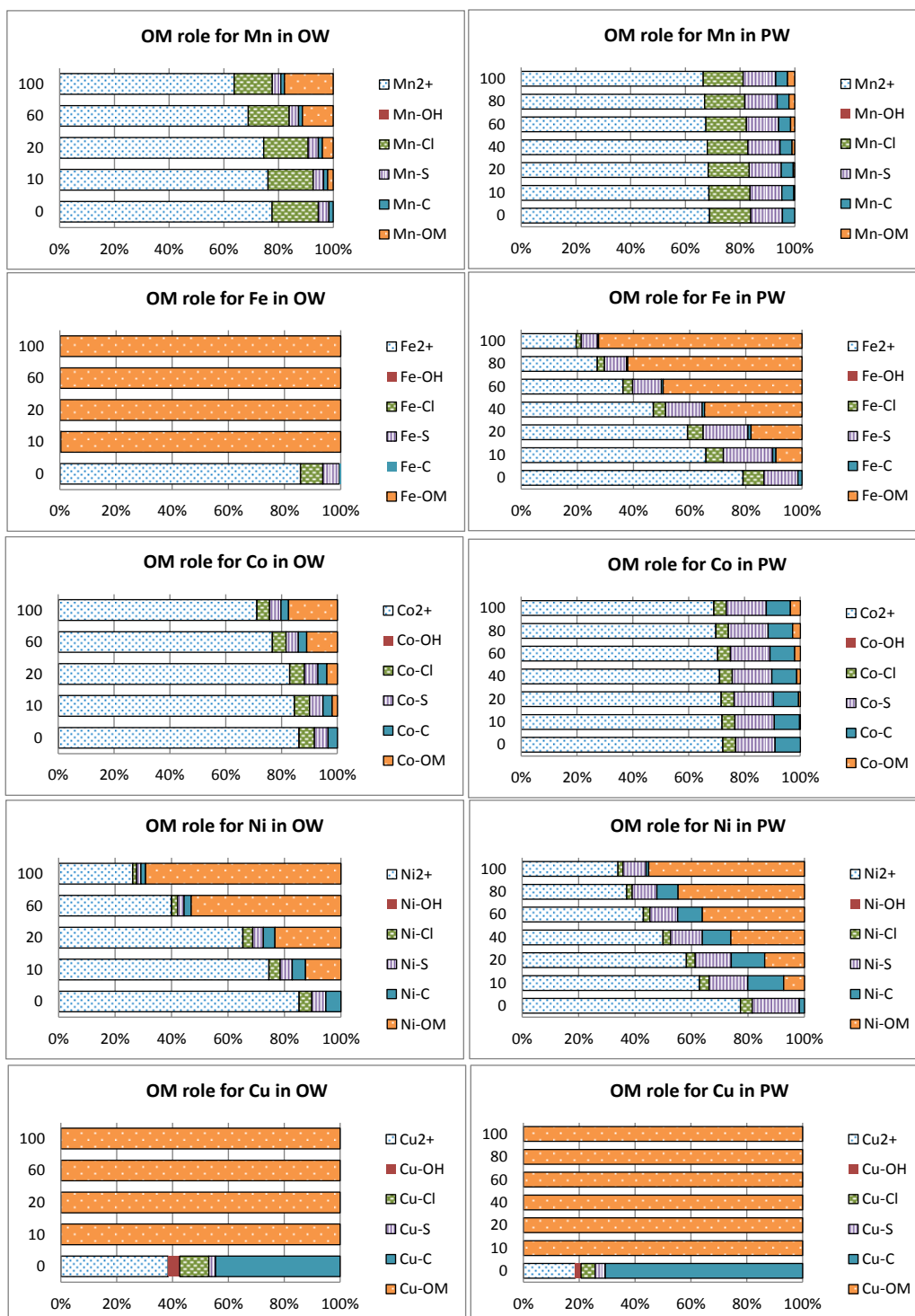


Figure 41. Percentage of free ion, metal-OH (bound to hydroxides), metal-Cl (bound to chlorides), metal-S (bound to sulphur groups), metal-C (bound to carbonates), metal-P (bound to phosphates) and metal-organic matter (OM) complexes calculated with Visual Minteq for Mn, Fe, Co, Ni and Cu in overlying water (OW) and porewaters (PW) (depth: -1 cm) of a control core (core 1) in function of OM (contents in DOC from 0 to 100 mg L<sup>-1</sup>).

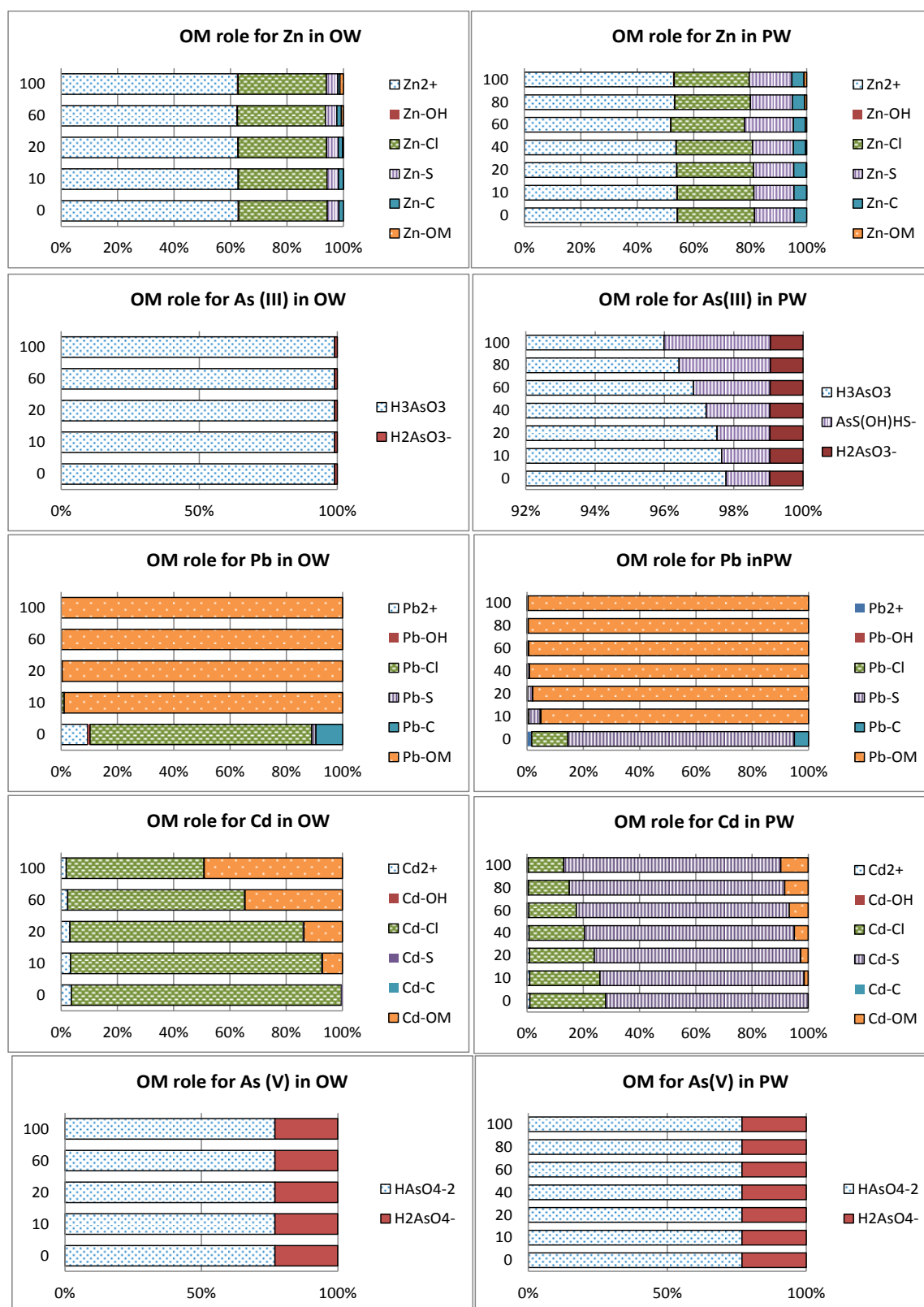


Figure 42. Percentage of free ion, metal-OH, metal-Cl, metal-S, metal-C, metal-P and metal-organic matter complexes calculated with Visual Minteq for Zn, As(III), Pb, Cd and As(V) in overlying water and porewaters (depth -1 cm) of a control core (core 1) in function of organic matter (contents in DOC from 0 to 100 mg / L).



Figure 43. Percentage of free ion, metal-OH (bound to hydroxides), metal-Cl (bound to chlorides), metal-S (bound to sulphur groups), metal-C (bound to carbonates), metal-P (bound to phosphates) and metal-organic matter (OM) complexes calculated with Visual Minteq for Mn, Fe, Co, Ni, Cu, Zn, As(III), Pb, Cd and As (V) in porewaters (depth -1 cm) of a control core (core 1) in function of sulphides [contents in S(-II) from 0 to 1000 μM].

Arsenic is a metalloid, with two main redox forms (III and V), that does not behave like other metals since its species are mainly oxoanions. Eh-pH diagrams using pH and redox potential values obtained in our work show that arsenic is mostly present as As (III) (as  $\text{H}_3\text{AsO}_3$ ), but also as As (V) ( $\text{H}_2\text{AsO}_4^-$  and  $\text{HAsO}_4^{2-}$ ). The most toxic species are inorganic As(III), followed by inorganic As(V). The less toxic species are the organic ones; Methylated compounds such as methylarsonate (MMA), dimethylarsinate (DMA), trimethylarsine oxide (TMAO) and tetramethylarsonium (TETRA) are considered moderately toxic, while more complex organoarsenic compounds like arsenobetaines (AsB), arsenocholines (AsC) and arsenosugars (AsS) are not harmful (Kumaresan 2001, Leverone 2007).

### 2.4.5.3. Mineral saturation

The saturation index (SI) was calculated to know the extent of porewater saturation with respect to a mineral phase. Thermodynamic calculations carried out from experimental data obtained from control and experimental cores of the LABOSI-4 experiment predict the speciation of numerous compounds with respect to carbonates, phosphates and sulfides.

The aim of this section is to underline how trace metals are presumed to be removed from the porewaters and trapped in the particles, under pure phases, coprecipitation, or even adsorption. It will also permit to predict how the stock of metals present in the sediment can be released, following the modification of several key parameters as mentioned previously (mainly OM and sulphides).

Calcium ↓ The SI value of calcite is near equilibrium at the first centimetres of the surface sediment (1–2 cm; see Figure 44) and becomes slightly supersaturated below a depth of ca –3 cm in the experimental core and –5 cm in the control core. Hydroxylapatite was found to be undersaturated in both the experimental and control cores in the first centimeters (–1 cm to –4 cm) and near equilibrium from –5 cm depth.

Magnesium ↓ Comparison of the IAP values corresponding to  $\text{MgCO}_3$  in experimental and control cores (Figure 44) shows that anoxic porewaters extracted from these sediments are undersaturated with respect to the pure magnesite in the first centimeters. In the experimental core magnesite becomes saturated at –3 cm depth, whereas in control core it appears from –5 cm of depth. Sediments were found to be oversaturated with respect to  $\text{CaMgCO}_3$  in both cores at all depths (Figure 44).

Manganese ↓ The IAP profile vs depth for manganese reveals that anoxic porewaters are slightly oversaturated with respect to the solubility product of the pure  $\text{MnCO}_3$  (rhodochrosite) along the entire length of the studied sediment core (Figure 44). The affinity of Mn for carbonates was indeed proved in the previous part: in porewaters, Mn was significantly associated with  $\text{HCO}_3^-$  and  $\text{CO}_3^{2-}$ . On the other hand, by calculating the ionic activity product of MnS, the possibility of Mn-sulfide precipitation is explored:  $-\log(\text{IAP})$  values varying from 3 to 5 (Figure 45) are much higher than the solubility product of MnS. This implies that Mn (II) cannot react with sulphide ions to generate pure and separate MnS phases, and thereby its concentration in porewaters is certainly not controlled by MnS minerals. With respect to phosphates, the experimental core was found to be slightly saturated over the whole profile, whereas the control core was found to be undersaturated in the three first cm and becomes oversaturated from –4 cm.

Iron ↓ As shown in Figure 44, porewater is supersaturated with respect to siderite ( $\text{FeCO}_3$ ) in both cores between –2 cm and –4 cm depth. This mineral would,

therefore, be expected to precipitate in these sediments. Iron-phosphate precipitation is also investigated in the present work by calculating the ionic activity product of vivianite vs depth, (Figure 44). It was found to be near equilibrium over the whole profile for the experimental core, whereas it was found to be oversaturated from a depth of  $-4$  cm in the control core, as confirmed by the distribution obtained from thermodynamic calculations. It is also shown that anoxic porewaters extracted from sediments are oversaturated with respect to  $\text{FeCuS}_2$  and undersaturated with respect to pure iron sulfides and (Figure 45). Conversely, it has been clearly demonstrated that AVS composed mainly of FeS is present in our sediments. Calculations were done only with respect to FeS mackinawite, but there are also others like greigite, pyrrhotite or troilite, which were not taken into account and could precipitate (Gao et al. 2009, Huerta-Diaz et al. 1998). Moreover, sulphide concentrations used here correspond to field campaigns (2007–2008), which could also explain this undersaturation state.

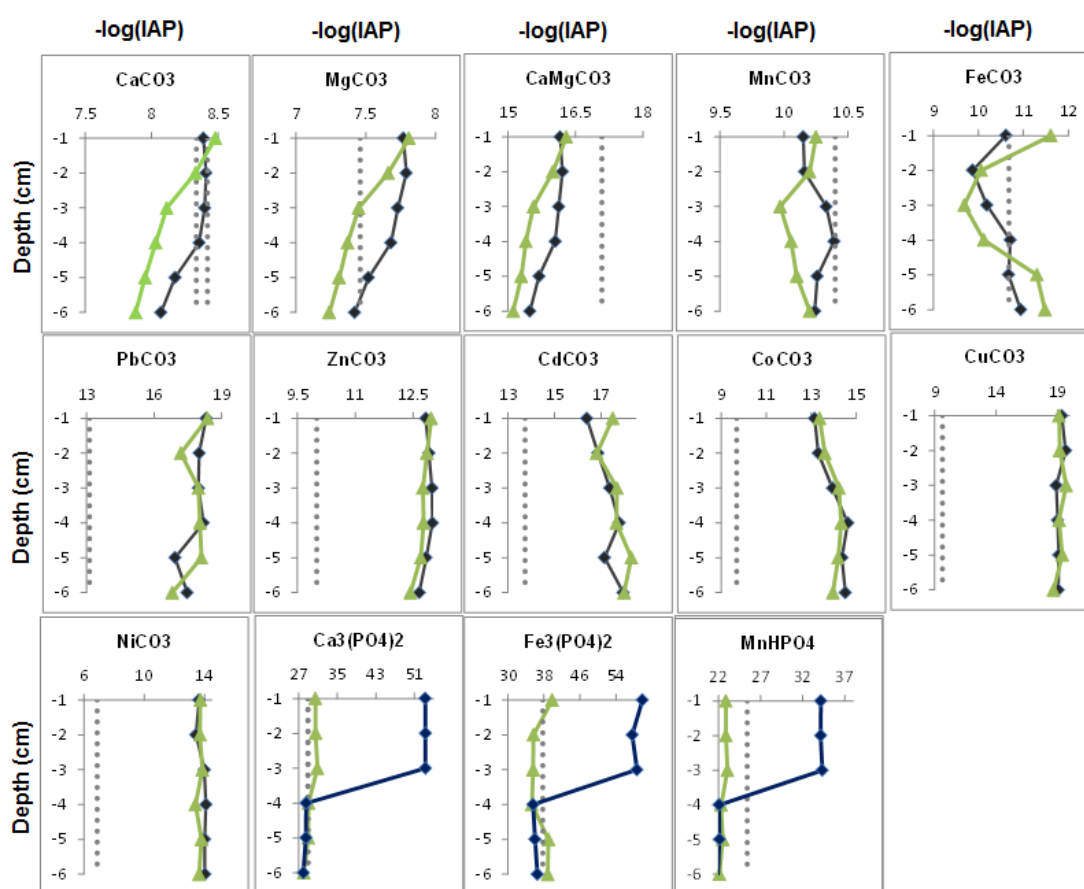


Figure 44: cologarithms of ionic activity products (IAP) profiles for  $\text{Ca}^{2+}$ ,  $\text{Mg}^{2+}$ ,  $\text{Mn}^{2+}$ ,  $\text{Fe}^{2+}$ ,  $\text{Pb}^{2+}$ ,  $\text{Zn}^{2+}$ ,  $\text{Cd}^{2+}$ ,  $\text{Co}^{2+}$ ,  $\text{Cu}^{2+}$  and  $\text{Ni}^{2+}$  in interaction with carbonates for a control core (line blue) and an experimental core (line green), and for  $\text{Ca}^{2+}$ ,  $\text{Fe}^{2+}$  and  $\text{Mn}^{2+}$  interactions with phosphates. These values were compared to the solubility products of the different minerals (lines in dots): calcite ( $\text{CaCO}_3$ ,  $\text{pKs} = 8.42$ ); aragonite ( $\text{CaCO}_3$ ,  $\text{pKs} = 8.46$ ); magnesite ( $\text{MgCO}_3$ ,  $\text{pKs} = 7.46$ ); dolomite ( $\text{CaMgCO}_3$ ,  $\text{pKs} = 17.09$ ); rhodochrosite ( $\text{MnCO}_3$ ,  $\text{pKs} = 10.4$ ); siderite ( $\text{FeCO}_3$ ,  $\text{pKs} = 10.68$ ); cerussite ( $\text{PbCO}_3$ ,  $\text{pKs} = 13.13$ ); smithsonite ( $\text{ZnCO}_3$ ,  $\text{pKs} = 10.0$ ); octavite ( $\text{CdCO}_3$ ,  $\text{pKs} = 13.74$ ); cobaltocalcite ( $\text{CoCO}_3$ ,  $\text{pKs} = 9.68$ );  $\text{CuCO}_3$  solid ( $\text{pKs} = 9.63$ ); gaspeite ( $\text{NiCO}_3$ ,  $\text{pKs} = 6.87$ );  $[\text{Ca}_3(\text{PO}_4)_2]$ ,  $\text{pKs} = 28.92$ ]; vivianite [ $\text{Fe}_3(\text{PO}_4)_2$ ,  $\text{pKs} = 37.76$ ] and  $\text{MnHPO}_4$  ( $\text{pk} = 25.4$ ) (values from Visual Minteq data base corresponding to the reaction  $\text{MeS} + \text{H}^+ \rightleftharpoons \text{Me}^{2+} + \text{HS}^-$ ).

Lead ↓ The SI values corresponding to  $\text{PbCO}_3$  indicate that the porewater is undersaturated over the whole depth (Figure 44). In addition, chemical speciation on this metal obtained from thermodynamic calculations and sequential extractions show that Pb is not associated with the carbonate phase. This suggests that cerussite ( $\text{PbCO}_3$ ) would not be expected to form in this sedimentary medium. In contrast, porewaters are supersaturated with respect to galena ( $\text{PbS}$ ), see Figure 45, suggesting the precipitation of this mineral in interstitial waters, as seen from chemical speciation calculations and sequential extractions. Furthermore, the low percentages of Pb found in the exchangeable and Fe/Mn oxides/hydroxides phases are probably due to the relative stability of galena in excess when anoxic sediments samples are treated according to the two first chemical extraction procedures described by Rauret et al. (1999 and 2000).

Zinc ↓ The values of  $-\log(\text{IAP})$  for  $\text{ZnCO}_3$  are, over the entire pore water profile, higher than the cologarithm of the solubility product of smithsonite (Figure 44), indicating that this mineral would not be expected to precipitate in sediments. Also, chemical speciation calculations show that Zn is associated with carbonates. This leads us to assume the existence of solid solutions composed associating Ca, Zn and carbonates (or  $\text{Ca}_{1-x}\text{Zn}_x\text{CO}_3$ ) in these sediments. On the other hand, porewaters are found to be oversaturated with respect to ZnS crystals (Figure 45) as expected from sequential extraction results. Our thermodynamic calculations further show that both wurtzite and sphalerite should precipitate in interstitial waters.

Cadmium ↓ To raise the possibility of cadmium-carbonate precipitation, the ionic activity product of  $\text{CdCO}_3$  was calculated with depth (Figure 44). The results of  $-\log(\text{IAP})$  indicate that porewaters are undersaturated with respect to  $\text{CdCO}_3$  crystals. Furthermore, chemical speciation data obtained for Cd show that this metal was very weakly detectable in the carbonate phase. All these findings suggest that cadmium (II) solute does not precipitate with carbonate ions as a pure and separate  $\text{CdCO}_3$  phase in the sedimentary medium. In contrast, cadmium-sulfide precipitation might occur in these sediments since sequential extractions show a high percentage of Cd extracted in the two last steps. To support this, the IAP values corresponding to the product of CdS are determined with depth (Figure 45), and the obtained results reveal that anoxic porewaters are supersaturated with respect to greenockite, revealing the possibility of precipitation of  $\text{Cd}^{2+}$  ions with sulphide ions.

Cobalt ↓ The  $-\log(\text{IAP})$  values corresponding to  $\text{CoCO}_3$  were determined with depth (Figure 44). Results show that porewaters are highly undersaturated with respect to cobaltocalcite,  $\text{CoCO}_3$ , which is supported by sequential extractions. Cobalt-sulfide formation is also examined by calculating the ionic activity product at various depths (Figure 45), suggesting that porewaters are, in most cases, undersaturated with respect to alpha CoS, but are oversaturated with respect to beta CoS. Co speciation shows that cobalt is well associated with the oxidizing phase. This implies that cobalt would be either complexed with sedimentary organic matter and/or associated [by (co)precipitation/adsorption] with iron sulphide(s). In this latter case, this would agree well with general studies carried out by Morse and Luther (III) (1999) on trace metals pyritization in anoxic sediments.

Copper ↓ The cologarithms of the IAP for  $\text{CuCO}_3$  are much higher than the pKs values reported for the  $\text{CuCO}_3$  solid (Figure 44). As a result, this precipitate would not be expected to be generated in the pore water medium. This agrees well with chemical distribution study, showing very weak proportions of copper presumably bound to sedimentary carbonates which were eliminated during the first step of the sequential extraction procedure. Note, however, that understanding the

behaviour of copper is difficult because Cu generates very strong complexes with a wide variety of dissolved compounds including organic matter and (poly)sulfides (Morse and Luther III 1999; Shea and Helz 1988). Thermodynamic calculations show that porewaters are supersaturated (Figure 45) with respect to covellite (CuS) and chalcopyrite (CuFeS<sub>2</sub>), as observed in a previous work of our group (Gao et al. 2009) indicating that these minerals would be expected to precipitate and therefore to control copper concentration in the sediment. This is supported by the high percentages of this metal found in the oxidizable phases by using chemical sequential extraction.

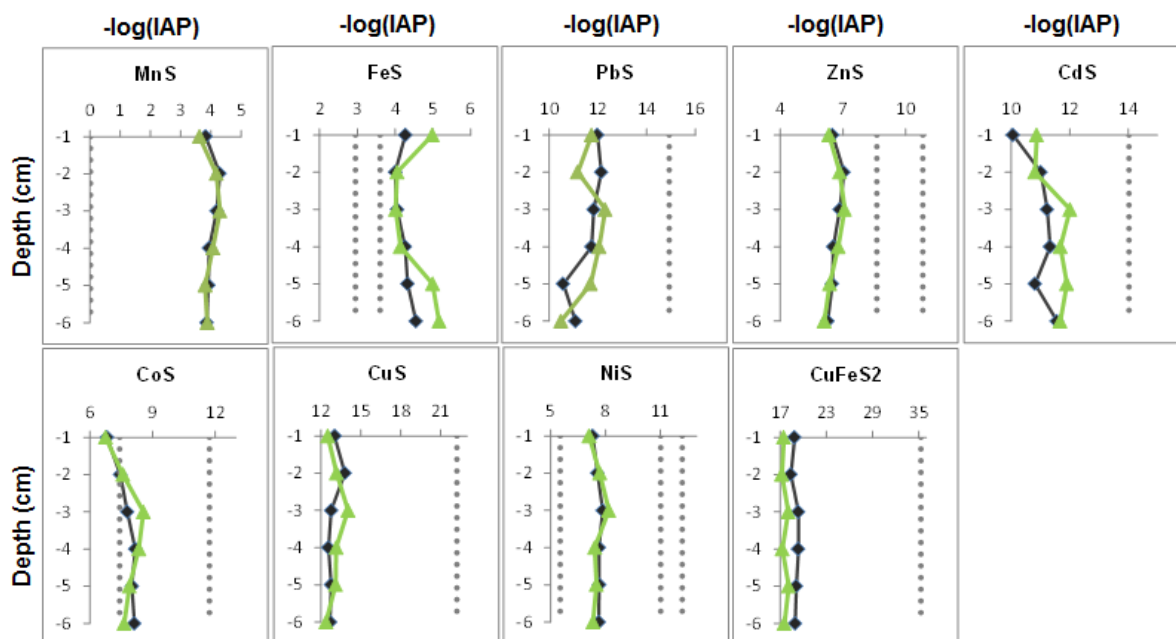


Figure 45: cologarithms of ionic activity products (IAP) profiles for Mn<sup>2+</sup>, Fe<sup>2+</sup>, Pb<sup>2+</sup>, Zn<sup>2+</sup>, Cd<sup>2+</sup>, Co<sup>2+</sup>, Cu<sup>2+</sup> and Ni<sup>2+</sup> in interaction with sulfides for a control core (line blue) and an experimental core (line green). These values were compared to the solubility products of the different sulfide minerals (lines in dots). MnS green (pKs = 0.02); mackinawite (FeS<sub>(1-x)</sub>, pKs = 3.6); FeS ppt (pKs = 2.95); galena (PbS, pKs = 14.92); sphalerite (ZnS, pKs = 10.82); wurtzite (ZnS, pKs = 8.62); greenockite (CdS, pKs = 14.02); CoS α (pKs = 7.42); CoS β (pKs = 11.72); covellite (CuS, pKs = 22.22); NiS α (pKs = 5.52); NiS β (pKs = 11.02); NiS γ (pKs = 12.02); and chalcopyrite (CuFeS<sub>2</sub>, pKs = 35.27) (values from Visual Minteq data base corresponding to the reaction  $\text{MeS} + \text{H}^+ \rightleftharpoons \text{Me}^{2+} + \text{HS}^-$ ).

Nickel ↓ Computational calculations permit to reach the ionic activity product of NiCO<sub>3</sub> at different depths in porewaters. IAP values show that these porewaters are highly undersaturated with respect to NiCO<sub>3</sub> precipitate, suggesting that gaspeite would not precipitate in the medium (Figure 45). Accordingly, nickel carbonate cannot be formed as a separate phase in the sediment. However, sequential extractions reveal the presence of Ni in the carbonate fraction. The incorporation/adsorption of Ni(II) ions into the calcite lattice would be expected to occur, at least partially, in the sediment in order to generate nickel calcites: Ni<sub>x</sub>Ca<sub>1-x</sub>CO<sub>3</sub>. The possibility of nickel-sulfide precipitation is also raised in this work by assessing the ionic activity product of NiS. The corresponding IAP values indicate that porewaters are supersaturated to NiS crystals except for the α form (Figure 45).

### Influence of pH, temperature, DOC and sulfides in mineral saturation

Calculations were carried out to simulate the behaviour of the system when different conditions from those observed in the LABOSI-4 experiment could occur. This is also an important feature of such a software: to propose predictive results from possible changes of sediment properties (input of OM, increase of sulfatoreduction bacteria activity, variation of the temperature, acidification, etc.). Results should not be interpreted as quantitative values but rather as qualitative trends to better understand the dynamic of biogeochemical exchanges of trace metals between the solid and the liquid phases of the sediment.

With respect to sulfides, when concentrations are high ( $> 50 \mu\text{M}$ ), as measured in some field campaigns, the precipitation of mackinawite ( $\text{FeS}_{1-x}$ ) is observed. Precipitation of  $\text{CoS}_2$  was also observed to increase with higher sulfides contents. Nevertheless, no relevant changes in saturation were found when different DOC contents were observed. Temperature variations, between  $5\text{--}20^\circ\text{C}$ , show that when temperature is lower than  $15^\circ\text{C}$  there is no precipitation of calcite, whereas higher temperatures (than  $15^\circ\text{C}$ ) lead to siderite precipitation ( $\text{FeCO}_3$ ). pH changes result in small changes in saturation indices; when pH is lower than 7 there is no precipitation of calcite, CoS alfa, dolomite, magnesite,  $\text{MnCO}_3$  and siderite. When pH is higher than 7.5, precipitates that were not originally presented at some depths such as siderite will appear.

#### **2.4.5.4. Ferrihydrite-metal adsorption calculations**

As shown previously, the calculations only referred to the porewater composition without any solid phase considerations. In order to give to the model a better view on the whole system (composed of particles, porewaters, bacteria, etc.), we decided also to include in some simple calculations surface complexation modeling of ions adsorption onto the iron hydroxides present in the first layers of surface sediments (the thickness of this layer depends on the anoxia set up by early diagenetic processes). For this study, two surface complexation models were used: (i) the Diffusive double Layer Model (DLM), using the predefined parameter set Two-line ferrihydrite with DLM, and the database feo-dlm\_2008.vdb (Dzombak and Morel, 1990); and (ii) the Three Plane Model (TPM) CD-MUSIC, with the predefined parameter set for ferrihydrite of Fh-gen\_CD.vdb, using the parameterization of Gustafsson et al (2009). Both models show similar results, and only results from the TPM are shown here.

To predict the fate of metals in this environment, different concentrations of iron oxihydroxides were tested in this work (from 0 to  $2 \text{ g L}^{-1}$ ), since these adsorption processes restrict their mobility (Gustafsson, 2007). Arsenic and cobalt were observed to be strongly influenced by adsorption reactions to particle surfaces (Figure 46), whereas the other studied metals were found to be weakly affected, as previously seen in many other works [Anninou and Cave (2009), Edenborn et al. (1986), Cornelis et al. (2008), Sracek et al. (2004)] and from sequential extractions. When the concentration of the solid phases increases, these metals will be more strongly adsorbed (Wilkie and Hering, 1996), especially in the case of As (V), which was found to be almost 100% adsorbed to ferrihydrite when the concentration of this iron oxihydroxide is higher than  $0.5 \text{ g L}^{-1}$  (Figure 46).

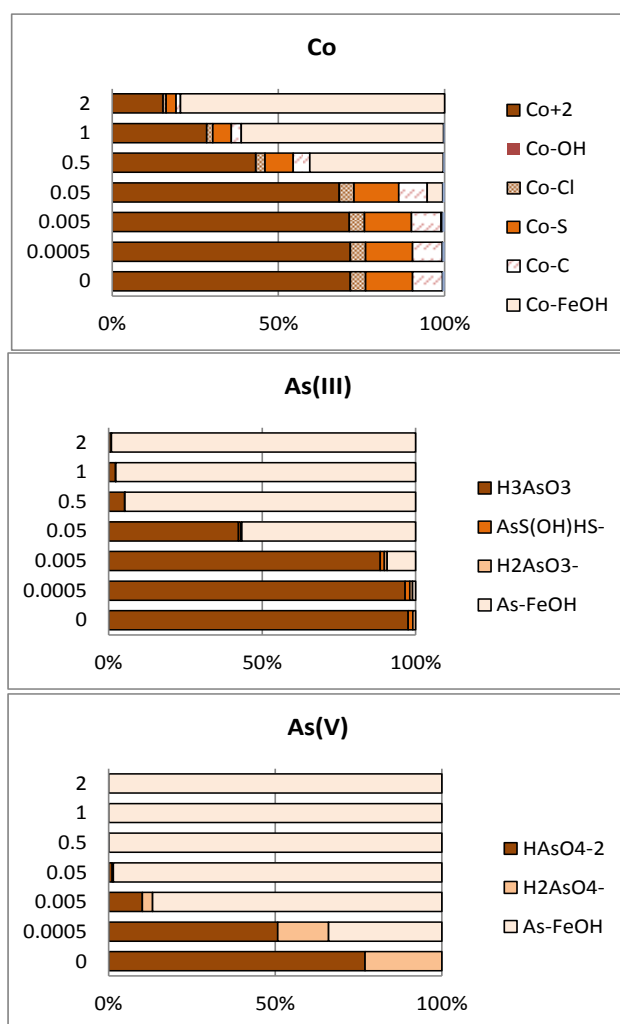


Figure 46. Thermodynamic chemical speciation of Co, As(III) and As(V) calculated with Visual Minteq in porewaters (depth –1 cm) of a control core (core 1) in function of iron oxihydroxides contents (from 0 to 2 g L<sup>-1</sup>).

Iron oxihydroxides will be reduced with depth, liberating in this case adsorbed elements. As observed in Figure 40, cobalt and arsenic (III) concentrations slightly increase in the first centimeters of the sediment, but then decrease at higher depths. This could be explained by a partial precipitation of sulphides (as seen in Figure 45, cobalt is expected to precipitate with sulphides).

In the future, it will be interesting to know the fraction of As and Co adsorbed on iron oxihydroxides to see if it corresponds with the quantity predicted by thermodynamic calculations.

#### 2.4.6. Numerical modeling conclusions

Thermodynamic calculations were carried out in surface waters and porewaters of control and experimental cores, mainly in samples from the LABOSI–4 experiment. Tests were done with concentrations obtained from DGT, DET and ICP-MS analyses, showing in general good agreement. These calculations were done in order to study metal speciation and predict the existence of solids adsorbing trace metals in order to know the fate of metals in this environment. To better understand the observed vertical profiles several parameters such as temperature, pH, organic

matter and sulfides were modified, since they can partly control the mobility of trace elements. With respect to the speciation, most of the metals were found to be mainly present in the labile form in the following order:  $\text{Co}^{2+} > \text{Mn}^{2+} > \text{Fe}^{2+} > \text{Ni}^{2+} > \text{Zn}^{2+}$ . Conversely, Cu and Pb were mainly associated with organic matter; Cd with inorganic complexes (sulfides); As (III) as  $\text{H}_3\text{AsO}_3$  [and to a lesser extent as  $\text{AsS(OH)HS}^-$ ]; and As(V) as  $\text{HAsO}_4^{2-}$  [as arsenic speciation was not measured, two different cases were simulated: one with As(III) and another with As(V)]. Calculations showed that sulfides played an important role for all metals, whereas none of the studied metals seemed to be highly dependent on temperature or pH. For pH, it was previously observed to be, in general, a key parameter (Lourino et al. 2011, Byrne 1988); may be in our case the values are too basic to start the decomplexation and dissolution process. Organic matter was observed to be an important parameter to take into account for Fe, Co Cu, As(III), Pb and Cd since they are highly dependent on its concentration, with an availability order of:  $\text{Fe}^{2+} \geq \text{Co}^{2+} > \text{Mn}^{2+} \geq \text{Ni}^{2+} > \text{Zn}^{2+} \gg \text{Cu}^{2+} \gg \text{Pb}^{2+} > \text{Cd}^{2+}$ . Saturation indices were calculated with respect to carbonate, sulphide and phosphate minerals. For carbonates, only  $\text{MnCO}_3$  was oversaturated over the whole depth, whereas  $\text{CaCO}_3$ ,  $\text{MgCO}_3$  and  $\text{FeCO}_3$  were found to precipitate at some depths, which means that carbonates don't play a significant role in the speciation of trace metals. On the other hand, most of the metallic sulfides were found to precipitate, such as FeS, PbS, ZnS, CdS, CoS, CuS, NiS and  $\text{CuFeS}_2$ , which clearly indicates that metal speciation in these sediments is controlled by sulfides, but also by organic matter. Numerous metals associate efficiently with fulvic and humic acids in the porewaters, but probably also in the particulate organic matter.

These results show that early diagenesis processes were observed in this study case; the bacterial/reductive dissolution of Mn(III and IV) and Fe(III) oxides/hydroxides to Mn(II) and Fe(II) accompanied with microbial degradation of OM led to an increase of trace metals in porewaters at levels that raised the possibility of minerals precipitation. Metal simulations showed different behaviours of elements in sediments through their removal from interstitial waters by associations with carbonates and/or sulphides: either by direct precipitation to form pure solid phases or by coprecipitation/sorption processes. Overall, results obtained from thermodynamic calculations showed good agreement with experimental obtained data.

Adsorption studies were also done by using the surface complexation model in order to examine the adsorption of metals to iron oxihydroxides. As and Co were found to be dependent on the contents of iron oxihydroxides, with higher adsorption at higher contents. These iron hydroxides participate to slow down the diffusion rate of Co and As. In anoxic sediments, Co and As should be released from HFO in porewaters (slight increase with depth near the sediment water interface). However, as shown by the calculations, they can also re-precipitate with sulfides [in the case of  $\text{Co}^{2+}$  and As(III)] or be stabilized in porewater by organic complexation.

### 3. POLICY SUPPORT

The contamination of the Belgian Continental Plate (BCP) by transition metals and metalloids is significant. According to the background levels of trace metals in sediments in the North Sea reported by OSPAR (2000) [Cu/Al ( $2.2\text{--}5.7 \cdot 10^{-4}$ ), Pb/Al ( $1.8\text{--}4.0 \cdot 10^{-4}$ ) and Cd/Al ( $0.007\text{--}0.030 \cdot 10^{-4}$ )], values on the BCZ are equal to the upper value for Cu, are 2.5 times higher than the upper value for Pb and 5 times higher than the upper value for Cd. Efforts should be made to reduce the human impact on that zone, especially in the area extending up to 3-4 km in the open sea between Oostende and Zeebrugge. Sediments are able to accumulate large quantities of contaminants that may affect benthic biodiversity and ecology of many invertebrates and vertebrates.

Bacterial diversity of the BCP area is reduced (at least during the winter months) in the zone extending up to 3-4 km in the open sea, when compared to sediment stations far from the coast. However, in itself, bacterial diversity as measured with Denaturing Gradient Gel Electrophoresis (DGGE) is not a variable which can be considered as a good indicator of marine sediment quality. The same conclusion may be applied to Micro-Eukaryotes. This is probably the result of adaptation to elevated concentrations of toxic metals, especially in areas with a long history of contamination.

Bacterial biomass is a variable which is a better indicator than biodiversity for marine sediment quality, especially for arsenic in porewaters. Future studies should concentrate on arsenic speciation but also on the effect of microorganisms on the arsenic cycle.

Benthic upward fluxes of toxic metals and metalloids (such as Co, Mn and As) have been identified in the BCP coastal zone extending up to 3-4 km in the open sea (especially near stations 130, 140 and 700 on the eastern part of the Belgian coast). Arsenic is problematic as it is very toxic for man and marine life. It was demonstrated that arsenic may be released from muddy sediments of the BCP, especially during the spring phytoplankton blooms, at rates of ca.  $1 \mu\text{mol m}^{-2} \text{d}^{-1}$  (Gao et al. 2011). A clear link was thus established between arsenic effluxes and phytodetritus mineralization at the sediment-water interface (SWI) and it was estimated that about 55 kg of arsenic may be released into the seawater of the BCZ, in only two days and for an area of 720 km<sup>2</sup>, when only 5.2 g (dw) of phytodetritus are mineralized on each square meter of this area (Gao et al. 2011, Gillan et al., submitted). Products from fisheries (especially benthic and demersal fishes) and mussel-farming from this zone should be carefully monitored for metals and metalloids, especially arsenic.

The large phytoplankton blooms which inevitably occur each year on the Belgian continental plate are expected to increase effluxes of toxic metals from the sediments, especially from coastal muddy sediments on the eastern part of the Belgian coast. Efforts should be maintained to reduce nutrient inputs from the Scheldt estuary.

In October 2000 the EU Water Framework Directive (WFD) entered into force. The implementation of this WFD is currently raising a number of technical challenges for the Member States, particularly for Belgium, which should meet the WFD environmental objectives in 2015. Clearly, measurements performed during the MICROMET project between 2007 and 2010 suggested that a "good ecological and chemical status" will not be met in 2015 for the Belgian coastal ecosystem extending up to 3-4 km in the open sea between Oostende and Zeebrugge. A less stringent goal should be considered for this area.



## 4. DISSEMINATION AND VALORISATION

### 4.1. PhD thesis including MICROMET data

Ludovic LESVEN. 2008. Devenir des éléments traces métalliques au sein du sédiment, un compartiment clé de l'environnement aquatique. USTL, Lille, France. 181 pp.

Yue GAO. 2009. Trace metal behavior in sedimentary environments. VUB, Brussels, Belgium. 310 pp.

Annelies PEDE. 2011. Diversity and dynamics of protist communities in subtidal North Sea sediments in relation to metal pollution and algal bloom deposition. PAE-UGent, Gent, Belgium. 222pp. (Thesis submitted 14th October 2011)

### 4.2. Poster presentations and oral communications

- Gillan DC (2007) The MICROMET Project : Microbial Diversity and Metal Fluxes in Contaminated North Sea Sediments. Programme Science for Sustainable Development. Kick-off Meeting, Belgian Science Policy, Brussels, 26-27 Mars (oral communication).

- Pede A., Verstraete T., Vyverman W., Sabbe K. (2007) Eukaryotic Microbial Diversity and Metal Fluxes in Contaminated North Sea Sediments (MICROMET) : preliminary results. NecoV working group on Ecology of Aquatic Microorganisms, University of Amsterdam, 7th December (oral communication).

- Baeyens W, Bechara R, Billon G, Dubois P, Fischer JC, Gao Y, Gillan DC, Leermakers M, Lesven L, Pede A, Sabbe K (2008) Preliminary results of potential correlations between geochemical parameters, metals contamination and microbial diversity in North Sea sediments. 35th International Symposium on Environmental Analytical Chemistry, ISEAC 35, Gdansk, Poland, June, 22-26 (poster).

- Gao Y, Lesven L, Gillan D, Sabbe K, Billon G, Baeyens W (2008) Geochemical behavior of trace elements in sediments inside the Scheldt estuary plume. 10th International Estuarine Biogeochemistry Symposium, 18th May, Xiamen, China (poster).

- Gillan DC. (2008) The structure of microbial communities in North Sea sediments contaminated by metallic pollutants. Symposium ECODIM V: Interaction between microbes and metals. University of Concepcion, Chile, 18th January (oral communication).

- Pede A., Gillan D., Gao Y., Billon G., Lesven L., Leermakers M., Baeyens W., Vyverman W. & Sabbe K. (2009) Patterns in microbial diversity in North Sea sediments; correlations with specific sediment characteristics and heavy metal pollution. VLIZ jongerencontactdag, Brugge, 6th March (poster).

- Pede A., Gillan D., Gao Y., Billon G., Lesven L., Leermakers M., Baeyens W., Vyverman W. & Sabbe K. (2009) Spatial And Seasonal Variation In Microbial Diversity In Marine Subtidal Sediments In Relation To Sediment Geochemistry And Heavy Metal Pollution. ASLO Aquatic Sciences Meeting 2009, Nice (France), January, 25-30 (poster).
- Pede A., Gillan D., Gao Y., Billon G., Lesven L., Leermakers M., Baeyens W., Vyverman W. & Sabbe K. (2009) Spatial And Temporal Microbial Dynamics In Metal Contaminated North Sea Sediments. 44th EMBS 2009 (Liverpool), September, 7-11 (oral communication).
- Pede A., Gillan D., Gao Y., Billon G., Lesven L., Leermakers M., Baeyens W., Vyverman W. & Sabbe K. (2009). Analyzing Spatial and Temporal Trends in Eukaryotic Microbial Communities In Metal Contaminated North Sea Sediments. VLIZ Young Scientists' Day 2009 (Oostende), November, 27th (oral communication).
- Pede A., Gillan D., Gao Y., Billon G., Lesven L., Leermakers M., Baeyens W., Rousseau V., Vyverman W. & Sabbe K. (2011). Impact of phytoplankton bloom deposition on microbial communities and metal fluxes in contaminated North Sea sediments. VLIZ Young Scientists' Day 2011 (Brugge), 25<sup>th</sup> of February (oral communication).
- David C. GILLAN, Annelies PEDE, Koen SABBE, Yue GAO, Martine LEERMAKERS, Willy BAEYENS, Beatriz LOURINO CABANA & Gabriel BILLON (2011). Efflux of Metals from Contaminated Marine Sediments due to Bacterial Remineralisation of Phytodetritus. 7th international SedNet event, 6-9 April 2011, Venice, Italy (poster).

#### **4.3. Other activities**

- Design and implementation of the MICROMET website (<http://www.ulb.ac.be/sciences/micromet>) [12 465 connections since January 2007]
- Radio programme : "Histoire de Savoir" broadcasted on Radio Campus Brussels 92.1 FM on the 30 November 2009. Presentation of the MICROMET project [duration: 45 min]. Rebroadcasted two times.
- Presentation of the MICROMET project and results to students in Biology at Mons University and Université Libre de Bruxelles (ULB) [lectures of D.C. Gillan and Philippe Dubois : General Microbiology, Microbial Ecology, Marine Biology].

## 5. PUBLICATIONS OF THE TEAM

### 5.1. Published manuscripts

Gao Y, Lesven L, Gillan D, Sabbe K, Billon G, De Galan S, Elskens M, Baeyens W, Leermakers M (2009). Geochemical behavior of trace elements in sub-tidal marine sediments of the Belgian coast. *Mar Chem* 117:88–96.

Gao Y, Leermakers M, Pede A, Magnier A, Sabbe K, Lourino Cabana B, Billon G, Baeyens W, Gillan DC (2011) Response of DET and DGT trace metal profiles in sediments to phytodetritus mineralization. *J Environ Chem*, in press.

Gillan DC, Baeyens W, Bechara R, Billon G, Denis K, Grosjean P, Leermakers M, Lesven L, Pede A, Sabbe K, Gao Y. Links between bacterial communities in marine sediments and trace metal geochemistry as measured by in situ DET/DGT approaches. *Marine Pollution Bulletin*, in press.

### 5.2. Submitted manuscripts

Gillan DC, Pede A, Sabbe K, Gao Y, Leermakers M, Baeyens W, Lourino Cabana B, Billon G (submitted). Effect of bacterial mineralisation of phytoplankton-derived phytodetritus on the release of arsenic, cobalt and manganese from muddy sediments in the Southern North Sea. A microcosm study.

### 5.3. Manuscripts in preparation

Pede, A., Gillan, D., Gao, Y., Billon, G., Lesven, L., Verstraete, T., Baeyens, W., Vyverman, W. & Sabbe K. (in prep. a). Microbial eukaryote diversity and community structure in relation to natural stressors and trace metal pollutants in subtidal coastal marine sediments (North sea, Belgium).

Pede, A., Gillan, D., Gao, Y., Billon, G., Lesven, L., Leermakers, M., Baeyens, W., Verstraete, T., Vyverman, W. & Sabbe K. (in prep. b). Effects of spring phytoplankton bloom deposition on seasonal dynamics and vertical distribution of microbial eukaryotes in a silty, metal-contaminated sediment in the southern North sea.

Pede, A., Gillan, D., Gao, Y., Billon, G., Verstraete, T., Leermakers, M., Vyverman, W. & Sabbe K. (in prep. c). Impact of phytoplankton bloom deposition and concomitant metal fluxes on the composition and activity of benthic microbial communities in subtidal marine sediments: a microcosm study.

Pede, A., Gillan, D., Verstraete, T., Baré, J., Vyverman, W. & Sabbe K. (in prep. d). Short-term response of active microeukaryotic communities to arsenic ( $\text{KH}_2\text{AsO}_4$ ) contamination in silty and sandy subtidal coastal marine sediments.



## 6. ACKNOWLEDGMENTS

The MICROMET research was supported by the Belgian Science Policy Office (BELSPO) through the SSD research program (Science for a Sustainable Development, contract MICROMET n° SD/NS/04A and SD/NS/04B). Annelies Pede and Koen Sabbe acknowledge financial support from BOF-GOA projects 01GZ0705 and of Ghent University (Belgium). Contribution of the "Centre Interuniversitaire de Biologie Marine" (CIBIM). The MICROMET partners are indebted to Jean-Yves Parents and Dr. Véronique Rousseau (ULB, Brussels) for their help with the cultivation of *Phaeocystis* and *Skeletonema*, to Kevin Denis and Prof. Philippe Grosjean (Mons University) for their help with the automatic counting of bacteria using ZooPhytoImage. Many thanks also to André Cattrijsse and all the crew of the RV Zeeleeuw, and to Mathieu Bauwens (ULB) for his help in the laboratory.



## 7. REFERENCES

- Allen et al. (1980). *Envir. Sci. Technol.* 14, 441-443.
- Aller (1990) *Phil. Trans. R. Soc. London A* 331:51– 68.
- Aller (1994) *J. Mar. Res.* 52:259–295.
- Alongi et al. 1996. *Estuar Coast Shelf Sci* 42:197-211.
- Aminot A, Kerouel R. *Hydrologie des ecosystems marins. Paramètres et analyses*, Ifremer (Eds), 2004:336.
- Anderson et al (2008) *PERMANOVA Primer Guidance*
- Anninou and Cave (2009). *Estuarine, Coastal and Shelf Science* 82, 515-524.
- Baeyens et al (1986) In: Nihoul J. C. J (Eds.), *Marine Interfaces Ecohydrodynamics*. Elsevier Oceanography Series 42, pp 453-466.
- Baeyens et al. (2003) *Arch. Env. Cont. Toxicol.* 45:498-508.
- Bak et al. (1995) *Microb Ecol* 29:173-182.
- Balistrieri et al. (2008) *Appl Geochem* 23:3355–3371.
- Bass and Cavalier-Smith (2004) *Int J Syst Evol Microbiol* 54: 2393-2404.
- Bates et al. (1992) *Am J Epidemiol* 1992;135:462–476.
- Battin (1997) *Sci Tot Environ* 198:51–60.
- Bender & Heggie (1984) *Geochim. Cosmochim. Acta* 48:977-986.
- Benedetti et al. (1996). *Environ. Sci. and Technol.* 30(6), 1805-1813.
- Benedetti et al.(1995). *Environ. Sci. Technol.* 29, 446-457.
- Berelson et al. (2003) *Cont Shelf Res* 23:457-481.
- Billon et al. (2001) *Analyst* 126:1805-1809.
- Billon et al. (2007) *J Soils Sed* 7:17-24.
- Blair et al. (1985) *Appl Environ Microbiol.* 50, 996-1001.
- Boivin et al. (2006) *Env. Poll.* 140:239-246.
- Boon et al. (1999) *Est Coastal and Shelf Science* 49: 747-761.
- Bott, A.W. (1995) *Current Separation* 14 (1) 24–30.
- Böttcher et al. (2000) *Continental Shelf Res* 20:1749-1769.
- Bowman et al. (2005) *Microb Ecol* 49:451-460.
- Burdige & Gieskes (1983) *Am. J. Sci.* 283:29– 47.
- Byrne (1988). *Marine Chemistry*, 25, 163-181.
- Cadée (199) *J Sea Res* 36:227-230.
- Calmano W, Förstner U (1996) *Sediments and toxic substances*. Springer, Berlin, 335 pp.
- Canfield et al. (1986). *Chem Geol* 54:149-155.
- Canfield DE, Kristensen E, Thamdrup B (2005) *Aquatic geomicrobiology. Advances in marine biology volume 48*. Elsevier Academic Press, Amsterdam, 640 pp.
- Canfield et al. (1993) *Geochim. Cosmochim. Acta* 57:3867– 3883.
- Canavan et al. (2007) *Sci Total Environ.* 381, 263-279.
- Cernansky et al. (2009) *Bioresource Technology* 100: 1037-1040
- Chang et al (1993) *Plant Mol Biol Repr.* 11, 113-116
- Chantangsi & Leander (2010) *Int J Syst Evol Microb* 60: 1962-1977.
- Ciceri et al. (1992) *Hydrobiologia* 235/236:501-517.
- Clark RB (2001) *Marine pollution*. Oxford University Press, 236 pp.
- Clarke & Gorley (2006) *Primer V6 User Manual*, Plymouth UK, 192 pp.
- Cooksey & Wigglesworth-Cooksey (1995) *Aquat. Microb. Ecol.* 9:87-96.
- Corinaldesi et al. (2005) *Appl Environ Microbiol* 71:46-50.
- Cornelis et al. (2008). *Journal of Hazardous Materials* 159, 271-279.
- Coteur et al. (2003) *Environ Toxicol Chem* 22:2136-2144.
- Countway et al. (2005) *J. Euk. Microbiol.* 52:95-106.
- Créach et al. (2006) *J. Phycol.* 42: 1142-1154.
- Danis et al. ( 2004) *Sci. Tot. Environ.* 333:149-165.
- Davison (1980) *Geochim Cosmochim Acta* 44, 803-808.
- Davison & Zhang (1994) *Nature.* 367, 546-548.
- Davison et al. (1991) *Nature* 352:323-325.

- Davison (1991) *Aquat Sci.* 53, 300-329.
- de Beer et al. (2005) *Limnol Oceanogr* 50:113-127.
- De Gieter et al. (2002) *Arch. Env. Cont. Toxicol.* 43:406-417.
- Denis & Desroy (2008) *Mar Pollut Bull* 56:1844-1854.
- Desroy & Denis (2004) *Mar Ecol Prog Ser* 270:41-53.
- Diaz et al. (2006) *Environment International* 32: 711-717.
- Dietrich & Arndt (2000) *Mar. Biol.* 136:309-322.
- Diez et al. (2001) *Appl Environ Microbiol* 67:2932-2941.
- Di Toro et al. (1992) *Environ Sci Technol* 26:96-101.
- Docekalova et al. (2002) *Talanta* 57:145-155.
- Dowdle et al. (1996) *Appl. Environ. Microbiol.*,62(5), 1664-1669.
- Du Plessis et al. (2005) *J. Appl. Microbiol.* 98:901-909.
- Dzombak & More (1990) *Surface Complexation Modeling*. Wiley, New York.
- Edenborn et al (1986). *Biogeochemistry* 2, 359-376.
- Ehrlich (1997) *Appl Microbiol Biotechnol* 48:687-692.
- Ekelund et al. (2001) *Protist* 152:301-314.
- Ekelund et al. (2003) *Soil Biol Biochem* 35:1507-1516.
- Elderfield et al. (1981) *Am. J. Sci.* 281, 768–787.
- Epstein (1997) *Microb. Ecol.* 34:188-198.
- Fones et al. (2004) *Continent Shelf Res* 24:1485-1504.
- Ford & Ryan (1995) *Environ. Health. Perspect.* 103(Suppl 1):25-28.
- Fossing & Jørgensen (1989) *Biogeochem* 8:205-222.
- Franco et al. (2007) *Aquat Microb Ecol* 48:241-254.
- Franco et al. (2008) *Mar Ecol Prog Ser* 358:51-62.
- Froelich et al. (1979) *Geochim. Cosmochim. Acta* 43, 1075–1090.
- Gadd (2004) *Geoderma* 122:109-119.
- Gao et al. (2006) *Sci Tot Environ* 362:266-277.
- Gao et al. (2009) *Marine Chemistry* 117:88-96.
- Garland & Mills (1991) *Appl Environ Microbiol* 57:2351–2359.
- Gillan (2004) *Mar Pollut Bull* 49:504-513.
- Gillan et al. (2005) *Appl Environ Microbiol* 71:679-690.
- Gillan & Pernet (2007) *Biofouling* 23:1-13.
- Giller et al. (1998) *Soil Biol Biochem* 30:1389-1414.
- Gohin et al. (2003) *Cont Shelf Res* 23:1117–1141.
- Green N, Bjerking B, Hylland K, Ruus A, Rygg B (2003) Hazardous substances in the European marine environment: Trends in metals and persistent organic pollutants. Topic report 2/2003, European Environment Agency, Copenhagen, 83 pp.
- Gustafsson, J. P., 1999. WINHUMICV for Win95/98/NT (<http://www.lwr.kth.se/english/OurSoftware/WinHumicV/index.htm>).
- Gustafsson, (2006). Visual Minteq. Stockholm, <http://www.lwr.kth.se/English/OurSoftware/vminteq/>.
- Gustafsson and Bhattacharya (2007). In: Arsenic in soil and groundwater environment. Trace metals and other contaminants in the environment, Vol. 9, pp. 159-206. Elsevier
- Gustafsson et al. (2009). *Appl. Geochem.* 24(3), 454-462.
- Gutierrez et al (2009) *Bioessays* 31: 805-816.
- Gypens et al. (2007) *J sea Res* 57:19-35.
- Hamels et al. (2004) *Microb Ecol* 47:18-29.
- Hamels et al. (2005) *Eur J Protist* 41:241-250.
- Harnstrom et al. (2011) *Proc Nat Acad Sci USA* 108: 4252-4257.
- Hausmann et al. (2002) *Deep Sea Res.* 49:1959-1970.
- Heggie et al. (1987) *Geochim Cosmochim Acta* 51:1059-1070.
- Hitzl et al. (1997) *FEMS Microbiol Ecol* 22:167–174.
- Holmes (1986) *Mar Chem* 20:13-27.
- Holtze et al. (2003) *Soil Biol Biochem* 35:1175-1181.
- Hondeveld et al. (1994) *Mar. Ecol. Prog. Ser.* 109:235-243.

- Hondeveld et al. (1995) *Neth J Sea Res* 34:275–287.
- Hondeveld et al. (1999) *J. Sea Res.* 41:255-268.
- Hoppenrath & Leander (2006) *J Euk Microb* 53: 327-342.
- Huerta-Diaz et al. (1998) *Appl. Geochem.* 13, 213-233.
- Hunt (1983) *Limnol Oceanogr* 28:913–923.
- Iskrenova-Tchoukova et al. 2010. *Langmuir* 26:15909-15919.
- Jensen et al. (1990) *Mar Ecol Prog Ser* 61:87-96.
- Jongman et al. (1987) *Data analysis in community and landscape ecology.* Pudoc Wageningen.
- Jørgensen (1978) *Geomicrobiol J* 1:11-27.
- Jørgensen & DesMarais (1990) *Limnol Oceanogr* 35:1343-1355.
- Kennish MJ (1998) *Pollution impacts on marine biotic communities.* Kennish MJ & Lutz PL (eds) *CRC Marine Science Series*, CRC Press, New York, 310 pp.
- Knowles & Benson (1983) *Trends Biochem Sci* 8:178–180.
- Konstantinidis et al. (2009) *Appl Environ Microbiol* 75:5345–5355.
- Köpke et al. 2005) *Appl Environ Microbiol* 71:7819-7830.
- Kristensen et al. (1995) *Limnology and Oceanography* 40: 1430-1437.
- Kröncke et al. (2004) *Mar. Ecol. Progr. Ser.* 282:13-31.
- Kuehl (2000) *Design of experiments – statistical principles of research design and analysis.* Duxbury, USA.
- Kumaresan M. and Riyazzuddun P (2001). *Current Science*, 80(7).
- Kuwabara et al. (1996) In: *San Francisco Bay: The Ecosystem* (ed. J. T. Hollibaugh), pp. 157–172. *Pacific Div. Am. Assoc. Adv. Sci.*
- Lam et al. (2003) *Mar Ecol Prog Ser* 263: 83–92.
- Lancelot et al. (1987) *Ambio* 16:38–46.
- Lancelot et al. (2005) *Mar. Ecol. Progr. Ser.* 289, 63–78.
- Lancelot et al. (2007) *Journal of Marine Systems* 64:216–228.
- Lara et al. (2007) *FEMS Microbiol Ecol* 62 (3): 365-373.
- Lee et al.(2000). *JCHESS.* In: *ARMINES – Centre d’informatique Géologique*, Ecole de Mines de Paris.
- Leermakers et al. (2005) *Water Air Soil Pollut* 166:265-286.
- Lehman et al. (1997) *Environ Toxicol Chem* 16:2232-2241.
- Lesven et al. (2010). *Appl. Geochem.* 25, 1361-1373.
- Leverone, J.R. (2007) *Development of New Technologies for Removal of Arsenic from Water Supplies Through Biomimicry of Natural Systems.* Final Report.
- Lopez & Levinton (1987) *Q Rev Biol* 62, 235-260.
- Lourino et al. (2011). *J of Environ Monit.* 13, 2124-2133.
- Luo et al. (2009) *Hydrobiologia* 636: 233-248.
- Madrid et al. (2001) *Appl Environ Microbiol* 67:1663-1674.
- Mc Cune & Grace (2002) *Analysis of ecological communities.* MjM software design, Oregon, USA.
- Meyer-Reil & Köster (1992) *Mar. Ecol. Progr. Ser.* 81:65-72.
- Meysman et al. (2003a) *Comput Geosci* 29:291-300.
- Meysman et al. (2003b) *Comput Geosci* 29:301-318.
- M'Harzi et al. (1998) *J Plankton Research* 20:231-2052
- Michener, R. H., Schell, D. M., 1994. In: *Lajtha, D. K., Michener, R. H., (Eds). Stable Isotopes in Ecology and Environmental Science.* Blackwell, Oxford, 138-157.
- Moriarty et al. (1985) *Mar. Biol.* 85. 293-300.
- Morris et al. (2010) *The ISME J* 4:673–685.
- Morse & Luther-III (1999) *Geochim Cosmochim Acta* 63, 3373-3378.
- Mußmann et al. (2005) *Environ Microbiol* 7:405-418.
- Mukhopadhyay et al. (2002) *FEMS Microbiol Rev* 26:311–325.
- Muylaert et al. (2006) *J Sea Res* 55:253–265.
- Muyzer et al. (1993) *Appl Environ Microbiol* 59:695-700.
- Myers & Neelson (1988) *Science* 240, 1319–1321.

- Nakamura & Takaya (2003) *Mar Pollut Bull* 47:5-9.
- Newell (1965). *Proc. zool. Soc. Lond.* 144: 25-45.
- Nriagu JO (Ed.). (1994) *Arsenic in the Environment: Human Health and Ecosystem Effects*. *Adv. Environ. Sci. Technol.*, Vol. 27. John Wiley and Sons, New York.
- QSR (2000) *Quality Status Report 2000, Region II – Greater North Sea*. OSPAR Commission, London. 136 pp.
- Pakhomova et al. (2007) *Mar Chem* 107:319–331.
- Patterson et al. (1989) *Progress in Protistology* 3: 185-277.
- Pearce & Scheibling (1991) *J Exp Mar Biol Ecol* 147:147–162.
- Peperzak et al. (1998) *J Plankton Res* 20:517-537.
- Pershagen (1985) *Am J Epidemiol* 122:684–694.
- Petersen et al. (1996) In: Calmano W, Förstner U (eds) *Sediments and toxic substances*. Springer, Berlin, p. 37-50.
- Phillips (1984) *Bull Mar Sci* 35:283-298.
- Polymenakou et al. (2005) *Cont. Shelf. Res* 25:2570-2584.
- Powell et al. (2003) *FEMS Microbiol Ecol* 45:135-145.
- Rauch et al. (2008) *Marine Pollution Bulletin* 56:1284–1293.
- Rauret et al. (2000). *J. Environ. Monit.* 2: 228-233.
- Rauret et al.(1999). *J. Environ. Monit.* 1: 57-61.
- Richards & Bass (2005) *Curr. Opin. Microbiol.* 8:240-252.
- Rickard, D., Morse, J. W., 2005. *Mar. Chem.* 97, 141-197.
- Riebesell (1993) *Mar Ecol Prog Ser* 96:281-289.
- Riedel et al. (1987) *Est Coast Shelf Sci* 25:693–706.
- Rivera-Duarte & Flegal (1994) *Geochim Cosmochim Acta* 58:3307-3313.
- Rousseau et al. (2000) *J Sea Res* 43:357-372.
- Rousseau et al. (2002) *Mar. Ecol., Prog. Ser.* 236:61–73.
- Rousseau et al. (2008) In: V. Rousseau, C. Lancelot and D. Cox (Eds). *Presses Universitaires de Bruxelles*, Bruxelles, pp 45-59.
- Ruddick K, Lacroix G. (2008) In: *Current status of eutrophication in the Belgian coastal zone*. V. Rousseau, C. Lancelot and D. Cox (Eds). *Presses Universitaires de Bruxelles*, Bruxelles, 2008; 1–15.
- Rygg (1985) *Mar Ecol Prog Ser* 25:83-89.
- Schoemann et al. (1998) *Limnol Oceanogr* 43:1427-1441.
- Schoemann et al. (2005) *J. Sea Res.* 53, 43–66.
- Servais (1990) *Oceanol Acta* 13:229–235.
- Shea and Helz (1988). *Geochim. Cosmochim. Acta* 52, 1815-1825.
- Shimeta et al. (2007) *Aquat Microb Ecol* 48: 91-104.
- Skrabal et al. (1997) *Limnol. Oceanogr.* 42, 992–996.
- Skrabal et al. (2000) *Geochim Cosmochim Acta* 64:1843-1857.
- Sracek et al. (2004). *Applied Geochemistry*, 19, 169-180.
- Starink et al. (1994) *Appl Environ Microbiol* 60:167-173.
- Stefanowicz (2006) *Polish J Environ Stud* 2006;15:669–676.
- Stoeck et al. (2003) *Appl. Env. Microbiol.* 69:6856-6863.
- Stoeck et al. (2006) *Protist* 157:31-43.
- Sullivan & Aller (1996) *Geochim Cosmochim Acta* 60:1465–1477.
- Sunda and Lewis (1978) *Limnol. Oceanogr* 23:870-876.
- Sundby et al. (1986) *Geochim Cosmochim Acta* 50:1281–1288.
- Sutherland (2002) *Appl Geochem* 17:353-365.
- Teasdale et al. (1999) *Anal Chem* 71:2186-2191.
- Ter Braak et al. (1998) *CANOCO 4.5 reference guide and user's manual*.
- Thamdrup et al. (1994) *Geochim. Cosmochim. Acta* 58, 2563–2570.
- Tipping and Hurley (1992). *Geochim. Cosmochim. Acta* 56: 3627-3641.
- Thompson et al. (1991) *Can J Zool* 69: 1048-1070.
- Tillman et al. (1999) *J Sea Res* 42: 255–261.
- Turley & Lochte (1990) *Paleoeco. Palaeoclim. Palaeoecol.* 89:3-23.

- Vala AK (2010) *Bioresource Technology* 101: 2565-2567.
- USEPA (1998). "Minteqa2/Prodefa2, a Geochemical Assessment Model for Environmental Systems: User Manual Supplement for Version 4.0."
- Vanaverbeke et al (2004a) *Mar Ecol Prog Ser* 273: 139-146.
- Vanaverbeke et al. (2004b) *J Sea Res* 52:281-292.
- Vanaverbeke et al. (2008) In: Current status of eutrophication in the Belgian coastal zone. V. Rousseau, C. Lancelot, D. Cox (Eds). Presses Universitaires de Bruxelles, Bruxelles, pp 73-90.
- Van den Eynde (2004) *J. Mar. Systems* 48:171-189.
- Van der Gucht et al. (2005) *FEMS Microbiol Ecol* 53:205-220.
- Van der Zee et al. (2003) *Cont. Shelf Res.* 23:625–646.
- Van der Zee & Van Raaphorst (2004) *J Sea Res* 2004;52:73–85.
- Van Duyl et al. (1992) *Hydrobiologia* 235/236:267-281.
- Van Hannen et al. (1998) *J Phycol* 34:206-213.
- Veldhuis & Admiraal (1987) *Mar Biol* 1987;95:47–54.
- Venter et al. (2004) *Science* 304:66–74.
- Vincx M (1990) *Neth. J. Sea Res.* 25:181-188.
- Von der Heiden & Cavalier-Smith (2005) *Int J Syst Evol Microbiol* 55: 2605-2621.
- Warnken et al. (2001) *Mar Chem* 73:215–231.
- Westerlund et al. (1986) *Geochim. Cosmochim. Acta* 50, 1289–1296.
- Wey et al. (2008) *Aquatic Microbial Ecology* 52: 283-296.
- Wilkie & Hering (1996). *Colloids and Surfaces. A: Physicochemical and Engineering Aspects* 107, 97-110.
- Wilms et al. (2006) *Appl Environ Microbiol* 72:2756-2764.
- Wright et al. (1991) *Mar Ecol Prog Ser* 77:183-196.
- Zevenhuizen et al. (1979) *Microb. Ecol.* 5, 139-146.
- Zhang et al. (2002) *Sci Total Environ* 296:175-187.
- Zhang (2004) *Environ. Sci. Technol.* 38, 1421-1427.
- Zhang & Davison (1999) *Anal Chim Acta.* 398, 329-340.
- Zwart et al. (1998) *FEMS Microbiol Ecol* 25:159-1.